HOW DOES MITOCHONDRIAL HETEROPLASMY AFFECT CELL PROLIFERATION?

A thesis

Submitted in partial fulfilment

of the requirements for the Degree

of

Master of Science

in

Cellular and Molecular Biology

in the

School of Biological Sciences

University of Canterbury

by

Selina Kaye Sutton

University of Canterbury

2005

“Better a little faith, dearly won, better launched alone on the infinite bewilderment of truth, than to perish on the splendid plenty of the richest creeds”

HENRY DRUMMOND

ABSTRACT

Mitochondrial mutations and heteroplasmy have been associated with disease states that result from inadequate cellular energy production. As mitochondrial DNA (mtDNA) encodes many of the polypeptides involved in oxidative phosphorylation (OXPHOS), mtDNA mutations may lower energy production which is required for cell division and sustained ATP synthesis. In order to test the relationship between mtDNA mutations and the rate of cell division, a mammary epithelial cancer cell line, MCF-7, is used as a model. Nine proliferate single cell clones have been isolated from MCF-7. Population doubling times of six single cell clones and the MCF-7 stock have been determined. Clones with distinctly different growth rates were selected for mutational analysis. Growth rates of these clones appeared to be different from each other. Using polymerase chain reaction (PCR) and DNA sequencing, three cases of heteroplasmy have been identified in the mitochondrial genes of the MCF-7 stock and four single cell clones (ATPase C9119T, ND6 T14300G, Cytb G15807A). Heteroplasmy present in the Cytb gene is differs between single cell clones. Differences between the growth rates may be indicative of metabolic variations in these single cell clones. The OXPHOS enzymes encoded by the mutated genes were quantified by standard enzymatic assays. The assays demonstrated significant differences in specific activity between the clones, but were not correlated with mitochondrial heteroplasmy. This thesis determines that the differences in specific activity observed between clones is of nuclear origin.

CONTENTS

List of Figures

List of Tables

List of Equations

CHAPTER 1

INTRODUCTION

1.1 Mitochondria

1.1.1 The Mitochondrion

Mitochondria consist of an outer membrane encasing an inner membrane of an undulating appearance, known as the inner cristae (Figure 1.1). This inner membrane hosts the protein complexes of oxidative phosphorylation (OXPHOS) (Ruiz-Pesini *et al*., 2000a; Shoubridge, 2001; Barrientos, 2002). Oxidative phosphorylation requires the concerted effort of the mitochondrial and nuclear genomes to produce functional membrane protein complexes (Ruiz-Pesini *et al*., 2000b; Diez-Sanchez *et al*., 2003; Ballard and Whitlock, 2004).

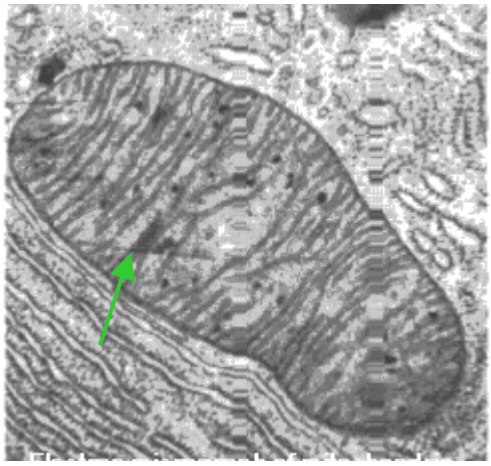

Figure 1.1. **The Human Mitochondrion.** Indicated are the inner cristae in which the OXPHOS enzymes are embedded. Figure taken from J. D. Ross is an electron micrograph approximately 30,000 x.

1.1.2 The Mitochondrial Genome

The mitochondrial genome (Figure 1.2) consists of a circular, double stranded DNA molecule of 16,659 base pairs (Anderson *et al*., 1981; Wallace, 1999). It contains 37 genes (2 encoding ribosomal RNAs, 22 encoding transfer RNAs, and 13 encoding polypeptides) partially encoding the enzymes of OXPHOS. The mitochondrion is also capable of independently replicating its own genome (Emmerson *et al*., 2001; Diaz *et al*., 2002; Chen *et al*., 2003). The majority of mammalian cells contain between 10^2 and 10^4 copies of mtDNA (Wallace *et al*., 1999; Cavelier *et al*., 2000; DiMauro *et al*.,

2000; Chen *et al*., 2003). The existence of so many copies of mtDNA is due to the mitochondria's main function of producing cellular energy. This occurs through three energy conversion pathways; glycolysis, the tri-carboxylic acid (TCA) cycle and OXPHOS.

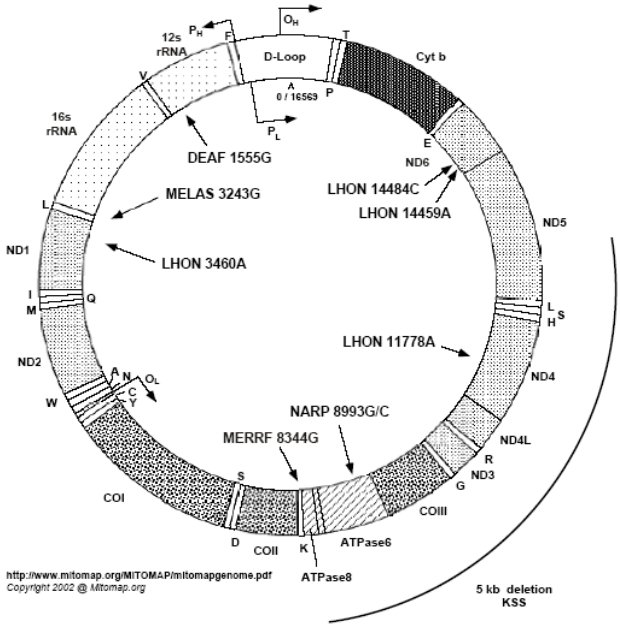

Figure 1.2. **The Mitochondrial Genome.** Figure taken from MITOMAP- a human mitochondrial genome database www.mitomap.org

1.2 Energy Conversion Pathways

1.2.1 Glycolysis

Glycolysis is an anaerobic process that occurs in the cellular cytosol. The glycolytic pathway primarily involves the catabolic degradation of glucose and simple sugars. Phase 1 involves the phosphorylation of glucose and subsequent conversion of

glucose-6-phosphate to two molecules of glyceraldehyde-3-phosphate (G3P) through a series of steps, consuming two molecules of ATP in the process. Phase 2 of glycolysis converts the G3P through a series of steps into pyruvate yielding four molecules of ATP. This results in a net production of two molecules of ATP and two of pyruvate per molecule of glucose. Figure 1.3 provides a simplified overview of glycolysis.

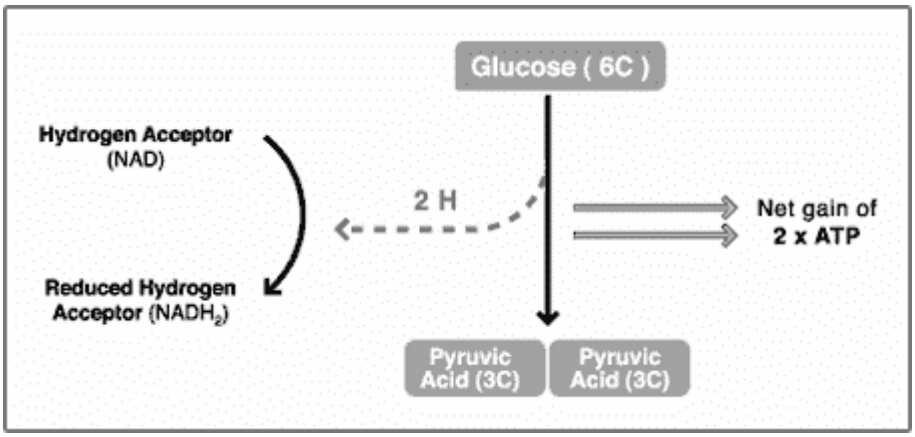

Figure 1.3. **A simplified schematic of glycolysis in which a net gain of 2 ATP molecules are produced.** Figure from the British Broadcasting Corporation www.bbc.co.uk.

The production of pyruvic acid is in preparation for the next metabolic step- the TCA cycle.

1.2.2 The Tricarboxylic Acid Cycle

The TCA cycle utilises acetyl-CoA primarily produced from the conversion of pyuvate by pyruvate dehydrogenase. Carbon units enter the TCA cycle as acetyl-CoA and are expelled as carbon dioxide through a series of reactions. Figure 1.4 provides a simplified schematic of the changes in carbon units and concomitant loss of carbon dioxide experienced through the TCA cycle.

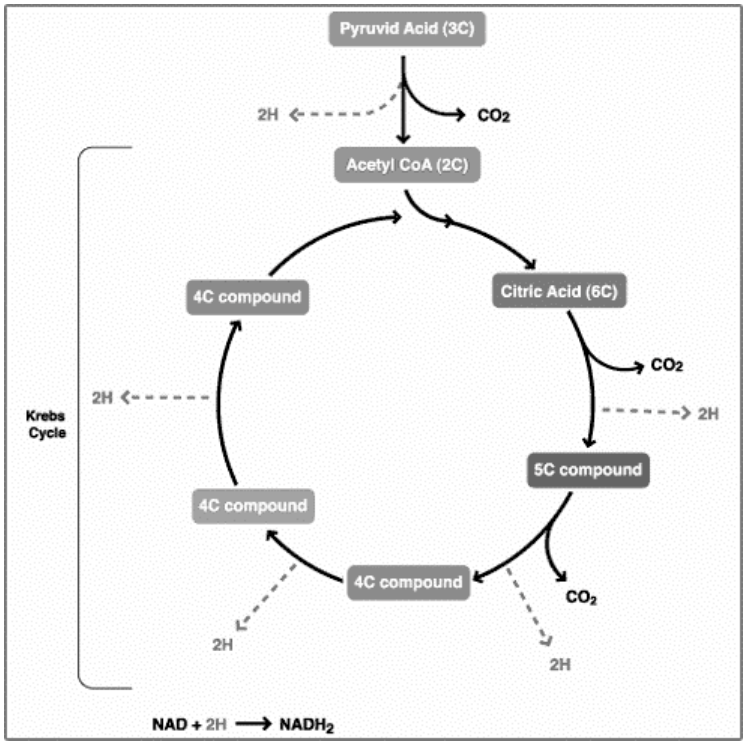

Figure 1.4. **The Tricarboxylic Acid Cycle.** Figure from the British Broadcasting Corporation www.bbc.co.uk.

Energy is yielded from the TCA cycle in a variety of forms including adenosine tri-phosphate (ATP), nicotinamide adenine dinucleotide (NADH) and membrane bound reduced flavin adenine dinucleotide ($FADH_2$). These are summarized in Equation 1.1 (Garrett and Grisham, 1999). P_i represents inorganic phosphate.

Equation 1.1

$$\text{Acetyl-CoA} + 3\ NAD^+ + [FAD] + ADP + P_i + 2\ H_2O \rightleftharpoons 2\ CO_2 + 3\ NADH + 3\ H^+ + [FADH_2] + ATP + CoASH$$

This thesis focuses on the next step in metabolism-oxidative phosphorylation. The stoichiometric relationship between the processes of glycolysis, the TCA cycle and OXPHOS is as follows in Equation 1.2:

Equation 1.2

$$NADH + H^+ + \tfrac{1}{2}\, O_2 + 3\ ADP + 3P_i \rightleftharpoons NAD^+ + 3\ ATP + 4\ H_2O$$

$$[FADH_2] + \tfrac{1}{2}\, O_2 + 2\ ADP + 2\ P_i \rightleftharpoons [FAD] + 2\ ATP + 3\ H_2O$$

A maximum of thirty-four molecules of ATP is produced during the entire process of energy conversion, with three ATP molecules per NADH and two ATP molecules per $FADH_2$ (Garrett and Grisham, 1999). This will be detailed in the following section. Mitochondria act as the powerhouse of a cell, supplying the bulk of the cellular energy request by means of the last step energy conversion step, OXPHOS (Wallace *et al*., 1999). This energy is stored via an electrochemical gradient ($\Delta\Psi m$) created by active transport of protons across the inner mitochondrial membrane. Passive diffusion of protons through ATP synthase produces ATP (Wallace *et al*., 1999; Barrientos, 2002; Smith, 2004). The first four complexes of OXPHOS are known as the respiratory chain.

1.2.3 The Respiratory Chain

The respiratory chain consists of four multimeric complexes (I-IV) (Figure 1.5) and two enzymes (ubiquinone and cytochrome c) that act as mobile electron carriers (Garrett and Grisham, 1999). This electron transfer from reducing equivalents creates a proton gradient across the inner membrane through a detailed system of chemiosmotic coupling (Garrett and Grisham, 1999; Barrientos, 2002).

The thirteen mtDNA translation products make up the subunits of four of the five complexes of OXPHOS (Complexes I, III, IV (respiratory chain) and ATP synthase, complex V) (Shoubridge, 2001; Jacobs, 2003).

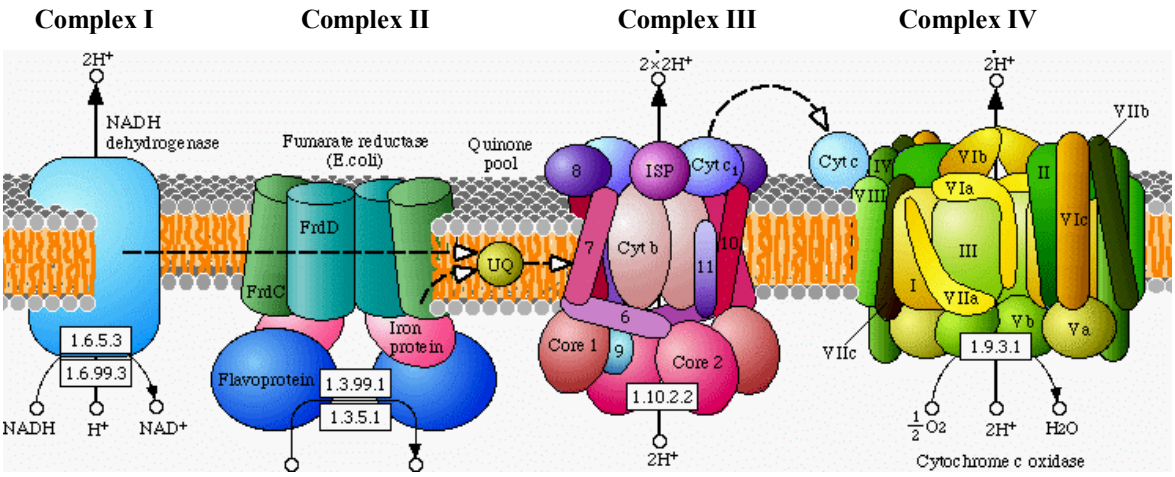

Figure 1.5. **Complexes I-IV of the electron transport chain involved in oxidative phosphorylation.** Figure taken from Homo sapiens draft oxidative phosphorylation GenomeNet 2004

1.2.3.1 Complex I –NADH-Coenzyme Q Reductase

Complex I supplies ubiquinone to complex III through the electron acceptor, ferricyanide (Rustin *et al.*, 1996; Barrientos, 2002). It achieves this by the oxidation of reduced NADH to NAD+ coupled with the reduction of flavin mononucleotide (FMN) (Equation 1.3, Garrett and Grisham, 1999).

Equation 1.3

$$NADH + [FMN] + H^+ \rightarrow [FMNH_2] + NAD^+$$

It is the most structurally complex of all the OXPHOS enzymes with at least 40 subunits (Hofhaus *et al.*, 1995; Barrientos, 2002). It has a molecular mass of 900 kDa

and is under dual (mitochondrial and nuclear) genetic control (Hofhaus *et al*., 1993; Hofhaus *et al*., 1995; Bourges *et al*., 2004).

1.2.3.2 Complex II –Succinate-Coenzyme Q Reductase

Complex II is solely encoded by nDNA, producing four non-equivalent polypeptides (Garrett and Grisham, 1999; Barrientos, 2002). These subunits are associated with anchor proteins in the mitochondrial membrane. A flavin is covalently linked to a 70 kDa peptide, known as the flavoprotein subunit (Fp) (Figure 4.2). Complex II is a 140 kDa multimeric complex that catalyses the oxidation of succinate to fumarate, coupled with the reduction of ubiquinone (UQ) (Equation 1.4, Garrett and Grisham, 1999). Complex II produces reduced ubiquinone (UQH_2), the substrate of complex III but does not directly transport protons across the inner membrane.

Equation 1.4

$$\text{Succinate} \rightarrow \text{Fumarate} + 2H^+ + 2e^-$$

$$UQ + 2\,H^+ + 2e^- \rightarrow UQH_2$$

1.2.3.3 Complex III- Coenzyme Q-Cytochrome c Reductase

Complex III supplies cytochrome c (II) to complex IV. Complex III is a 496 kDa complex, which also facilitates the transport of protons across the inner membrane increasing $\Delta\Psi m$. This requires the oxidation of UQH_2 yielding two electrons which are supplied to cytochrome c (III) (Garrett and Grisham, 1999; Barrientos, 2002). The

reduction of cytochrome c (III) involves a complex redox pathway known as the Q cycle. Briefly, UQH_2 diffuses into a complex III site termed Qp. A series of redox steps occur forming an intermediate product, semiquinone ($UQ\cdot^-$), at the Qp site. Semiquinone is converted to ubiquinone as electrons are again acquired from the oxidation of UQH_2 at the Qp site. This results in the reduction of cytochrome c. The overall process for complex III is represented in Equation 1.5.

Equation 1.5

$$UQH_2 + 2\ H^+_{in} + 2\ \text{Cyt c (III)} \rightarrow 4\ H^+_{out} + 2\ \text{Cyt c (II)} + UQ$$

Reduced cytochrome c is the mobile electron carrier between complexes III and IV.

1.2.3.4 Complex IV- Cytochrome c Oxidase

Cytochrome c oxidase (complex IV) catalyses the transfer of electrons from cytochrome c (II) to molecular oxygen (D'Aurelio *et al*., 2001; Barrientos, 2002). It has thirteen subunits of mitochondrial and nuclear origin comprising a 204 kDa complex (Garrett and Grisham, 1999). The catalytic core contains three mtDNA encoded subunits. The reaction is represented in Equation 1.6 (Garrett and Grisham, 1999). Protons are also actively transported across the membrane during complex IV activity.

Equation 1.6

$$4\ \text{Cyt c}\ (Fe^{2+}) + 4\ H^+ + O_2 \rightarrow 4\ \text{Cyt c}\ (Fe^{3+}) + 2\ H_2O$$

1.2.3.5 ATP Synthase

ATP synthase (complex V) promotes the synthesis of ATP by the diffusion of protons through the F_o and F_1 rotating components of the complex, spanning the mitochondrial membrane (Aggeler *et al*., 2002). It is the only OXPHOS complex that allows diffusion of protons into the inner membrane. (Garrett and Grisham, 1999; Barrientos, 2002; Aggeler *et al*., 2002; Smith, 2004). ATP hydrolysis (cleavage of hydrolytic bonds) is the primary energy source for the processes of biosynthesis and muscle contraction (Smith, 2004) creating a free energy change (ΔG°) of -31 kJ/mol. ATP is in fact, an energy carrier as close to a 40 kg turnover of ATP per day is experienced in the average human body, with only 50-70 mg of adenosine phosphates present at any given time (Smith, 2004). Any change in the capacity of OXPHOS in high energy demanding tissues may noticeably impair cellular function in terms of reduced cell proliferation.

1.3 Reactive Oxygen Species

In metabolism, reactive oxygen species (ROS) are formed by the reaction of superoxide with surrounding bio-molecules (Halliwell and Gutteridge, 1999). These can be proteins, other ROS, or nucleic acid. A typical formation of free radicals is the homolytic fission of hydrogen peroxide, producing two hydroxyl radicals (Equation 1.7). This may occur in a biological system increasing hydroxyl radical concentration.

Equation 1.7

$$H_2O_2 \rightarrow 2\ ^{\cdot}OH$$

The hydroxyl radical can react with nitrogen bases in purines and pyrimidines in a biological system as follows in Figure 1.6;

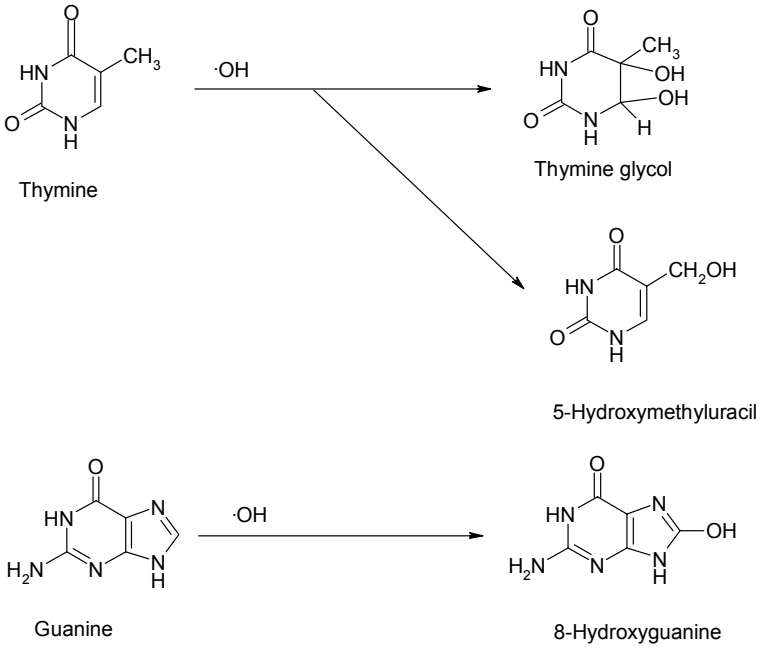

Figure 1.6. **Nucleic acid damage mediated by the hydroxyl radical**

8-Hydroxyguanine (8-oxo-dG) is a common marker of DNA damage (Fujii *et al.*, 2002). A by-product of OXPHOS is the production of ROS in the form of superoxide. Superoxide is produced during metabolism in which leakage of electrons react with oxygen to form a reactive oxygen species. Superoxide reacts with local bio-molecules to produce a host of reactive species that can cause widespread damage. It is estimated that each mitochondrion may generate 10^7 radicals/day (Max, 1992). Additionally, due to the lack of stringent repair mechanism, it is proposed that mtDNA has a mutation rate of 5-10 times that of nuclear DNA due to ROS mediated damage and the absence of protective histone proteins (Brown *et al.*, 1979; Croteau and Bohr, 1997).

There is, however, a relationship between ROS, cell proliferation and growth-related signalling pathways (Arnold *et al*., 2001; Behrend *et al*., 2003). This gives ROS a positive role within a biological system, though much activity is counter production. Of particular relevance to cellular damage is the involvement of ROS in lipid peroxidation. Lipid accumulation is associated with a decrease in male fertility with age (Holstein *et al*., 2003), cellular transformation (Takabe *et al*., 2001) and apoptosis (Gieseg *et al*., 2000).

Reactive oxygen species have been implicated in human male infertility, atherosclerosis, neuro-degenerative disease, diabetes and a host of diseases (Twigg *et al*., 1998; Aitken and Krausz, 2001; Gil-Guzman *et al*., 2001; Behrend *et al*., 2003; Wang *et al*., 2003; Moustafa *et al*., 2004; Sanocka and Kurpisz, 2004). Indeed, there are reports of high levels of ROS in 20-40% of infertile men (Aitken *et al*., 1997; Gil-Guzman *et al*., 2001), though healthy sperm production and cellular function is dependant upon physiological levels of ROS (Zini *et al*., 1995; Aitken *et al*., 1997; Allen *et al*., 1997; de Lamirande *et al*., 1998; Richer and Ford, 2001; St John *et al*., 2001; Sanocka and Kurpisz, 2004). It is yet unknown at what level ROS induce damage and what levels are necessary for healthy cellular function (Behrend *et al*., 2003; Sanocka and Kurpisz, 2004).

1.3.1 Lipid Peroxidation

The plasma membrane is particularly susceptible to oxidative stress due to being enriched with polyunsaturated fatty acids (PUFAs) that are essential for membrane fluidity, which is required for membrane vesicle fusion (Aitken and Krausz, 2001; Khosrowbeygi *et al*., 2004) and functional ability (Sanocka and Kurpisz, 2004). Lipid

inclusions and peroxidation have been implicated in disease (Folgero *et al*., 1993; Aitken and Krausz, 2001; Miller *et al*., 2001).

Oxidative stress induces peroxidation of PUFAs in the plasma membrane, with the potential knock-on effect of DNA damage of both mitochondrial and nuclear genomes (Aitken and Krausz, 2001; Takabe *et al*., 2001). Mitochondrial DNA damage that results in less efficient metabolism may encourage greater superoxide production along with subsequent ROS reactions (Diaz *et al*., 2002).

1.3.2 Fenton Chemistry in Biological Systems

A mediator of the formation of highly damaging ROS in a biological system is free iron. Though generally tightly chelated, free iron is present at low levels in a biological system. Fenton chemistry is the reaction of ROS with free iron. In the presence of Fe^{3+}, hydroperoxides can undergo a reaction yielding Fe^{2+} by translocation of a proton. This is described in Equation 1.8.

Equation 1.8 $ROOH + Fe^{3+} \rightarrow RO^{\cdot}_2 + Fe^{2+} + H^{+}$

This yields the peroxyl radical ($HO^{\cdot}_2$) capable of undergoing the following reaction.

Equation 1.9

$$-CH2- + HO^{\cdot}_2 \rightarrow -\dot{C}H- + H_2O_2$$

This gives rise to hydrogen peroxide (H_2O_2). Hydrogen peroxide can also react with Fe^{2+} giving rise to the hydroxyl radical ($HO^{\cdot}$), a potent mediator of bio-molecular damage.

Equation 1.10

$$H_2O_2 + Fe^{2+} \rightarrow HO^{\cdot} + OH^{-} + Fe^{3+}$$

In the present research, AAPH (peroxyl radical generator) was selected to test the potential for mitochondrial DNA damage in MCF-7 cells. Azo initiators such as AAPH also produce superoxide, which rapidly converts to the protonated form and reacts with lipid hydroperoxides forming hydrogen peroxide, a key ROS in biological systems (Equation 1.10, Halliwell and Gutteridge, 1999). Superoxide releases iron from iron-sulphur centred proteins that can generate carbon centred radicals, which initiate lipid peroxidation (Murphy *et al.*, 2003). This can result in a chain reaction (propagation) of lipid peroxidation shown in Equation 1.11. (Simandan *et al.*, 1998).

Equation 1.11

$$\text{-}CHO^{\cdot}_2 + \text{-}CH_2 \rightarrow \text{-}CHO_2H + \text{-}C^{\cdot}H$$

Fenton chemistry is responsible for the production of many reactive oxygen species in a biological system. Understanding the role of hydrogen peroxide as a pro-oxidant species is important in the present research as H_2O_2 can produce a host of other reactive oxygen species in a biological system, with potential for nucleic acid modification. Figure 1.7 summarizes the key pathways in the neutralization of hydrogen peroxide, working to counter bio-molecular damage.

Key Pathways of Antioxidants Relating to Hydrogen Peroxide Neutralisation

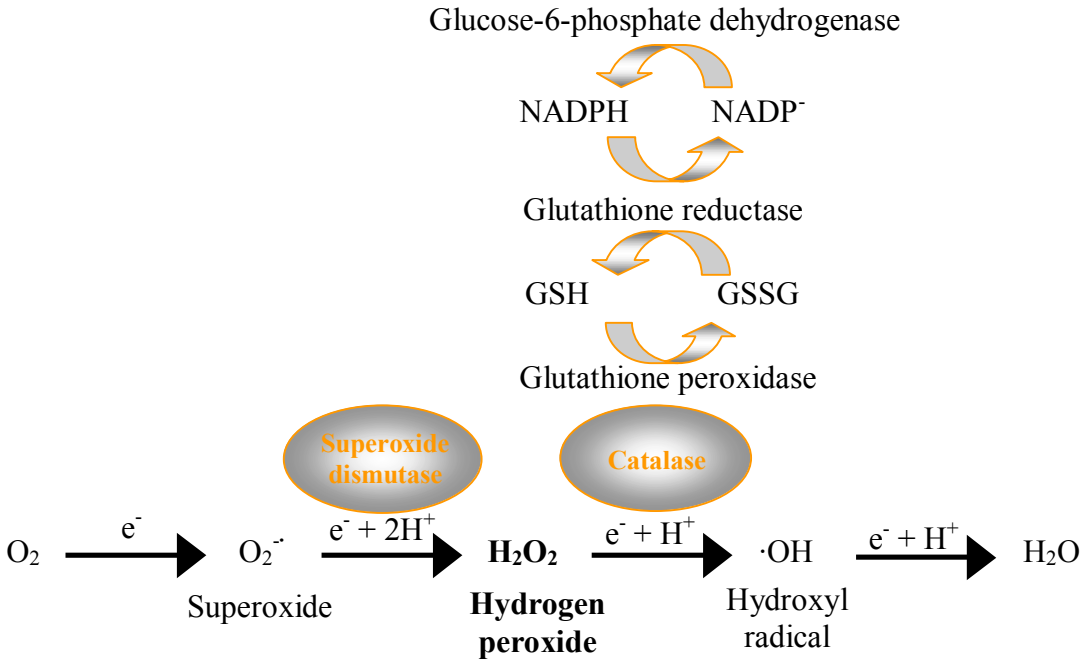

Figure 1.7. **Summary of the major antioxidant pathways relating to hydrogen peroxide.**

1.4 Mitochondrial DNA Mutation and Disease

Mitochondria play a key role in providing energy for cell proliferation and sustaining cellular activity (Snustad and Simmons, 1997; Ruiz-Pesini *et al*., 1998; Rossignol *et al*., 2000; Ruiz-Pesini *et al*., 2000a). Thus, mitochondrial heteroplasmy or mutation may influence ROS production (in the form of increase superoxide production), and induce disease states in organs that are dependant on consistent energy production and suffer when energy production declines (Halliwell and Gutteridge, 1999; Chomyn *et al*., 2000; DiMauro and Schon, 2001; Yasukawa *et al*., 2001; Kirino *et al*., 2005). The presence of mutant cells in laboratory cultures may be determined by slow cell proliferation and substantial cell death. Biochemical communication between

mitochondria and the cell nucleus has been associated with a degree of control of the signalling involved in apoptosis, cell proliferation and differentiation of normal and malignant cells (Felty and Roy, 2005).

1.4.1 Mitochondrial Mutation Load

The mutant load of mtDNA in tissues can be influenced in two ways. Firstly, there is an ever-present background of ROS production and tissue toxins. Secondly, mtDNA deletions producing a smaller genome tend to replicate faster, accumulating with age (Cummins *et al*., 1994; Diaz *et al*., 2002). This can result in decreased metabolic activity and increased ROS production causing more damage to both DNA and proteins (Diaz *et al*., 2002).

1.4.2 Human Mitochondrial Mutation Rate

Mitochondrial DNA mutates faster than nuclear DNA due to localized ROS production (Brown *et al*., 1979; Wallace *et al*., 1999; DiMauro and Andreu, 2000). Thus, tissues with a higher metabolic demand, in the form of increased ATP consumption, experience higher levels of mtDNA deletion (Cortopassi *et al*., 1992). Estimates of the human mitochondrial mutation rate vary greatly and can span up to two orders of magnitude (Siguroardottir *et al*., 2000). In the hypervariable region I (mt16024-16383) and hypervariable region II (mt57-371) a value of 0.0043 mutations per generation was estimated from mutational studies of 272 individuals (Siguroardottir *et al*., 2000). The higher mutation rate of mtDNA results in mitochondrial haplogroups that differ between populations (Wallace *et al*., 1999). It is

possible that haplogroups exist within a cell culture that contains sub-populations such as MCF-7.

Mitochondrial DNA mutations are responsible for a host of diseases that arise due to impaired energy output. These include mitochondrial myopathies, encephalopathy, lactic acidosis, stroke-like episode (MELAS) (Klug and Cummings, 1997; Chomyn *et al*., 2000; DiMauro and Andreu, 2000; Kirino *et al*., 2004; Kirino *et al*., 2005), myoclonus epilepsy associated with ragged red fibres (MERRF) (King and Attardi, 1989; Klug and Cummings, 1997; Yasukawa *et al*., 2001), Leber's hereditary optic neuropathy (LHON), progressive external ophthalmoplegia (PEO) and a host of others (Hofhaus *et al*., 1996; DiMauro and Schon, 2001; Kirino *et al*., 2005). These include the influence of mitochondrial haplotypes (Cummins *et al*., 1994; Folgero *et al*., 1993; Ruiz-Pesini et al., 2000), mutations or deletions and mitochondrial heteroplasmy (Cummins *et al*., 1994; Wallace *et al*., 1999; DiMauro and Andreu, 2000; Quintana-Murci *et al*., 2001; Diaz *et al*., 2002; Bai *et al*., 2004).

Mitochondrial DNA mutations exist in two broad categories; mutations that affect mitochondrial protein synthesis (single nucleotide deletions or substitutions involving rRNA and tRNA genes) (DiMauro and Schon, 2001; Suzuki *et al*, 2002; Kirino *et al*., 2004; MITOMAP, 2005) and those that are present in protein coding genes (DiMauro and Andreu, 2000; DiMauro and Schon, 2001; MITOMAP, 2005). Expectedly, cells harbouring pathological tRNA mutation within the mtDNA exhibit decreased OXPHOS complex activity, lowered oxygen consumption, and reduced cellular growth rates (Jacobs, 2003). Currently ninety pathogenic mitochondrial tRNA mutations are known (MITOMAP, 2005). The outcome of many of these mutations is

impaired energy output due to lowered efficiency of the OXPHOS enzymes, most evident in tissues requiring a large energy supply (DiMauro and Andreu, 2000) such as muscle tissue, spermatozoa and cancer cells.

1.4.3 Mitochondrial DNA Copy Number

The copy number of mitochondria DNA per cell is dependant on cellular energetic demand (May-Panloup *et al*., 2003). The majority of mammalian cells contain 10^2 to 10^4 copies of mtDNA. Some mitochondria contain up to 11 copies of mtDNA, others are devoid of mtDNA (Cavelier *et al*., 2000). At the molecular level, this reduction is due to the down regulation of the mitochondrial transcription factor A (tfam) controlling mitochondrial DNA copy number (Larsson *et al*., 1997; Rantanen *et al*., 2001). In the present research, citrate synthase activity will be monitored in cell clone cultures as an indicator of mitochondrial DNA copy number.

1.4.4 Mitochondrial Heteroplasmy

There exists a cell-to-cell variable load of mutant to wild-type mitochondrial DNA. (Wallace *et al*., 1999; DiMauro and Andreu, 2000; Quintana-Murci *et al*., 2001). Heteroplasmy is a state in which mutant and wild type mitochondrial DNA exists within a tissue or even a single cell. The situation in which cells or tissues have identical mitochondrial DNA is known as homoplasmy (DiMauro and Andreu, 2000).

The mutational state of heteroplasmy tends to drift towards homoplasmy over time. This process is known as replicative segregation (Wallace, 1986; Wallace *et al*., 1999;

D'Aurelio *et al*., 2001; Battersby *et al*., 2003). As cells divide it is by chance that one daughter cell may receive mutant mitochondrial DNA. Over time, the percentage of mutant or wild type mtDNA will drift toward a pure mutant, or a homoplasmic state (Wallace, 1986). For this reason, many mitochondrial myopathies will not be evident until later in life due to mutant DNA accumulation. Increase of mutant mtDNA is met with a concomitant decline in cellular energy production (Wallace *et al*., 1999).

The proportions of mutant and wild type mitochondrial genomes can vary between different tissue types (Cavelier *et al*., 2000) and the same tissue of an individual (Grzybowski, 2000; Quintana-Murci *et al*., 2001; Chen *et al*., 2003). Further, a given cell can exist in a heteroplasmic state (Grzybowski, 2000). The variation of mitochondrial deletion in different people of similar age appears to be less than the variation amongst different tissues of an individual (Cortopassi *et al*., 1992). Additionally, a state of heteroplasmic deletion can be present within the genome that is difficult to determine by conventional PCR and sequencing for single deletions, as the wild type sequence will still appear, but at a reduced level of the base in question (Holt *et al*., 1989).

1.4.5 Mitochondrial Hyper-mutagenesis in Some Cancer Cell Lines

A high frequency of homoplasmic point mutation is detected in a range of human tumours. The rates range from 70% in colon tumour cell lines to 15% in prostate (Chen *et al*., 2003). At the very least, a significant subset of human tumours experience frequent mutational events within the mtDNA. This is proposed to occur as the cell shifts from a benign epithelial cell to a malignant cell, of high oxygen

consumption particularly in prostate tumours (Costello and Franklin, 2000). This directly relates to OXPHOS, as mitochondria are the primary source of ROS, heightened with increased oxygen consumption. Chen *et al.* (2003) found a process of mitochondrial hyper-mutagenesis in place, potentially mediated by increased oxidative stress in three prostate tumour cell lines (Chen *et al*., 2003). This was proposed due to the discovery of local homoplasmy of mutation, and linkage of multiple mitochondrial mutations occurring along the course of tumour progression (Chen *et al*., 2003). It is as yet unknown whether the MCF-7 cell line has, or can be induced to high oxygen consumption. Moreover, it is an important aspect of using cancer cell line models in studying mitochondrial genetics, whether a process of hyper-mutagenesis is active.

1.5 The MCF-7 Cell Line as a Model

A cell line model can be employed to elucidate the influence of genetic factors on cellular proliferation and morphological changes, both of which may indicate DNA modification. Consistent treatment of a cell line during study is paramount to obtain meaningful results. Cell line models are also useful for *in organello* assessment of mitochondrial protein synthesis (Gaines and Attardi, 1984; Micol *et al*., 1997) and OXPHOS function (Barrientos, 2002). The MCF-7 cell line contains sub-populations (Devarajan *et al*., 2002; Zou and Matsumura, 2003), useful for the isolation of single cell clones with the potential for genetic variation. MCF-7 is a well-characterized cell line (Sutherland *et al*., 1983; Devarajan *et al*., 2002; Zou and Matsumura, 2003; Lacroix and Leclercq, 2004; Zivadinovic *et al*., 2004) which has been used in studying environmental factors (Zou and Matsumura, 2003), chemotherapeutic drugs

(Sutherland *et al*., 1983; Taylor *et al*., 1983), drug resistance (Devarjan *et al*., 2002), and reactive oxygen species (Hand and Craven, 2003).

1.6 Thesis Aspirations

The MCF-7 cell line will be used to assess the effect of free radical generators on mitochondrial mutation, OXPHOS activity and rate of cell proliferation. Morphological changes under the influence of free radical generators will be determined. In order to achieve the research goals, cell cultures with a homogenous genetic background will be established by isolating single cell clones from an MCF-7 stock culture. Mutations in the mitochondrial genome will be analysed by sequencing of selected genes and the activities of the OXPHOS enzymes will be assayed by standard biochemical technique. Further, mutation rates of the MCF-7 stock culture will be assessed after a known number of cell generations.

CHAPTER 2

MATERIALS AND METHODS

2.1 Materials

All materials were of molecular biology grade. Chemical abbreviations are listed in Appendix A. For a comprehensive list of suppliers, refer to Appendix C. Distilled, deionised water (ddH_2O) was prepared by ultra filtration with a Barnstead NANO Pure Ultrapure water system (IO, USA). Chemical solutions and ddH_2O were autoclaved before use.

2.2 Methodology

2.2.1 Cell Culture

2.2.1.1 MCF-7 Cell Line

MCF-7 is a cell line derived from mammary epithelial adenocarcinoma from a 69-year-old Caucasian woman (American type culture collection (ATCC) cell line HTB-22). It was derived from a pleural effusion metastatic site. Its morphology is polygonal and adherent and has been well characterized (ATCC; Mambo *et al*., 2002; Zou and Matsumura, 2003). Widely used by research laboratories, it is suitable as a cell line model (Sutherland, 1983; Devarajan, 2002; Lacroix and Leclercq, 2004).

2.2.1.2 Cell Culture Conditions

Aseptic techniques were strongly adhered to as outlined by Freshney (Freshney, 2001). Cultures were worked with in a vertical laminar flow hood (Figure 2.1 A) (Clyde-Apac BH2000 series) and the cultures were maintained at 37˚C in a CO_2 incubator (Sanyo MCO-20AIC) at 5% CO_2. All reagents for cell culture were pre-warmed to 37˚C before use. Cell cultures were grown to 80-95% confluence before sub-culturing or freezing. Cells morphology was visualised with an inverted microscope (Figure 2.1 B) (Leitz Diavert, Welzler, Germany) and photographed with a hand-held Sony Cybershot 5.1 Megapixel camera.

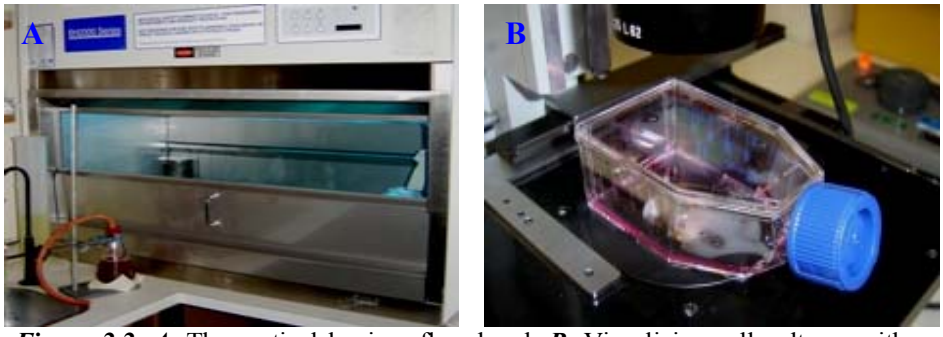

Figure 2.2. A, The vertical laminar flow hood, ***B,*** Visualizing cell cultures with an inverted microscope

2.2.1.3 Preparation of Cell Culture Medium

All cell culture reagents were obtained from Gibco, Invitrogen, New Zealand and stored as recommended by the manufacturer. Dulbecco's modified eagles medium (DMEM, 0.1 μm filtered) contained 4500 mg/L D-glucose, 584 mg/L L-glutamine, 110 mg/L sodium pyruvate and 4 mg/L pyridoxine hydrochloride, alongside standard DMEM reagents (Gibco, Invitrogen). The medium was supplemented with foetal

bovine sera (FBS, 9.85 %, Invitrogen, New Zealand source), and 49 units/ml penicillin-streptomycin (Gibco, Invitrogen).

2.2.1.4 Initial Cell Seeding

A 1.0 ml aliquot of MCF-7 cells (6.9×10^6) obtained from Dr Drusilla Mason (School of Biological Sciences, University of Canterbury, New Zealand) were seeded into a T-75 flask. Growth medium (GM, 19.0 ml) was dripped into the flask over two minutes to reduce osmotic shock. The cells were incubated for four hours (to adherence). The culture medium was refreshed to remove dimethyl sulfoxide (DMSO) from culture freezing.

2.2.1.5 Harvesting and Subculturing of MCF-7 Cells

To harvest the cells the culture medium was removed by aspiration and 2.0 ml trypsin/EDTA 0.25%/1 M was applied to the monolayer to detach cells. The culture was incubated for 2-5 minutes at 37˚C until all cells had detached from the surface. Eight ml of GM was added to dilute the trypsin and a cell count was taken.

2.2.1.6 Performing a Cell Count

Cultures were thoroughly mixed prior to an aliquot being removed for cell counting or seeding. For cell counting, a 100 µl aliquot was removed and diluted with 100 µl trypan blue (Gibco, Invitrogen, New Zealand) cellular viability dye. Trypan blue will stain all dead cells, while living cells will actively exclude the dye (Gibco, Invitrogen,

New Zealand). From the dye suspension 3 µl was taken for cell counting. A Makler counting chamber (Sefi-medical instruments) with a 0.01 mm^2 x 10 µm grid was used to determine the cell count. The cell count was adjusted for a dilution factor of two to correct for the addition of the dye. Percent viability was calculated by dividing viable cells by the total number of cells counted. Unless otherwise stated the percentage viability was above 90% (excluding plateau phase of population growth studies).

2.2.1.7 Cell Culture Cryopreservation

Aliquots (1.0 ml) of the cell culture suspension were centrifuged (Eppendorf 5417R) at 90 x *g* for 8 minutes. The supernatant was aspirated and the pellet washed with 1 x phosphate buffered saline (PBS, 0.26 M Na_2HPO_4, 0.09 M KH_2PO_4, 0.39 M NaCl), pH 7.4. The washed pellet was re-suspended in 1.0 ml 10% DMSO and transferred to cryotubes (Nunc-Nalgene). The cryotubes were slowly cooled in isopropanol for 2 minutes and stored in a -80˚C chest freezer (GFL).

2.2.1.8 Isolation of Single Cell Clones

Conditioning medium was prepared from an equal volume of fresh GM and GM from exponentially growing cell cultures. Briefly, GM from exponentially growing culture was centrifuged at 53 x *g* (Eppendorf 5810R) to remove floating cells and cell debris. The supernatant was used to make up conditioning medium. For single clone isolation, MCF-7 mammary epithelial cells (second passage) seeded at 7.6 x 10^6 cells/ml were grown to 90% confluence in 19.0 ml GM in a T-75 flask. The culture medium was aspirated and 2.0 ml of trypsin/EDTA 0.25%/1 M (Gibco, Invitrogen, New Zealand)

was applied to the monolayer and incubated at 37˚C for 3-4 minutes or until cells had detached. Eight ml of conditioned GM was added to dilute the trypsin/EDTA and a cell count was performed with the resulting cell suspension. This was determined to be 1.08 x 10^6 cells/ml. Based on the cell count, a serial dilution was performed until the cell concentration was 10.77 cells/ml. Aliquots of 65 µl of cell suspension were seeded into each well of a Nunc 96 well plate, giving an average count of 0.7 cell/well. The single cell wells were identified under a microscope and recorded. Wells with more than one cell were discarded. Conditioning medium was refreshed regularly until single cell clones had formed populations, after which standard growth media was introduced. Single cell clone cultures were established in T-75 flasks with GM.

2.2.1.9 WST-1 and Trypan Blue Cell Estimates

Trypan blue and the WST-1 cell proliferation assay are two methods for estimating cell population growth. The trypan blue cell count was performed by seeding 2 x 10^3 cells/well in a 12 well plate (3.5 cm^2) and performing cell counts (Section 2.2.1.6) at regular intervals.

The WST-1 (4-[3-(4-Iodophenyl)-2-(4-nitorphenyl)-2H-5-tetrazolio]-1,3-benzene disulfonate) assay functions by the cleavage of a tetrazolium salt to a formazan product (Figure 2.2). An absorbance shift occurs due to a colorimetric change by the reduction of tetrazolium salts caused by cellular membrane enzymes. A WST-1 calibration plot was formed by seeding wells with a know concentration of cells and measuring the absorbance at 450 nm with 690 nm as a reference wavelength. A

calibration curve was constructed from these measurements. Subsequent estimates of cell concentration could be determined by taking the average absorbance and calculating the corresponding cell count from the calibration curve. Culture medium was aspirated from wells to be assayed and replaced with 100 µl of phenol red free GM, supplemented with heat inactivated FBS. To the maintenance medium, 10 µl of WST-1 reagent was added and the culture was incubated for 4 hours. The plate was shaken prior to measurements being taken. Each time-point represents the mean (± SE) of the number of cells from eight separate wells.

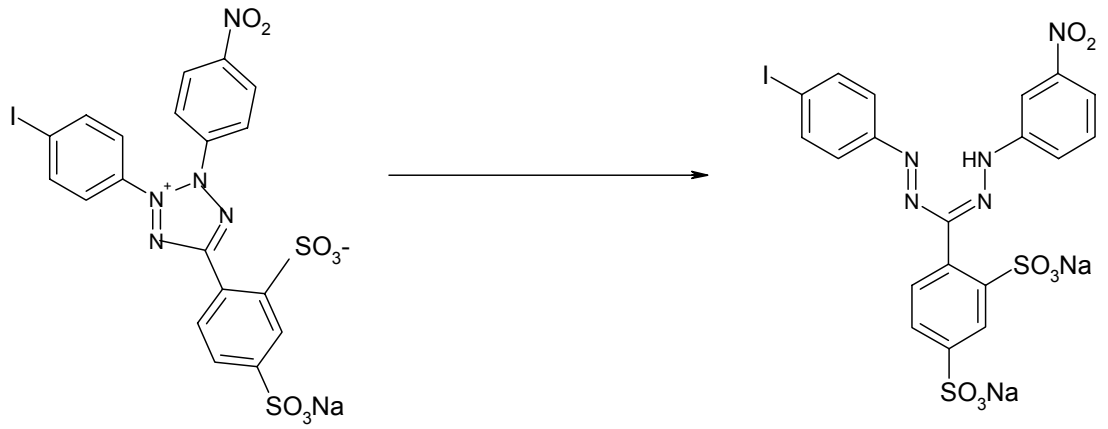

Figure 2.2. **WST-1 reagent.** The WST-1 assay functions by the cleavage of the tetrazolium salt to a formazan product.

2.2.1.10 Check for Bacterial Contamination

All cultures were checked for bacterial contamination immediately before population growth studies and mitochondria isolation. Aliquots (1.0 ml) from cultures were seeded into 12 well plates (three wells per culture), and incubated for five days with antibiotic free GM.

2.2.2 DNA Analysis

2.2.2.1 MCF-7 Cell Genomic DNA Extraction

Cells were grown to a minimum of 85% confluence in T-75 or T-25 flasks in all instances. The growth medium was aspirated and 2.0 ml or 1.0 ml, respectively, of trypsin/EDTA 0.25%/1 M (Gibco, Invitrogen, New Zealand) was added. Cells were monitored using an inverted microscope until all cells had lifted from the well surface. The cell suspension was transferred to 1.5 ml microfuge tubes and centrifuged at 86 x *g*, room temperature, for eight minutes. The medium was aspirated and cell the pellet was washed with PBS and centrifuged as before. The PBS was aspirated and the cell pellet was treated with extraction buffer (900 µl; 0.1 M Tris HCl, 0.1 M NaCl, 20 mM EDTA (pH8)) and lysis mix (100 µl; 100 µg/ml proteinase K, 10 mM DTT, 1% SDS). Extractions were mixed thoroughly and incubated in a waterbath at 50˚C overnight. One volume of Tris-EDTA pH8 (TE8) saturated phenol was added to the cell solution. This was mixed thoroughly and centrifuged at 15,300 x *g*, for five minutes at ambient temperature. The aqueous phase was transferred to a new tube and the original tube was back-extracted with an equivalent volume of TE8. The two aqueous phases were combined and treated with equal volumes of phenol and chloroform (chloroform:isoamyl alcohol/24:1). The extraction was thoroughly mixed for five minutes and centrifuged as above. The aqueous phase was transferred to a new tube and one volume of chloroform was added. The extraction was centrifuged as above. The aqueous phase was transferred to a new tube and the DNA was precipitated with 0.1 volume 3M NaOAc (pH 7.0) and two volumes of 100% cold ethanol. The resulting solution containing visible white strands of DNA was stored in the freezer (-

20˚C) overnight. The DNA was pelleted at 15,300 x *g* for 20 minutes at 4˚C. The supernatant was aspirated and the DNA was washed with 70% cold ethanol. The DNA was re-suspended in TE8.

2.2.2.2 Visualization of Isolated Genomic DNA

Successful DNA extraction was confirmed by electrophoresis on a 1% (w/v) agarose (Sigma) gel prepared with 1 x TAE (Tris-acetate/EDTA 0.04 M/0.001 M, pH8). DNA (1 µl) with 1 x orange G loading buffer (30% glycerol, 0.35% orange G) was loaded into the gel and run at 80V (5V/cm) for 25 minutes. Gels were stained with ethidium bromide solution (0.5 µg/ml) for 15 minutes, with agitation, and visualized on an ultra-violet (UV) transilluminator at 300 nm.

2.2.2.3 Genomic DNA Quantification

DNA was quantified by determining the absorbance of 5 µl genomic DNA in 495 µl ddH_2O at 260 nm and 280 nm. DNA concentration was calculated from the absorbance at 260 nm (one optical density (OD) unit at 260 nm is equivalent to 50 µg dsDNA/ml). The concentration of DNA was calculated with the following equation.

$$\text{DNA concentration (µg/µl)} = \frac{OD_{260} \times 10^2 \times 50 \text{ µg/ml}}{1000}$$

DNA was also quantified visually by a spotting technique. Quantities of λ DNA (0.3, 0.1, 0.08, 0.06, 0.04 and 0.01 µg/µl) were spotted on a 1 % agarose gel as a concentration standard. Aliquots of 1 µl of each single clone isolated DNA and the

MCF-7 stock were spotted beside the marker. These were allowed to dry, stained in ethidium bromide, and visualised as above. The concentration of MCF-7 stock DNA and clone DNA were estimated by comparison to the λ DNA standards.

2.2.2.4 Polymerase Chain Reaction (PCR)

PCR reactions were performed in a 25 µl reaction volume and contained 1 x PCR buffer, 2 mM dNTP mix (dATP, dGTP, dCTP, dTTP) (Eppendorf), 2 mM $MgCl_2$, 0.5 units *Taq* DNA polymerase (Roche), 8 mM of forward and reverse primer (Hermann-GbR)

PCR was performed on a Perkin-Elmer DNA thermal-cycler 480 as follows:

80˚C	2 min (DNA added)	
94˚C	2 min	
94˚C	30 seconds	┐
56-59˚C	30 seconds	30 x
72˚C	1 minute	┘
72˚C	5 minutes	
4˚C	SOAK	

The annealing temperature varied depending on the primer pair used (Table 2.1).

Table 2.1. **Human mitochondrial genome primer pairs.**

Primer pair	Gene	Position	Product size	Tm values	
				F	R
12S F 12SR	12S	628-1705	1077	68	70
16S F 16S R	16S	1591-2646	1055	71	68
16SF1 16SR1	16S	2334-3366	1032	68	66
ND1F ND1R	ND1	3245-4370	1125	66	66
ND1F3 ND2R2	ND1/ND2	3930-4885	955	66	64
ND2F2 ND2R3	ND2	4712-5309	597	68	68
ND2F3 COI IR	ND2/tRNA/COI	5198-6758	1560	66	67
COI IF COI IR	COI	5815-6758	943	68	67
COI 2F COI 2R	COI	6611-7600	989	66	66
T7COII IF T3COII IR	COII	7495-8485	990	82	83
T7ATPaseF T3ATPaseR	ATPase6, 8	8466-9336	870	84	84
T7COII IF T3COIII IR	COIII	9184-10176	992	84	84
HMTL 10123 HMTH 10859	ND3	10123-10859	736	64	66
HMTL 10123 HMTH 12143	ND3/ND4	10123-12143	2020	64	63
HMTL10763 HMTH 12211	ND4	10763-12211	1448	68	69
ND5A ND5D	ND5	12066-13512	1446	64	66
ND5C ND5D	ND5	12890-13512	622	64	66
ND5C ND5B	ND5	12890-14151	1261	64	64
ND6F ND6R	ND6	14050-14755	705	70	68
CytbF CytbR	Cytb	14621-16006	1385	68	68
DloopF DloopR	Dloop	15882-710	1389	67	68
T7 tag	taatacgactcactataggg				
T3 tag	attaaccctcactaaaggga				

T7 and T3 are tags required for Licor sequencing

2.2.2.4.1 Design of PCR Primers

PCR primers were obtained from Hermann GbR (Bio-Strategy Distribution Ltd). Primers were designed using the Primer3 design software. Additional primers were designed with T7 and T3 tags for fluorescent tag binding in preparation for Licor DNA sequencing (Table 2.1). Primer pairs were designed to have complementary Tm values and an approximate 50% GC content. Tm values were supplied by Primer 3.

2.2.2.4.2 Ethanol Precipitation of PCR Products

PCR product was purified by ethanol precipitation. One volume of 4 M ammonium acetate (NH_4OAc) and two volumes of isopropanol were added to 20 µl of PCR product. The solution was mixed by gentle inversion and incubated at room temperature for 20 minutes. The solution was centrifuged at 15,300 x *g* at room temperature for 20 minutes. The supernatant was removed and the pellet was washed with 70 % ethanol. The tube was centrifuged as before and the supernatant removed. Washing was repeated with 100% ethanol. The residual alcohol was removed with a finely drawn glass pipette and evaporated at ambient temperature before being re-suspended in 10 µl TE8. Purified products (1 µl) were confirmed by electrophoresis and visualized as above.

2.2.2.5 DNA Sequencing

Mitochondrial DNA sequencing was achieve by employing Licor fluorescent DNA sequencing, and ABI Big Dye® Terminator sequencing version 3.1.

2.2.2.5.1 DNA Sequencing with Licor 4000L DNA Sequencer

Thermosequenase reactions were performed using fluorescent primers (T7 forward, T3 reverse, Table 1) and a 1% mix of dideoxy termination nucleoside triphosphate bases (ddNTP's). A single reaction contained the following:

DNA + H_2O	5.75 µl
Reaction buffer	1.0 µl
Fluorescent primer	1.0 µl (1 picomol)
Thermosequenase	1.0 µl
Volume	8.75 µl

The mix was added to tubes containing 1.0 µl of each ddNTP, A, G, C, or T respectively. For this reaction A, G, C, T sequencing is performed separately. Forward and reverse priming reactions were also performed separately. The thermal sequencing reaction was performed using an Eppendorf Mastercycler® gradient as follows:

95˚C	5 min	
95˚C	30 seconds	29 x
50˚C	15 seconds	
70˚C	1 minute	
95˚C	30 seconds	9 x
72˚C	1 minute	
4˚C	SOAK	

Following thermal cycle amplification, 2.0 µl of stop buffer (bromophenol blue/ xylene cyanol, 1%, USB) was added. Samples were denatured at 95˚C for 5 minutes and chilled on ice immediately before electrophoresis and were loaded into a 6% polyacrylimide gel perforations made by a 0.25 mm 'shark tooth' comb. A tank containing 1 x TBE (Tris-borate/EDTA) was used as a buffer. Samples were run at

2250 V, 68.8 W, 30.6 mA for up to 12 hours. Image analysis was performed with Base ImageR software and sequences were assembled with Clustal X software v 1.7.

A 6% polyacrylimide gel was prepared at a cross-linking ratio of 19:1; 190 g acrylimide to 10 g N,N'-methylene-bis-acrylimide in a 40% (w/v) solution (Biorad). This consisted of 29.4 g urea, 7.0 ml 10 x Tris-borate/EDTA (TBE, pH 8), 5.6 ml long ranger polyacrylamide (19:1), made up to 70 ml with ddH_2O. The mixture was gently heated until urea had dissolved. Immediately before pouring, 440 µl 10% APS (ammonium persulphate, Roche) and 35 µl TEMED (N, N, N', N'-Tetramethyl-etheylenediamine, Sigma) was thoroughly mixed through the gel solution. The gel was immediately poured between two glass plates with a 0.25 mm spacer. This was allowed to polymerize at room temperature for two hours.

2.2.2.5.2 DNA sequencing with ABI Prism version 3.1

The majority of sequencing was performed using a BigDye®Terminator v 3.1 cycle sequencing kit. This technique utilises fluorescent dideoxy nucleoside triphosphates (dNTPs) which are inserted into the sequence as varying loci when the sequencing reaction is performed. The reaction conditions were:

96˚C	10 seconds	┐
50˚C	10 seconds	24 x
60˚C	1 minute	┘
15˚C	SOAK	

Samples are read at high voltage with an ABI 3100 genetic analyzer (Applied Biosciences). Sequences were visualized and aligned using the Bioedit software v 7.0.4.

2.2.3 Oxidative Phosphorylation

2.2.3.1 Isolation of Intact Mitochondria by Differential Centrifugation

Exponentially growing MCF-7 cells were trypsinized and collected by centrifugation at 86 x *g* for eight minutes at room temperature. The resulting pellet was washed with 1 x PBS (pH 7.4) and centrifuged as above. The cells were incubated for seven minutes at 4˚C with 400 µl 2 mg/ml digitonin, 600 µl of 0.1 M sucrose and 400 µl of 1x PBS. The cells were then homogenized with a hand held grinder and centrifuged at 2000 x *g* for five minutes at 4˚C to pellet the nucleus and unbroken cells (Sottocasa *et al*., 1967; Gaines and Attardi, 1984). The digitonin treatment was repeated to ensure complete lysis of the cells. The combined supernatant was layered on top of a two-step gradient consisting of 400 µl 0.3M sucrose, 400 µl 1 x PBS (pH 7.4), 400 µl of 1 mg/ml BSA (bovine serum albumin) fraction V (Boehringer, Germany) and 200 µl mineral oil chilled to 4˚C. The layered supernatant was centrifuged at 3000 x *g* for 40 minutes. After centrifugation, a dark brown pellet with a top white fluffy layer was observed. The upper supernatant was discarded. The lower mitochondrial rich fraction should be free of contaminating cytosolic lactic dehydrogenase. The final supernatant was transferred into 1.5 ml tubes and spun at 19,000 x *g* for 40 minutes. The pellet was re-suspended in 0.6M sucrose and 20 mM HEPES (Sottocasa *et al*., 1967; Diekert *et al*., 2001). The suspensions were stored at -80˚C (Tryoen-Toth *et al.,* 2003) for no longer than three weeks before assay. When required, the sample was thawed on ice and centrifuged at 19,000 x *g* for 40 minutes. The pellet was re-suspended in hypotonic media consisting of 25 mM KH_2PO_4 and 5 mM $MgCl_2$ and freeze-thawed (Ruiz-Pesini *et al,* 1998) five times. This was accompanied with 5 x 1

minute bursts of sonication on a soniclear bath sonicator. The chilled mitochondrial homogenate was used for enzyme analysis.

2.2.3.2 Protein Determination

Protein content of the mitochondrial fractions was determined by the method of Bradford (Bradford, 1976). This was achieved using the BioRad protein assay (BioRad protocols) with a BSA standard. Briefly, assay reagent was diluted with four volumes of ddH_2O and mixed thoroughly. To 980 µl dilute reagent, 20µl of protein sample was added, mixed, and the sample read at 595 nm. A standard curve was constructed using BSA at concentrations 50, 75, 100, 125, 150, 250, 500, 1000, 1500 and 2000 µg/ml. The protein content of the unknown mitochondrial fraction was determined from this standard curve.

2.2.3.3 Analysis of Oxidative Phosphorylation Enzymes

Kinetic analysis of all the complexes of OXPHOS was performed in triplicate in 1.0 ml glass cuvettes on a Shimandzu UV-160 1PC UV visible spectrophotometer at room temperature. Samples were kept at -80˚C in storage or 4˚C immediately before assay

2.2.3.3.1 Citrate Synthase

Citrate syntase activity was monitored spectrophotometrically by the formation of the mercaptide ion upon cleavage of DTNB (5,5'-dithiobis-(2-nitrobenzoate)) (Srere, 1960). This was indicative of mitochondrial copy number per cell (Ruiz-Pesini *et al*.,

1998). Reagents were prepared as follows. DNTB, 1 mM, was prepared by dissolving 3.9 mg of DNTB (free acid) in 10.0 ml of 1 M Tris-HCl, pH 8.1. Acetyl-CoA, 10 mM, was prepared by dissolving 10 mg of Acetyl-CoA in ddH_2O. Oxaloacetate, 10 mM, was prepared by dissolving 1.32 mg oxaloacetate in 1 ml of Tris-HCl buffer (freshly prepared). The assay reagents were DTNB, 0.1 ml; acetyl CoA, 0.03 ml; 10 µg enzyme homogenate, 0.77 ml ddH_2O (Srere, 1960). Absorption was followed at 412 nm for 3 minutes to measure possible acetyl-CoA deacylase activity. The citrate synthase reaction was started by the addition of 0.05 ml oxaloacetate. Linear rates were obtained for at least 3 minutes (Srere, 1960).

2.2.3.3.2 Complex I

Complex I activity was determined as the decrease in absorbance due to the oxidation of NADH (nicotinamide adenine dinucleotide) at 340 nm with 425 nm as the reference wavelength (ε= 6.81 $mM^{-1}.cm^{-1}$). Mitochondria were added to buffer containing 25 mM KH_2PO_4 (pH 7.2), 5 mM $MgCl_2$, 2 mM KCN, 2.5 mg/ml BSA fraction V, 0.13 mM NADH, and 65 µM ubiquinone. The NADH-ubiquinone oxidoreductase activity was measured for an additional three minutes. Complex I activity is measured as rotenone sensitive NADH-ubiquinone oxidoreductase activity in oxidative phosphorylation (Birch-Machin *et al.*, 1994). The absorption of this complex is detected at wavelengths require to assay complex III, and is blocked by rotenone.

2.2.3.3.3 Complex II

Complex II activity was determined as the reduction of 2,6-dichlorophenolindophenol at 600 nm (ε= 19.1 mM^{-1} . cm^{-1}). Mitochondria were pre-incubated in buffer containing 25 mM KH_2PO_4 (pH 7.2) and 5 mM $MgCl_2$ at 30˚C for 10 minutes. In addition, 2 µg/ml antimycin A, 2 µg/ml rotenone and 50 µM dichlorophenolindophenol were added and the baseline rate recorded for 3 minutes. The reaction was started with the addition of ubiquinone 65 µM. The enzyme-catalysed reduction on dichlorophenolindophenol was measured for 5 minutes as modified from Birch-Machin *et al.* (1994). Antimycin A was employed to inhibit complex III activity, whilst assaying for complex II.

2.2.3.3.4 Complex III

Complex III activity was determined as the reduction of cytochrome c (III) to cytochrome c (II). Activity was measured at 550 nm with 580 nm as the reference wavelength (ε= 19 mM^{-1} .cm^{-1}). The reaction buffer consisted of 25 mM KH_2PO_4 (pH 7.2), 5 mM $MgCl_2$, 5.5 mg/ml BSA, 2 µg/ml rotenone, and 15 µM cytochrome c. The non-enzymatic rate was measured with the addition of ubiquinol (35 µM) for one minute. The increase in absorbance was measured upon the addition of mitochondria. Ubiquinol was reduced with excess sodium borohydride and the ubiquinol isolated by filtration into ethanol acidified to pH 2 and stored at -80˚C until required as modified from Birch-Machin *et al.* (1994).

2.2.3.3.5 Complex IV

Complex IV activity was determined as the oxidation of cytochrome c (II) to cytochrome c (III). Activity was measured at 550 nm with 580 nm as the reference wavelength (ε=19.1 mM^{-1} .cm^{-1}). The reaction buffer contained 20 mM KH_2PO_4 (pH 7.0) and 15 µM cytochrome c (II). Mitochondria were added and the initial rate was measured for one minute. Potassium ferricyanide was added and absorbance measured over 5 minutes or until all the cytochrome c (II) was converted to cytochrome c (III). Cytochrome c (II) was prepared by the addition of ascorbate to cytochrome c (III) (Sigma). Separation of cytochrome c (II) was achieved by Sephadex G25 chromatography. Cytochrome c (II) aliquots were stored at -80˚C and the protein concentration determined by the method of Bradford immediately before enzymatic assays were performed (Bradford, 1976; Birch-Machin *et al*., 1994)

2.2.4 Free Radical Generation

2.2.4.1 Treatment of MCF-7 cells with AAPH

MCF-7 passage 4 cells were grown to 95% confluence in standard growth medium. The culture medium was aspirated and the monolayer treated with trypsin at 37˚C until cells detached from the surface of the flask (Section 2.2.1.8). The trypsin was inhibited with one volume of growth medium and a cell count taken. Six aliquots (300 µl each) of cell suspension were seeded into a 6-well plate (16 cm^2) at 6.7 x 10^4 cells/well. Cells were grown to 90% confluence. Growth medium was aspirated and the monolayer incubated with 20 mM AAPH (2,2′-azobis(2-amido-

propane)dihydrochloride) in EBSS (Earle's balanced salt solution). The monolayer was treated for one hour after which the AAPH/EBSS solution was aspirated. The culture was thoroughly washed three times with 1 x PBS (pH 7.4). A single well of culture was treated with trypsin/EDTA as above and a cell count taken, estimating 7.4 x 10^4 cells/ml. A control was cultured without AAPH, the cell count was 1.3 x 10^5 cells/ml. Both AAPH treated and control cells were seeded into 12 well plates (3.5 cm^2) at 10,510 and 10,400 cells/well respectively. The population growth study was performed as previously described. Cells for the WST-1 assay were seeded at 78 (control) and 80 (AAPH treated) cells/well (refer to Section 2.2.1.9).

2.2.4.2 Treatment of MCF-7 Cells with DPPH

MCF-7 passage 6 cells were grown to 90% confluence. Culture medium was aspirated and 5.0 ml of EBSS containing 250 nM DPPH (1,1-Diphenyl-2-picryl-hydrazyl) was added. Isopropanol was used as a carrier of DPPH and made up to the final volume with EBSS. The culture was incubated for 1 hour and washed three times with EBSS. The culture was then treated with trypsin and growth media as above and the resulting cell count was 1.5 x 10^5 cells/ml. DPPH treated cells were seeded into 12 well plates at 10,300 cells/well. Cells for the WST-1 assay were seeded at 70 cells/well in 96 well plates 0.32 cm^2.

2.2.4.3 Treatment of Intact Mitochondria with AAPH

Intact mitochondria were isolated as described in Section 2.2.3.1. Ten µl of mitochondrial suspension was placed in a 1.5 ml tube. AAPH (20 mM) was added in

1 x PBS buffer to a final volume of 20 µl. The tube was mixed gently by inversion and incubated at 37˚C for 1 hour. DNA was isolated using the phenol/chloroform method (Section 2.2.2.1) and the mitochondrial genes ND1, COI, Cytb and D-loop were amplified. The PCR product was visualized (Section 2.2.2.2) and precipitated (Section 2.2.2.6) and sequenced by ABI fluorescent sequencing (Section 2.2.2.8)

2.2.4.4 Treatment of Intact Mitochondria with DPPH

Treatment with DPPH was performed as described for AAPH in Section 2.2.4.3. DPPH was dissolved in 5 µl of isopropanol and made up to the final volume with 1 x PBS. This gave a final concentration of 250 nm DPPH.

2.2.4.5 AAPH Treatment of DNA

MCF-7 DNA (1.38 µg) was incubated individually with 15 µl of AAPH at concentrations 20 mM, 50 mM and 100 mM in 1 x PBS. Incubations were performed at 37˚C for one and three hours. The treated DNA was analyzed by electrophoresis (Section 2.2.2.2). Ethidium bromide was used to stain the gel and DNA visualized under UV light.

2.2.4.6 DPPH Treatment of DNA

MCF-7 DNA (2.75 µg) was treated individually with 100 nM, 250 nM and 500 nM of DPPH. Isopropanol (5 µl) was used as a carrier and made up to the final volume in 1

x PBS. The solution was incubated at 37˚C for one hour. The treated DNA was analysed as described in Section 2.2.4.5

2.2.4.7 Continuous Free Radical Assault

MCF-7 passage 7 cells were grown in a T-25 flask to 90 % confluence. The culture was treated with trypsin and a cell count estimated to be 4.0 x 10^5 cells/ml. Six twelve well plates were seeded at 10,474 cells/well. To three well plates, AAPH, 2 mM, 4 mM, and DPPH, 25 nM were added. To the remaining, 1 mM AAPH, 25 nM DPPH and a control incubation were performed. Plates were incubated at 37˚C/5% CO_2. DPPH was dissolved in 0.5 µl isopropanol, mixed with 2 ml of growth medium and allowed to evaporate from the culture before the lid was closed. The control was performed alongside, and consisted of the addition of 0.5 µl isopropanol alone. Cell counts were performed as previously described (Section 2.2.1.9). Treatment with low level free radical generator lasted for 72 hours, after which the cultures were washed thoroughly with 1 x PBS. Cultures were established from treated cells and grown to confluence (average 5 days) in T-75 flasks. DNA was isolated as described previously (Section 2.2.2.1) from these cultures for mutation analysis.

2.2.4.8 Extended MCF-7 Cell Growth

MCF-7 cells (passage 7) were grown to confluence and subcultured for a period of 60 days. This allowed an approximate 53 population doubling times to take place. This is

equivalent to cell culture generation number (Freshney, 2000). Care was taken to grow cultures to 85-90% confluence before subculture throughout. DNA was isolated from this culture and quantified (Section 2.2.2.1). Mitochondrial genes ND1, CO I, D-loop and Cyt b were amplified and sequenced as previously described (Section 2.2.2.4) for mutation analysis.

2.2.4.9 Genomic DNA Isolation and PCR

DNA was isolated from all free radical generator treated cells and extended MCF-7 growth cells by the aforementioned phenol/chloroform method as (Section 2.2.2.1). PCR amplification and ABI sequencing (Sections 2.2.2.4 and 2.2.2.8) were applied to the mitochondrial genes, ND1, Cytb, D-loop and COI. These genes form over one third of the mitochondrial genome.

CHAPTER 3

RESULTS

3.1 Cell Culture

3.1.1 Isolation of Single Cell Clones

Eleven single clones (B5, B12, C6, C12, D4, D9, E1, E8, F2, F9, G8) were obtained. From these, eight single cell clone cultures were established. These excluded clones C6, F2 and F9. The yield of single cell clones was not as high as anticipated due to some cell clumping during isolation. Figure 3.1 shows isolated single cell clones (A and C), and a culture with two cells (B) that was discarded during single clone isolation.

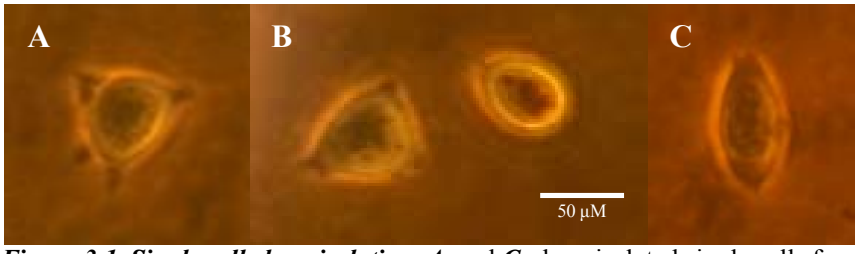

Figure 3.1. Single cell clone isolation, A, and ***C***, show isolated single cells for further culturing, ***B***, shows a discarded culture that contained two cells

The isolated single cell clones began to proliferate after a minimum of 10 days, with some taking as long as 15 days.

3.1.2 Growth Morphology

Growth morphology and characteristics were carefully studied. Clone C12 appeared to grow in very tight clusters (Figure 3.2 A) even with adequate room to spread out. Cultures of this particular clone were seeded in a uniform scatter of cells, but distinct clusters began to emerge within two days, favouring cluster growth habit. The cluster

cells were also smaller. This characteristic was not observed in the remaining clones. Culture B5 (Figure 3.2 B) grew with notable contact inhibition. This characteristic was not observed in other cultures. Cultures G8 (Figure 3.2 C) and E1 (Figure 3.2 D) grew in a similar fashion to the MCF-7 original culture (Figure 3.2 E).

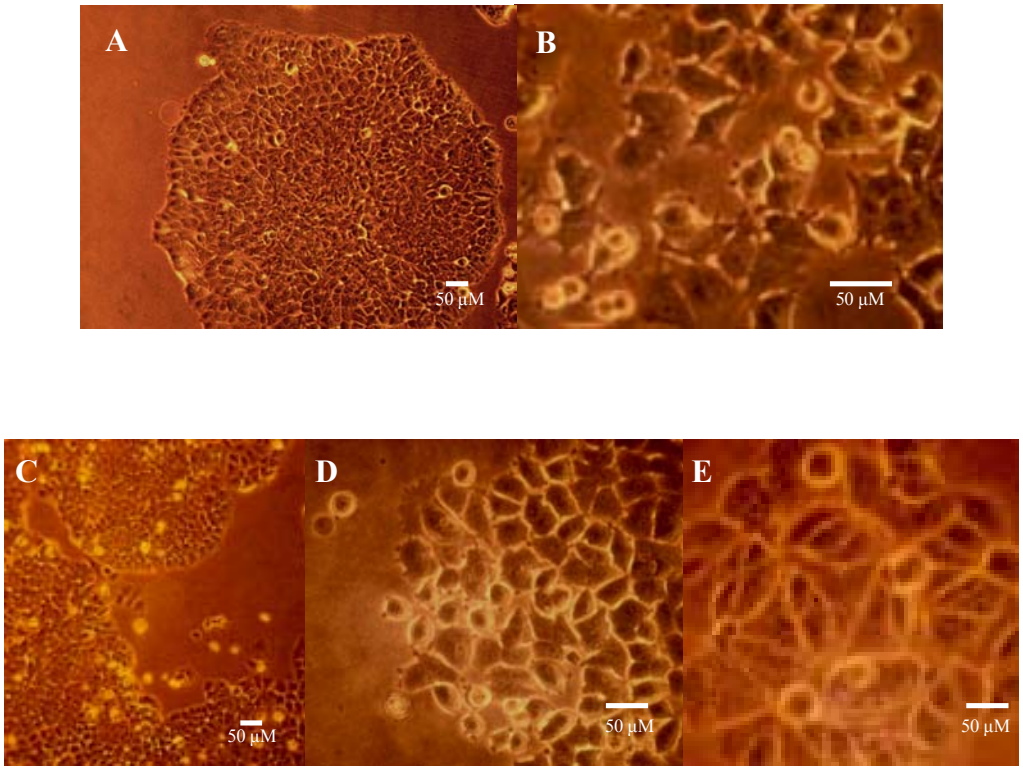

Figure 3.2. **Cultures of established single cell clones.** ***A***, C12 with distinct cluster formation; ***B***, B5 with notable contact inhibition; ***C***, G8; ***D***, E1; ***E***, MCF-7 culture from which the single clones were derived.

3.1.3 Isolation of Non-proliferate Clones

Cell clones C6, F2 and F9 did not proliferate within the 96 well plates after 45 days and were discarded. These clones proliferated to approximately 20 cells each clone, but did not grow further. DNA was obtained from clone C6, but was not successfully amplified. DNA was unable to be isolated from clones F2 and F9. The F2 and F9

culture grew to approximately 20-30 cells. The cell morphology for these clones appeared to be similar to E1 and G8, no cluster formation or distinct contact inhibition was observed.

3.1.4 Cell Proliferation with Trypan Blue

Preliminary growth studies on all viable single cell clone populations were performed. The cell cultures were in the second passage following isolation. From these, six single cell clones (B5, C12, D4, D9, E1 and G8) were selected for more detailed study. Figures 3.3 to 3.5 show the growth patterns of these clones using trypan blue cell counting. Figure 3 depicts growth curves of the clones D4 and D9 against the MCF-7 stock culture. These appear to grow in a similar fashion. Figure 3.4 depicts clones E1 and G8. Clone G8 displayed an early plateau phase, three factors below MCF-7. Clone E1 show a similar growth curve to that of the MCF-7 stock culture. Clones B5 and C12 (Figure 3.5) plateau at an earlier stage (factor of 10^2) than MCF-7. The average R^2 values for the trypan blue method of cell proliferation was 0.9735. The lag phase for B5, G8 and MCF-7 is approximately 24 hours. The lag phase for the remaining cultures was much shorter, or non-existent. All cultures were seeded at the same cell density, deviating less than 100 cells/well (Section 2.2.1.9).

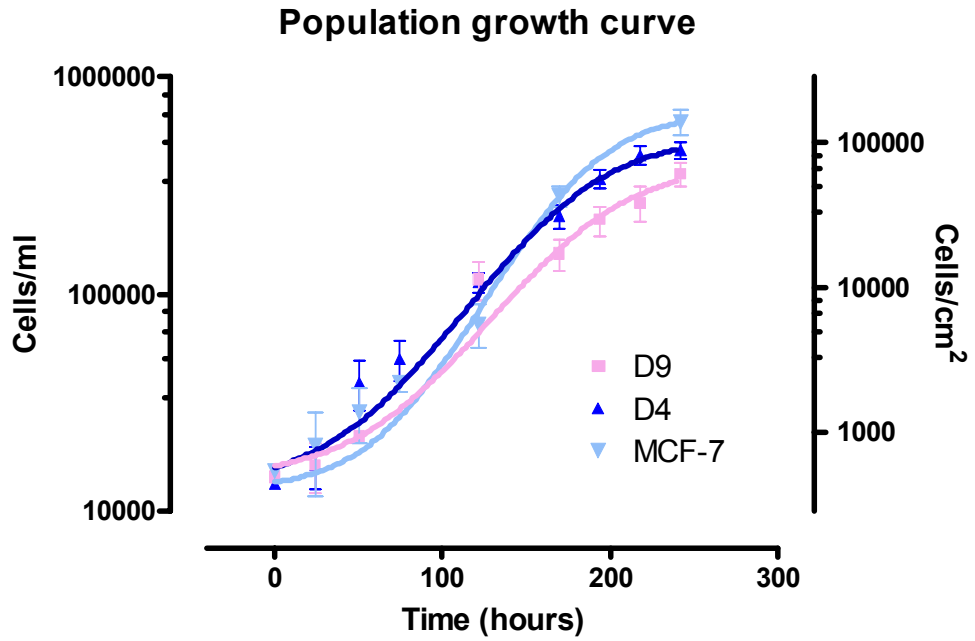

Figure 3.3. Population growth curve of single cell clones D9 ■ (R^2=0.9665) and D4▲ (R^2=0.9953), with the standard, MCF-7▼ (R^2=0.9995). Data shown as mean ± SE

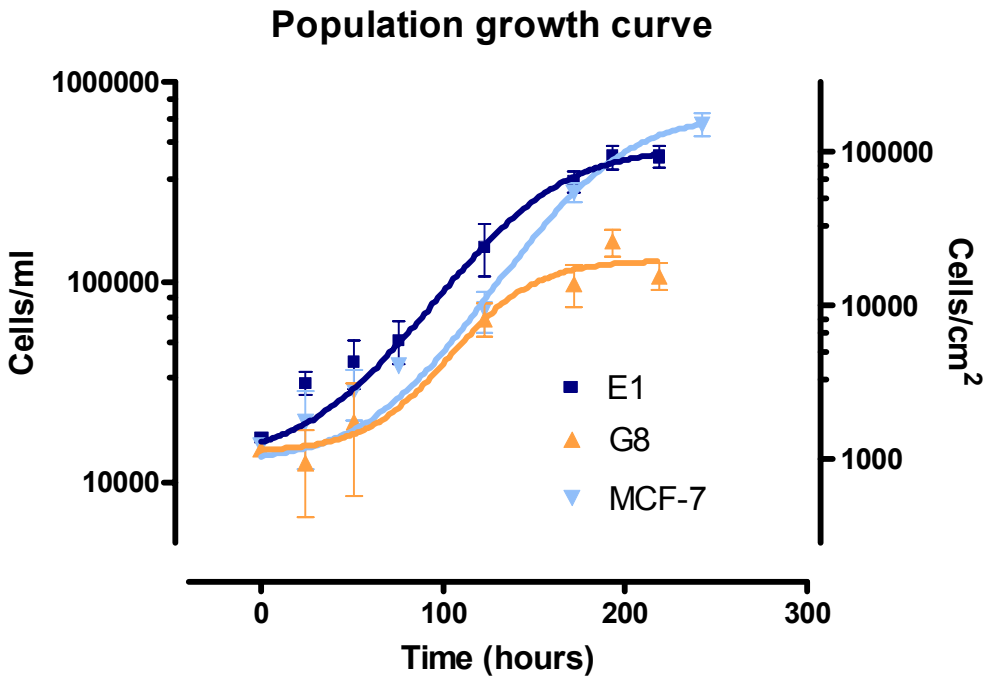

Figure 3.4. Population growth curve of clones E1 ■ (R^2=0.9925) and G8▲ (R^2=0.8957), with the standard, MCF-7 ▼. Data shown as mean ± SE

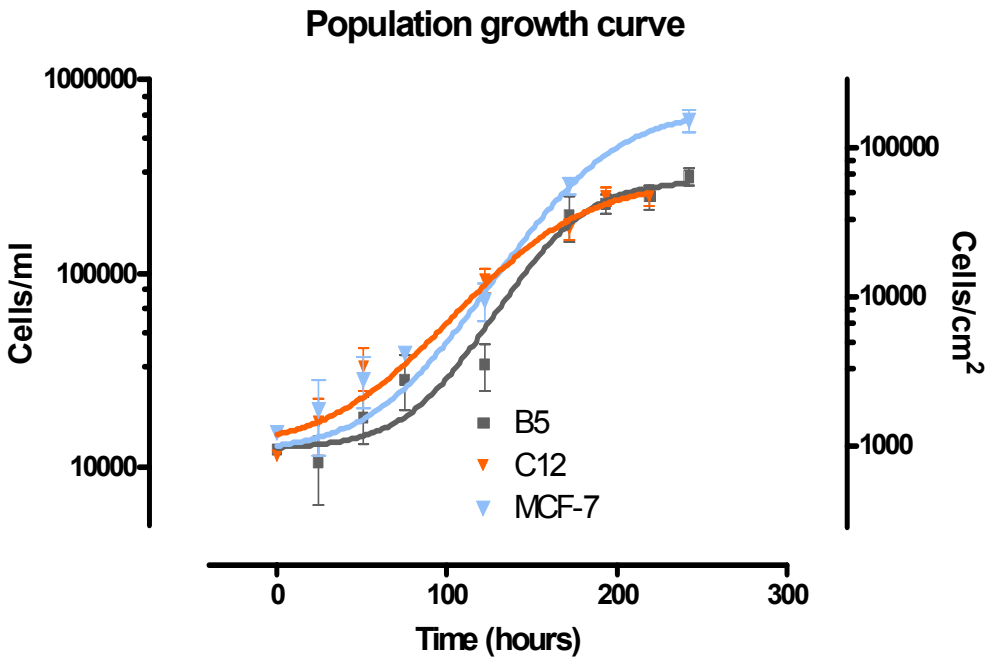

Figure 3.5. Population growth curve of clones B5 ■ (R^2=0.9825) and C12 ▼(R^2=0.9824), with the standard, MCF-7 ▼ . Data shown as mean ± SE

3.1.5 Cell Proliferation with WST-1

Figures 3.6 shows the colour change during the WST-1 assay. This is due to a cleavage of tetrazolium salt, producing a formazan product. GM was aspirated and replaced by the phenol free medium (pale yellow). The WST-1 reagent was a pale red colour, that became progressively more orange as the formazan adduct was produced. A UV visible microplate reader (Bio-Tek instruments) monitored this colorimetric shift.

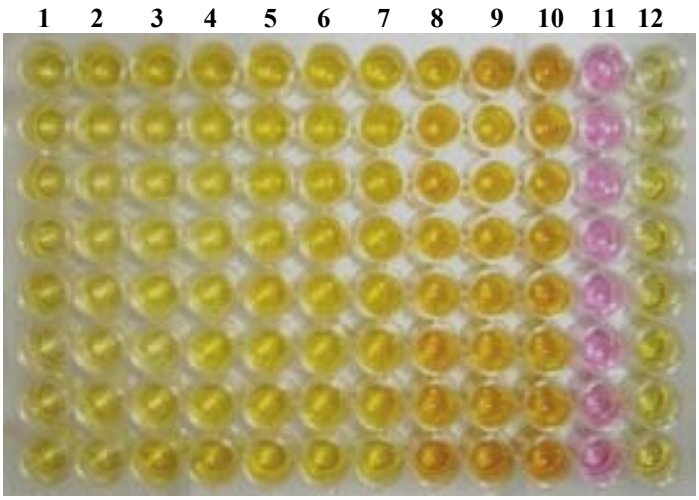

Figure 3.6. **The WST-1 assay.** ***Lane 1,*** wells seeded at 75 cells/well. Measurement taken at 24 hours; ***lane 2,*** 40 hours; ***lane 3,*** 98 hours; ***lane 4,*** 119 hours; ***lane 5,*** 155 hours; ***lane 6,*** 203 hours; ***lane 7,*** 301 hours; ***lane 8,*** 350 hours; ***lane 9,*** 398 hours; ***lane 10,*** 449 hours; ***lane 11,*** cells growing, not yet assayed; ***lane 12,*** control well for each measurement.

Figure 3.7 and 3.8 display growth curves derived from the absorbance values for the WST-1 assay. Cell number was estimated from a calibration curve of known cell concentration. Clone B5 displays the fastest cell population growth, and C12 the slowest. This is consistent with the growth curves constructed from the trypan blue cell estimates.

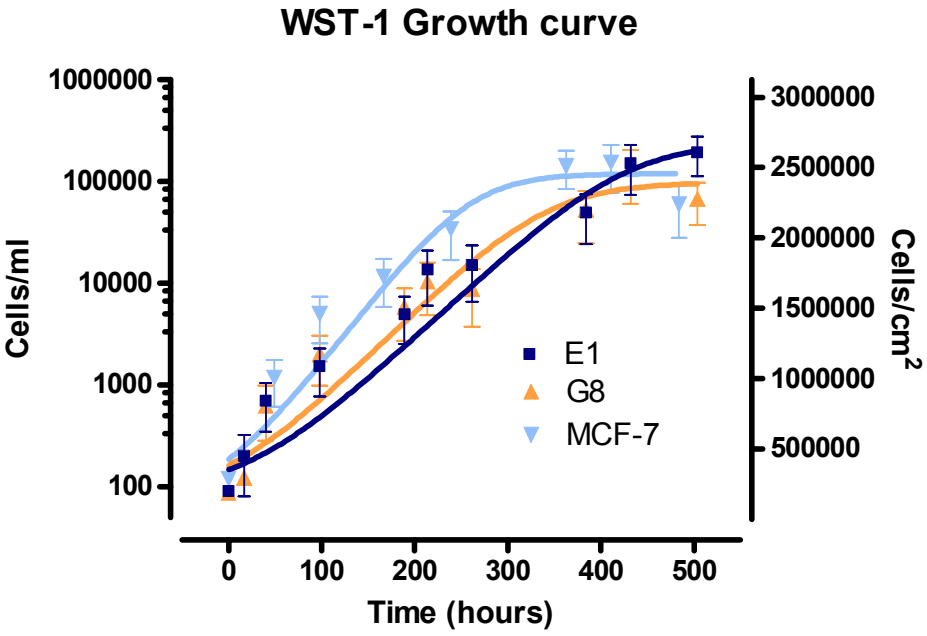

Figure 3.7. **WST-1 growth curve of clones.** E1 ■ (R^2=0.9706) and G8 ▲ (R^2=0.8058), with the standard, MCF-7 ▼ (R^2=0.8760). Data shown as mean ± SE

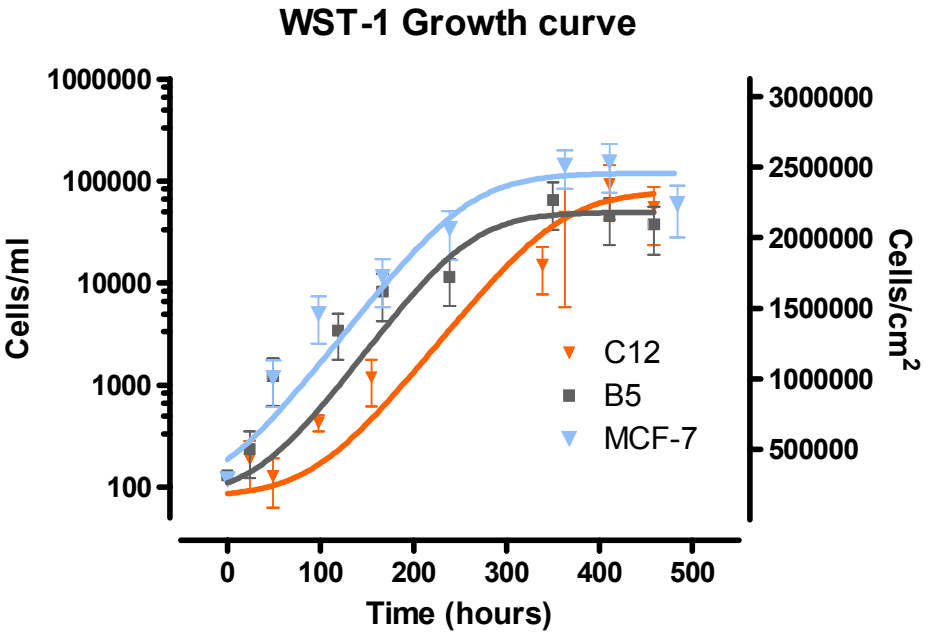

Figure 3.8. **WST-1 growth curve of clones.** C12 ▼ (R^2=0.8448) and B5■ (R^2=0.8705), with the standard, MCF-7 ▼. Data shown as mean ± SE

3.1.6 Comparison of Cell Proliferation Estimate Techniques

Table 3.1 and Figure 3.9 summarise the growth rates of different cell clones. B5 appears to be the fastest growing clone with a population doubling time (PDT) of 25.50 (trypan blue) and 25.75 (WST-1). This is followed by MCF-7 (27.00, 27.08), DPPH treated (27.00, 27.50), AAPH treated (28.00, 29.00), E1 (28.79, 32.41), G8 (31.76, 30.19), D4 (37.5, -), D9 (37.5, -) and the slowest, C12 (41.00, 35.00) (Table 3.1). Agreements between the two techniques for estimating PDT tend to decrease as PDT increases.

Table 3.1. **Trypan blue and WST-1 estimates of PDT (hours).**

Cell culture	Trypan Blue	WST-1
B5	25.5	25.75
MCF-7 (standard)	27.00	27.08
DPPH treated	27.00	27.50
AAPH treated	28.00	29.00
E1	28.79	32.41
G8	31.76	30.19
D4	37.50	-
D9	37.50	-
C12	41.00	35.00

MCF-7 estimate from ATCC in 29.00 hours (method unknown)

Figure 3.9 represents the relative population doubling times comparing trypan blue and WST-1 methods.

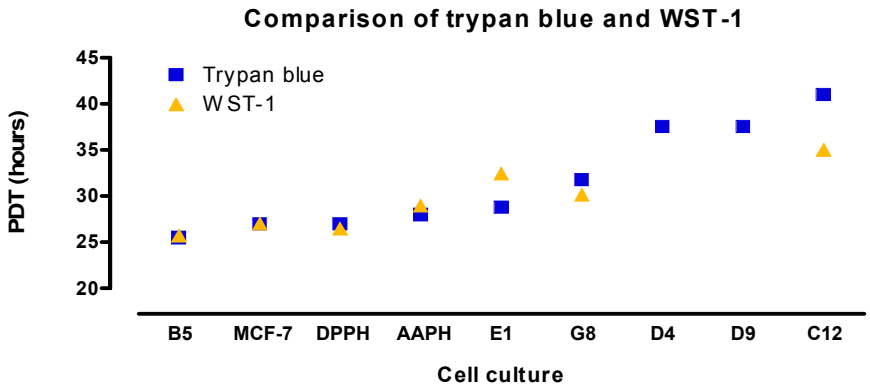

Figure 3.9. **Comparison of trypan blue and WST-1**. Comparative population doubling times of single cell clones and the standard MCF-7 using trypan blue cell viability counting and the WST-1 biochemical assay

3.2 DNA Analysis

3.2.1 DNA Isolation and Quantification

Figure 3.10 displays the quality of isolated DNA from the MCF-7 stock culture and derived single cell clones. Some protein contamination was present (Figure 3.10, lane 5); however, this did not interfere with amplification of DNA by PCR.

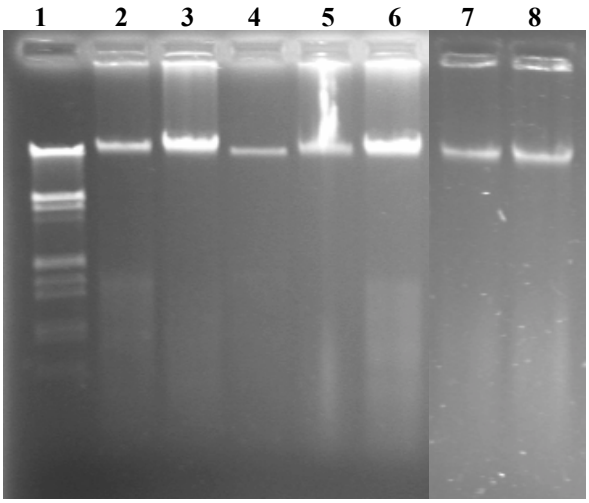

Figure 3.10. **Isolated cell culture DNA.** ***Lane 1,*** molecular marker λ*HindIII*/*EcoRI*; ***lane 2,*** MCF-7; ***lane 3,*** G8; ***lane 4,*** C12; ***lane 5,*** B5; ***lane 6,*** E1; ***lane 7 and 8***, Extracted MCF-7 DNA from cells treated with AAPH (20 mM).

Table 3.2 displays the concentration of isolated DNA. Purity was determined by the ratio between the absorbance at 260 nm and 280 nm. An increase above 1.8 indicates contamination by phenol, below is indicative of protein contamination.

Table 3.2. **Genomic DNA quantification.**

DNA	A_{260}	A_{280}	$A_{260/280}$	Quantity (μg/μl)
MCF-7	0.025	0.013	1.92	0.125
E1	0.130	0.077	1.69	0.650
G8	0.021	0.011	1.91	0.105
B5	0.093	0.049	1.90	0.465
C12	0.025	0.015	1.67	0.125
AAPH	0.055	0.029	1.90	0.275

Note: AAPH denotes DNA derived from AAPH treated MCF-7 cells

3.2.2 PCR of the Mitochondrial Genome

PCR was performed on all genes of the mitochondrial genome, in both forward and reverse direction. All supplementing PCR electrophoresis gels can be viewed in Appendix C (PCR and sequencing). Figures 3.11, 3.13 and 3.15 show gels of PCR amplicons and the corresponding ABI chromatograms are located directly beneath them. These sequences show varying levels of mitochondrial DNA heteroplasmy.

3.2.3 ABI and Licor Sequencing

The establishment of the MCF-7 baseling was achieved by employing Licor and ABI sequencing. The remaining sequencing was largely achieved with the ABI system.

3.2.3.1 Establishing the MCF-7 Baseline

The MCF-7 mitochondrial genome was sequenced, and determined to have 26 base changes in contrast to the NC_001078 homo-sapiens genome (NCBI, April, 2005). Table 3.3 lists these changes and their respective amino acid changes. This baseline was used to determine changes between the MCF-7 stock mtDNA and single cell clones.

Table 3.3. **Mitochondrial mutation baseline for MCF-7 mtDNA Sequence NC-001078 (April 2005).**

Gene	Nucleotide	Mutation	Amino acid change	ABI Prism	Licor
16S	2354	C→T	Q→L	12 x F	-
16S	2485	C→T	no change	12 x F 12 x R	-
$tRNA^{TYR}$	5970	A deletion	Stop→Y	7 x F	-
COI	6777	T→C	no change	7 x F	4 x F
ATPase6	8657	A→C	no change	11 x F	3 x R
ATPase6	8702	G→A	no change	11 x F	4 x F
ATPase6	8887	G→A	R→K	11 x F	-
COIII	9378	G→A	W→STOP	9 x F	4 x F
COIII	9541	C→T	no change	9 x F	4 x F
ND3	10399	G→A	A→T	4 x F	-
ND4	11018	C→T	A→V	6 x F	-
ND5	12706	T→C	no change	6 x F	-
ND5	12851	G→A	V→I	6 x F 6 x R	-
ND5	13261	T→C	no change	6 x F 6 x R	-
ND6	14581	G→A	A→T	8 x F	1 x Forward 2 x Reverse

Table 3.3 continued.

Gene	Nucleotide	Mutation	Amino acid change	ABI Prism	Licor
Cytb	14767	T→C	I→T	10 x F	-
Cytb	14906	A→G	I→M	10 x F	-
$tRNA^{PRO}$	15933	C→T	no change	11 x F	-
D-loop	16149	C→T	H→T	11 x F	-
D-loop	16173	C→T	no change	11 x F	-
D-loop	16184	C→A	N→K	11 x F	-
D-loop	16185	C→del	no change	11 x F	-
D-loop	16191	C→T	no change	11 x F	-
D-loop	16322	T→C	no change	11 x F	-
D-loop	73	G→A	V→MET	11 x F	-
D-loop	410	A→T	STOP→L	11 x F	-

F= Forward, R= Reverse

3.3.2.2 Heteroplasmy Between Single Cell Clones

Genes ND6 and ATPase (Figures 3.12 and 3.14) were sequenced with both ABI Big dye terminator and Licor fluorescent sequencing. The Cytb gene (Figures 3.16 to 3.19) was sequenced with ABI alone. All sequencing was performed in the forward and reverse direction. A summary of replicates for these sequences can be found in Table 3.3

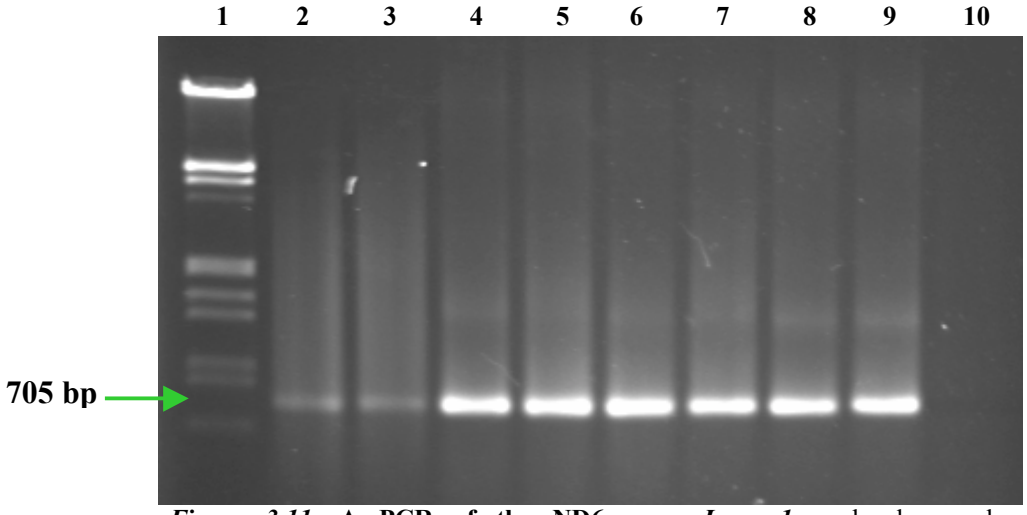

Figure 3.11. **A PCR of the ND6 gene.** ***Lane 1,*** molecular marker λ*HindIII*/*EcoRI*, ***lane 2 and 3,*** C12; ***lane 4 and 5,*** MCF-7; ***lane 6 and 7***, E1; ***lane 8 and 9,*** B5; ***lane 10***, negative control.

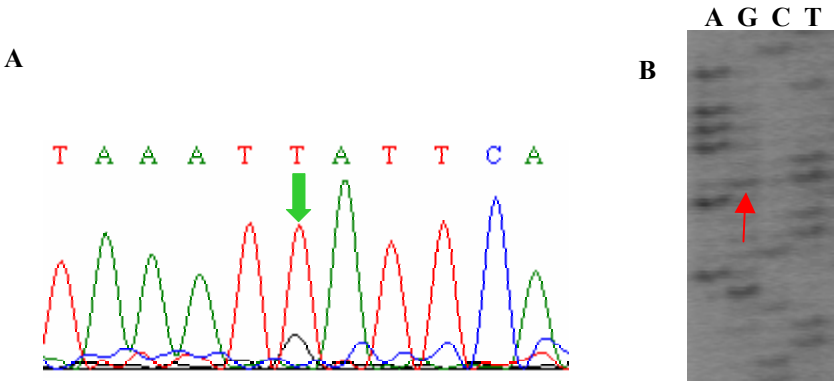

Figure 3.12. **C12 ABI chromatogram of the ND6 gene from the forward direction,** ***A.*** ABI sequence showing heteroplasmy; ***B.*** Licor sequence of the MCF-7 stock. The arrow indicates heteroplasmy between the T and G nucleotide bases (bp 14300).

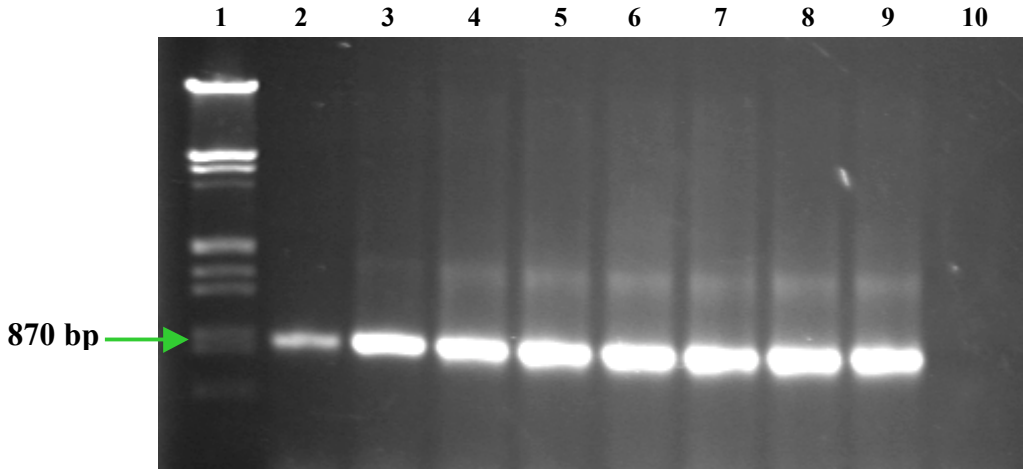

Figure 3.13. **A PCR product of the ATPase gene.** ***Lane 1,*** molecular marker λ*HindIII*/*EcoRI*, ***lane 2 and 3,*** C12; ***lane 4 and 5,*** MCF-7; ***lane 6 and 7,*** E1; ***lane 8 and 9***, B5; ***lane 10,*** negative control.

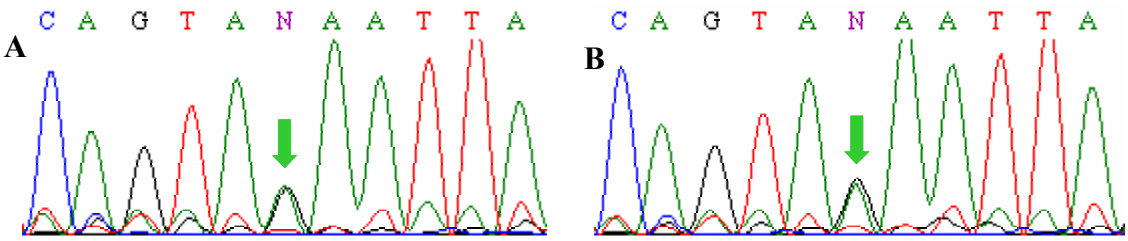

Figure 3.14. **ABI chromatographs of a portion of the ATPase6 gene displaying heteroplasmy** (bp 9119) ***A***, B5; ***B***, C12. The arrow indicates heteroplasmy between the C and T nucleotide bases (reverse sequence shown).

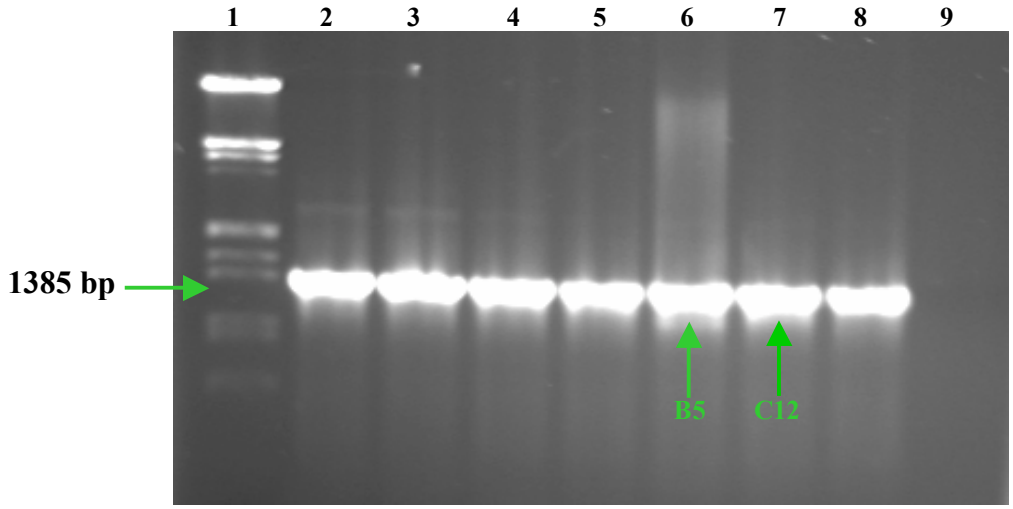

Figure 3.15. **A PCR product of the Cytb gene.** ***Lane 1,*** molecular marker λ*HindIII*/*EcoR*I, ***lane 2 and 3***, MCF-7; ***lane 4 and 5,*** G8; ***lane 6,*** B5; ***lane 7,*** C12; ***lane 8,*** E1; ***lane 9,*** negative control . The arrows indicate the PCR product for clones B5 and C12 harbouring different DNA heteroplasmy.

Figures 3.16 to 3.18 (below) show ABI chromatograms of the Cytb gene (reverse sequence) for clone B5 (Figure 3.16), MCF-7 original culture (Figure 3.17) and clone C12 (Figure 3.18). These figures demonstrate a level of heteroplasmy that is present

in clone B5, minimally present in the original MCF-7, but absent in clone C12. Clone E1 exhibited comparable heteroplasmy to the stock MCF-7. Clone G8 displayed mimimal heteroplasmy (Appendix C, PCR and sequencing). The level of heteroplasmy is estimated to be 15-20% (Clone B5, Figure 3.16) from studies performed in our laboratory (Angie Sin, personal communication).

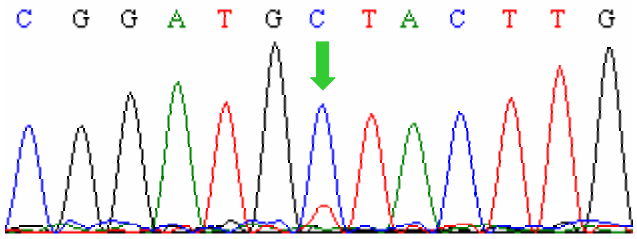

Figure 3.16. **ABI Chromatograph of a portion of the Cytb gene.** (bp 15807) The arrow indicates the B5 clone DNA heteroplasmy between the G and A bases (reverse sequence shown).

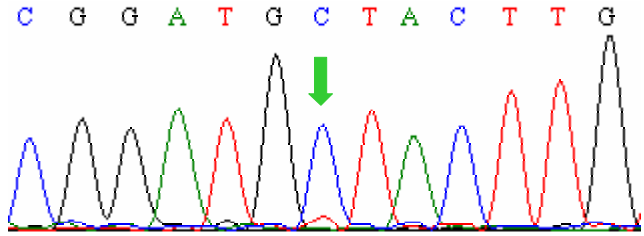

Figure 3.17. **ABI Chromatograph of a portion of the Cytb gene.** MCF-7 Cytb DNA displaying a degree of heteroplasmy (reverse sequence shown).

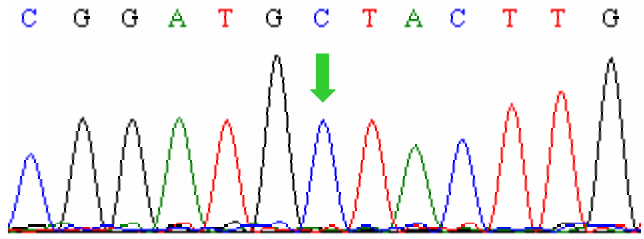

Figure 3.18. **ABI Chromatograph of a portion of the Cytb gene.** C12 clone DNA showing a lack of heteroplasmy (reverse sequence shown).

Table 3.4 summarises the relationship between the degree of mitochondrial DNA heteroplasmy and the samples harbouring the change. All clones and the MCF-7 stock present DNA heteroplasmy for the ATPase and ND6 genes. The Cytb gene

heteroplasmy is only present in the MCF-7 stock and clones B5 and E1. It is absent in clone G8 and C12.

Table 3.4. **Summary of Mitochondrial Heteroplasmy.**

Nucleotide	Gene	Degree of Heteroplasmy	Samples presenting	Amino acid change
9119	ATPase6	50%	MCF-7, B5 C12, E1, G8	no change
14300	ND6	20%	MCF-7, B5 C12, E1, G8	Y→STOP
15807	Cytb	15-20%	MCF-7, B5, E1	A→T

Confirmation for the sequencing results in Table 3.4, including supporting sequences can be found in Appendix C (PCR and sequencing) including a full list of sequencing replicas.

3.3 Oxidative Phosphorylation

3.3.1 Isolation of Intact Mitochondria

Table 3.5 shows the yield of protein from extracted mitochondria in relation to the number of cells used for isolation. This was determined after sonication and freeze-thawing in which the mitochondrial proteins of oxidative phosphorylation were accessible to quantification and enzyme assay. Clone E1 yielded a much higher amount of protein (683 μg/ml) for the number of cells used for isolation (1.1×10^6). Mitochondria for all samples were isolated concurrently.

Table 3.5. **Protein yield from mitochondrial extraction relative to cell number.**

Cell clone	Quantity of cells for isolation	Protein yield µg/ml
MCF-7	1.6×10^6	170
E1	1.1×10^6	683
G8	1.0×10^6	175
B5	6.9×10^5	317
C12	1.6×10^6	216

Enzyme assays were performed for complexes I-IV of the respiratory chain involved in the process of oxidative phosphorylation. Figure 3.19 shows the calibration curve from which the protein contents of mitochondrial extract were determined after intact mitochondria isolation.

3.3.2 Bovine Serum Albumin Standard Curve

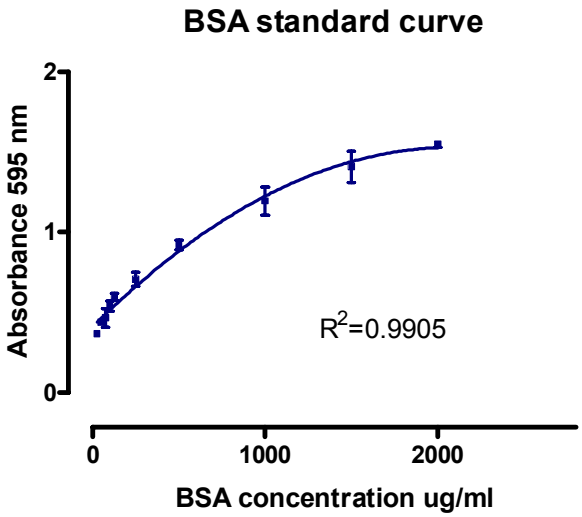

Figure 3.19. **BSA (fraction V) standard curve.** various concentrations were measure at 595 nm. The R^2 value indicates a strong curve fit

3.3.3 Assay for Citrate Synthase

The first step for enzyme assay was a measurement of the relative levels of citrate synthase (CS) in the mitochondrial extracts. This is indicative of mitochondrial copy

number (Srere, 1960) and hence important in standardizing clone fractions by the amount of target enzyme present. The CS assay utilized the reduction of DTNB to mercaptide ion (Figure 3.20) by an increase in absorbance in µmol/sec/mg protein (Table 3.6).

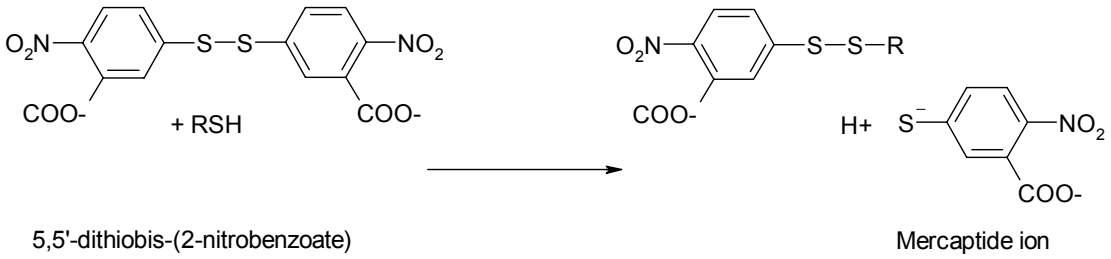

Figure 3.20. **Citrate synthase assay.** The citrate synthase assay was performed by the reduction of 5,5'-dithiobis-(2-nitrobenzoate) (DTNB) to the mecaptide ion product, resulting in an absorbance increase at 412 nm

Table 3.6 involved the addition of equal amount of protein (as determined from the BSA standard curve) for enzyme assay. From this, the specific activity of citrate synthase was determined in µmol/sec/mg protein. This gives comparative activity of samples with the same amount of protein.

Table 3.6. **Citrate Synthase enzyme activity.**

Cell culture	Enzyme activity/ml µmol/sec/ml (± SEM)	Specific activity µmol/sec/mg protein (+ SEM)
MCF-7	1.84×10^{-4} +/- 8.28×10^{-5}	0.018 +/- 8.12×10^{-3}
E1	2.15×10^{-4} +/- 5.31×10^{-5}	0.016 +/- 3.89×10^{-3}
G8	7.36×10^{-5} +/- 1.42×10^{-5}	8.41×10^{-3} +/- 1.62×10^{-3}
B5	2.15×10^{-4} +/- 7.08×10^{-5}	0.017 +/- 5.58×10^{-3}
C12	7.36×10^{-5} +/- 0	6.81×10^{-3} +/- 0

Values represent averages (+ SE) from triplicate enzyme assays

3.3.4 Complex I

Complex I is encoded by the mitochondrial genes ND1, ND2, ND3, ND4, ND5 and ND6 (MITOMAP). Complex I was assayed by the oxidation of NADH to NAD+ (Figure 3.21) giving an increase in absorbance at the rates indicated in Table 3.7. This and subsequent assays have been standardized with CS, displaying activity both before and after standardisation. Clone C12 had the highest activity at 82.23 ± 9.23 µmol/sec/mg protein with B5 the lowest 20.00 ± 1.35 µmol/sec/mg protein.

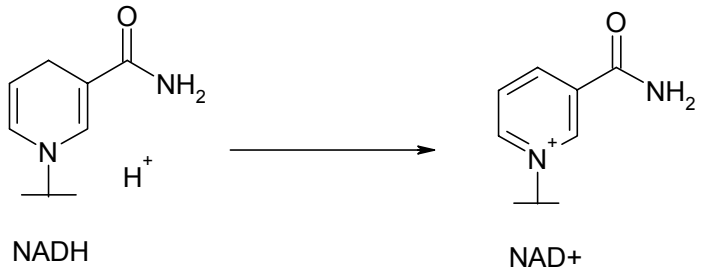

Figure 3.21. **The reduction of nicotinamide adenine dinucleotide (NADH) to NAD** at 340 nm (425 nm reference) by complex I.

Table 3.7. Complex I **- NADH dehydrogenase enzyme activity.**

Cell culture	Enzyme activity/ml µmol/sec/ml	Specific activity µmol/sec/mg protein	Standardize with citrate synthase µmol/sec/mg protein
MCF-7	1.02×10^{-3} +/- 1.51×10^{-4}	0.75 +/- 0.11	41.67 +/- 6.11
E1	2.38×10^{-3} +/- 3.24×10^{-4}	0.70 +/- 0.095	43.75 +/- 5.94
G8	8.60×10^{-4} +/-8.51×10^{-5}	0.61 +/- 0.061	72.53 +/-7.25
B5	7.55×10^{-4} +/-5.07×10^{-5}	0.34 +/- 0.023	20.00 +/- 1.35
C12	9.74×10^{-4} +/-1.08×10^{-4}	0.56 +/- 0.063	82.23 +/- 9.23

Values represent averages (+ SE) from triplicate enzyme assays. Enzyme activity/ml is activity/ ml final reaction volume used in assay

3.3.5 Complex II

Complex II is entirely encoded by nuclear DNA (nDNA). Activity for this complex was high relative to the mitochondrial encoded complexes. E1 had the highest activity at 629.38 µmol/sec/mg protein. The activity for clone B5 was markedly lower at 148.82 µmol/sec/mg protein (Table 3.8). Complex II is partially responsible for replenishing the quinone pool.

Table 3.8. **Complex II – Succinate dehydrogenase enzyme activity.**

Cell culture	Enzyme activity/ml µmol/sec/ml	Specific activity µmol/sec/mg protein	Standardize with citrate synthase µmol/sec/mg protein
MCF-7	0.016 +/- 4.5 x 10^{-3}	4.78 +/- 1.32	265.56 +/- 73.33
E1	0.055 +/- 3.58 x 10^{-3}	10.07 +/- 0.66	629.38 +/- 41.25
G8	8.19 x 10^{-3} +/- 1.44 x 10^{-3}	2.34 +/- 0.41	278.24 +/- 48.75
B5	0.012 +/- 1.33 x 10^{-3}	2.53 +/- 0.28	148.82 +/- 16.47
C12	0.013 +/- 1.92 x 10^{-3}	4.01 +/- 0.59	588.84 +/- 86.64

Values represent averages (+ SE) from triplicate enzyme assays. Enzyme activity/ml is activity/ ml final reaction volume used in assay

3.3.6 Complex III

Complex III is partially encoded by mitochondrial gene Cytb, the remaining genes are of nuclear origin. Figure 3.22 highlights two essential components for the assay of complex III. Rotenone is required to block complex I activity, detectible at 600 nm. Without this component, the enzyme activity for complex III would represent a

combination of complex I and complex III activities. The substrate for complex III, 2,6-dichlorophenol indophenol is readily detected at 600 nm. Clone G8 had the highest activity for complex III (592.15 +/- 24.97 µmol/sec/mg protein) whilst clone C12 was unable to be detected (Table 3.9).

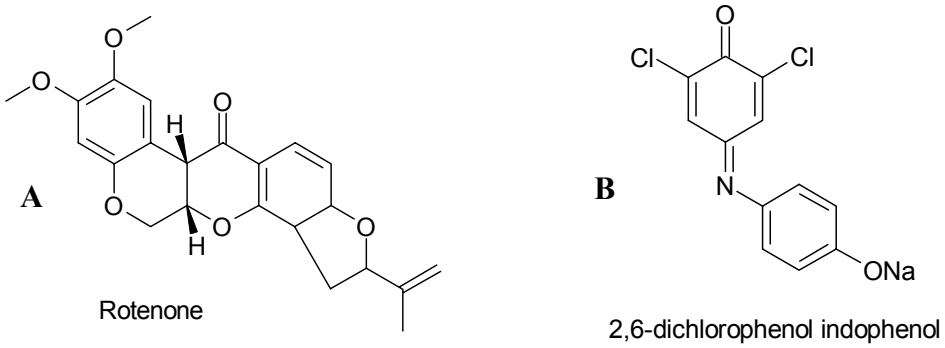

Figure 3.22. **Essential components of complex III enzyme assay. A,** Rotenone blocks complex I to assay for complex III by the reduction of 2,6-dichlorophenol indophenol ***(B)*** at 600 nm

Table 3.9. **Complex III – Ubiquinol cytochrome c- oxidoreductase enzyme activity.**

Cell culture	Enzyme activity/ml µmol/sec/ml	Specific activity µmol/sec/mg protein	Standardize with citrate synthase µmol/sec/mg protein
MCF-7	1.03×10^{-4} +/- 6.65×10^{-5}	0.061 +/- 0.039	3.39 +/-2.17
E1	9.58×10^{-3} +/- 1.24×10^{-3}	3.05 +/- 0.36	190.63 +/- 22.5
G8	8.72×10^{-3} +/- 3.62×10^{-4}	4.98 +/- 0 0.21	592.15 +/- 24.97
B5	0.0146 +/- 1.02×10^{-3}	5.76 +/- 0.40	338.82 +/- 23.53
C12	Could not detect activity		

Values represent averages (+ SE) from triplicate enzyme assays. Enzyme activity/ml is activity/ ml final reaction volume used in assay

3.3.7 Complex IV

Complex IV is encoded by the mitochondrial genes COI, COII, and COIII (MITOMAP). Complex IV activity is monitored by activity of cytochrome c oxidase, by the oxidation of cytochrome c. Enzyme activities are summarised in Table 3.10.

Table 3.10 **Complex IV – Cytochrome c oxidase enzyme activity.**

Cell culture	Enzyme activity/ml µmol/sec/ml	Specific activity µmol/sec/mg protein	Standardize with citrate synthase µmol/sec/mg protein
MCF-7	0.013 +/- 1.6×10^{-3}	7.65 +/- 0.94	425 +/- 52.2
E1	8.67×10^{-3} +/- 1.30×10^{-3}	2.54 +/- 0.38	158.75 +/- 23.75
G8	could not detect activity		
B5	6.5×10^{-3} +/- 7.00×10^{-4}	2.05 +/- 0.22	120.59 +/- 12.94
C12	5.2×10^{-4} +/- 3.00×10^{-4}	0.24 +/- 0.14	35.24 +/- 20.56

Values represent averages (+ SE) from triplicate enzyme assays. Enzyme activity/ml is activity/ ml final reaction volume used in assay

3.3.8 Summary of Relative Enzyme Activities

Figure 3.23 is a schematic representation of complex I-IV enzyme activities, with the greatest activity at the top and the lowest or undetected activity at the bottom. Interestingly, the fastest single cell clone (B5) is not enzymatically superior throughout all complexes and has the lowest activity in complexes I and II. The slowest single cell clone (C12) has very high activity for complexes I and II. The reverse occurs in complexes III and IV, in which B5 activity increases and C12 activity decreases.

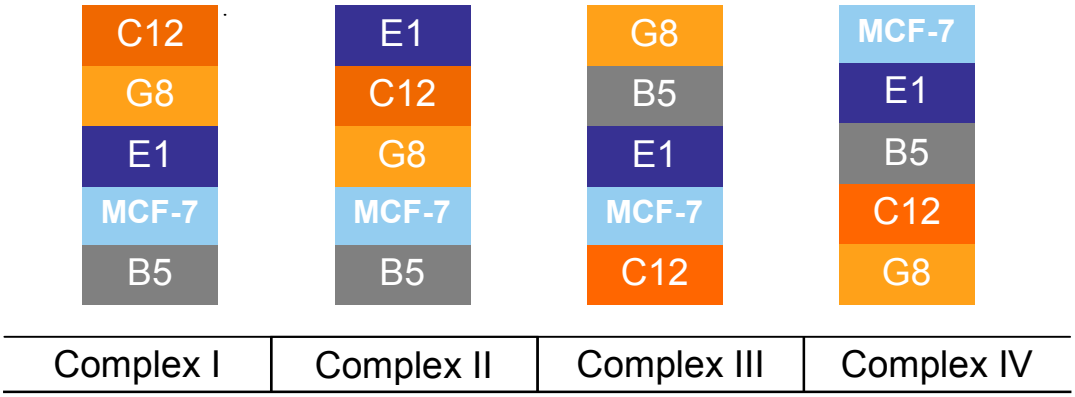

***Figure 3.23*. Schematic of relative enzyme activities with greatest activity at the top**. There was no detectable activity for C12 in complex III or G8 in complex IV

Table 3.11 provides a summary of the relationship between mitochondrial heteroplasmy and cell clone population doubling time.

Table 3.11. **Relationship between enzyme activity and mitochondrial heteroplasmy between clones.**

Nucleotide (heteroplasmic)	Degree of heteroplasmy	Gene	Amino acid change	Complex	Enzyme activity µmol/sec/mg protein ± SEM	Clone	PDT
9119	50%	ATPase6	no change	V	unknown	MCF-7, B5, C12, E1, G8	N/A
14300	20%	ND6	Y→STOP	I	41.67 +/- 6.11	MCF-7	27.00
14300	20%	ND6	Y→STOP	I	20.00 +/- 1.35	B5	25.50
14300	20%	ND6	Y→STOP	I	82.23 +/- 9.23	C12	41.00
14300	20%	ND6	Y→STOP	I	43.75 +/- 5.94	E1	28.79
14300	20%	ND6	Y→STOP	I	72.53 +/-7.25	G8	31.76
15807	20%	Cytb	A→T	III	3.39 +/-2.17	MCF-7	27.00
15807	25%	Cytb	A→T	III	338.82 +/- 23.53	B5	25.50
15807	0%	Cytb	A→T	III	could not detect activity	C12	41.00
15807	15%	Cytb	A→T	III	190.63 +/- 22.5	E1	28.79
15807	0%	Cytb	A→T	III	592.15 +/- 24.97	G8	31.76

Enzyme activity represents averages (+ SE) from triplicate enzyme assays. Enzyme activity/ml is activity/ml final reaction volume used in assay

3.4 Reactive Oxygen Species

3.4.1 Growth Morphology

The growth morphology changed significantly in some of the radical treatments. Treatment of the MCF-7 original culture with 20 mM AAPH for 1 hour did not appear to change cell size or morphology (Figure 3.24, A). Conversely, treatment with 2 mM (B) and 4 mM (C) AAPH for 72 hours dramatically changed cell appearance but not size. The addition of 2 mM AAPH induced a level of nuclear vacuolization, suggesting the cell may be undergoing apoptosis. The addition of 4 mM AAPH reduced the cell population ten-fold. Upon cell growth, distinct clusters emerged in an analogous manner to that of the C12 single cell clone (Section 3.1.1).

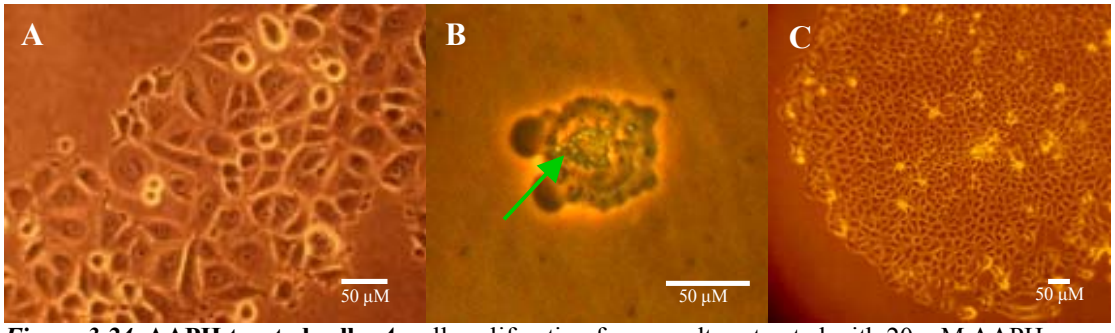

Figure 3.24. **AAPH treated cells.** ***A*****,** cell proliferation from a culture treated with 20 mM AAPH incubated for 1-hour; **B,** cell morphology from 2 mM AAPH incubated for 72 hours, there is notable cytoplasmic vacuolation and granulation; **C,** cluster morphology of cell culture grown from 4 mM AAPH treated cells.

Treatment of the original MCF-7 culture with DPPH at 250 nM (Figure 3.25, A) appeared to induce a slightly higher level of contact inhibition in approximately 20 % of the culture at confluence. A DPPH level of 25 nM (Figure 3.25, B, C) induced a similar morphology to that observed in the 2mM and 4 mM AAPH cultures. The control did not share these characteristics

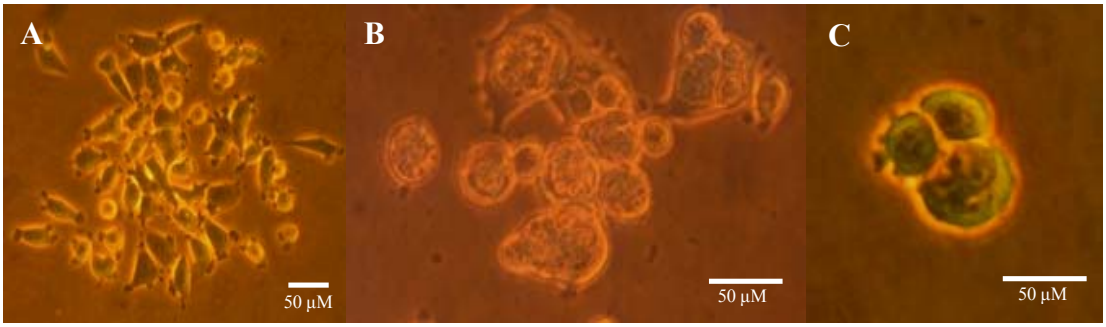

Figure 3.25*. DPPH treated cells.** ***A, cell proliferation from culture treated with 250 nM DPPH incubated for 1-hour; ***B and C,*** cell proliferation from 25 nM incubation over 72 hours.

MCF-7 cell were grown over an extended period of time. The morphology of the MCF-7 cells changed slightly (Figure 3.26) as the cells became elongated. The culture still grew as described in Section 3.1.2. DNA was successfully isolated from this culture and amplified for the same mitochondrial genes as the radical treated cells (ND1, COI, Cytb and D-loop). This was performed with particular interest in the D-loop region, to compare with the range of estimates mitochondrial mutation rate. The MCF-7 culture in Figure 3.26 was in its 53rd generation.

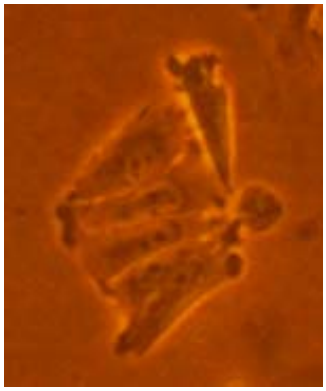

Figure 3.26. **Slightly elongated cells observed for MCF-7 in 53rd generation.**

3.4.2 Cell Proliferation

Growth curve methods and statistical analysis were performed as described in Sections 3.1.4 and 3.1.5.

Figure 3.27 shows the growth curves obtained from population studies using trypan blue cell viability dye and standard cell counting. The 20 mM AAPH treated culture shows a lower plateau phase, potentially due to a reduction in the surviving fraction, inducing a longer lag phase. This is confirmed by the WST-1 cell proliferation curve. The 250 nM DPPH treated culture follows the MCF-7 stock culture in Figure 3.27, but deviates between the AAPH treated and the MCF-7 stock in Figure 3.28. The experiments were performed alongside each other, with three replicas for Figure 3.27 (trypan blue) and eight replicas for Figure 3.28 (WST-1). A longer lag phase appears in Figure 3.28, after which the culture conforms to the MCF-7 stock after a period of 250 hours.

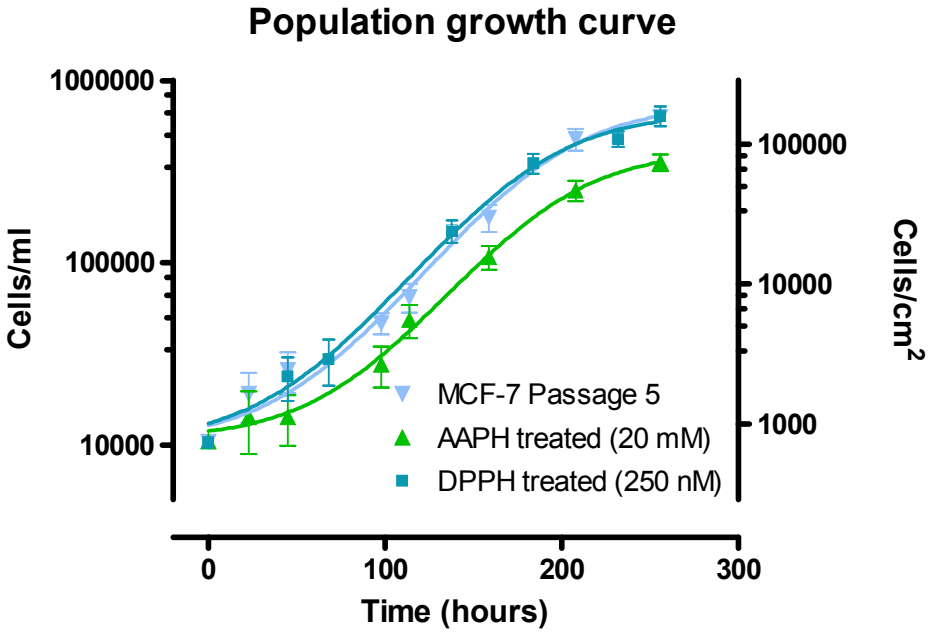

Figure 3.27. **Population growth curve.** ***MCF-7*** (▼, passage 5 R^2=0.9995); MCF-7 cells treated with ***20 mM AAPH*** ▲ (R^2=0.9995); MCF-7 cells treated with ***250 nM DPPH*** ■ (R^2=0.9959). Data shown as mean ± SE.

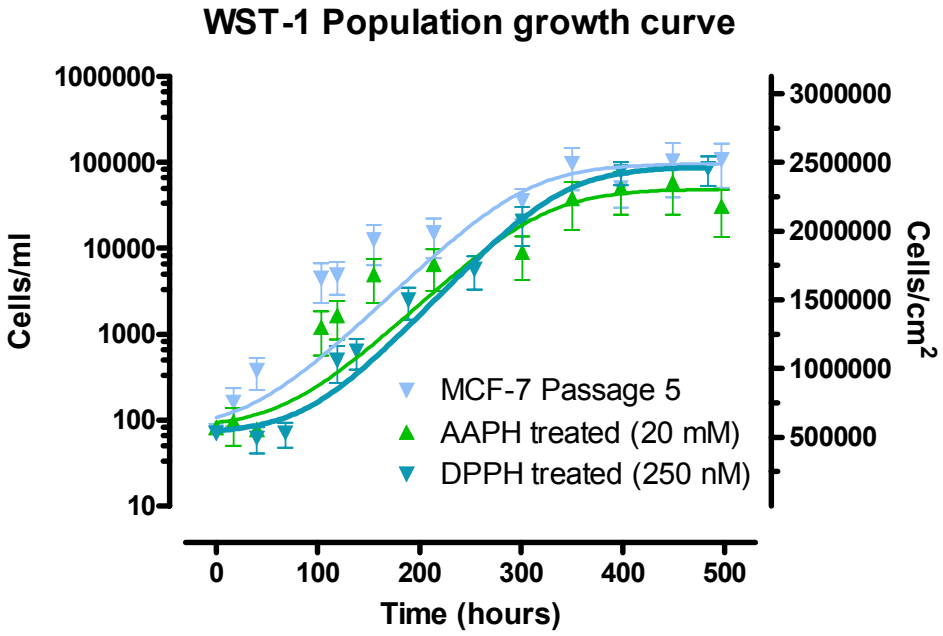

Figure 3.28*. WST-1 Population growth curve.** ***MCF-7 (▼, passage 5 R^2=0.8760); MCF-7 cells treated with ***20 mM AAPH*** ▲ (R^2=0.8729); MCF-7 cells treated with ***250 nM DPPH*** ■ (R^2=0.9980). Data shown as mean ± SE.

3.4.3 Cultures under Continuous Free Radical Assault

Figure 3.29 shows the difference in cell proliferation between the cultures treated with low-level free radical generators and the MCF-7 control. These were seeded at a higher level (10,000 cells/3.5 cm^2) as cell proliferation was unable to be detected at lower levels. The culture treated with 1 mM AAPH and 25 nM DPPH was more proliferative than that treated with 25 nM DPPH alone.

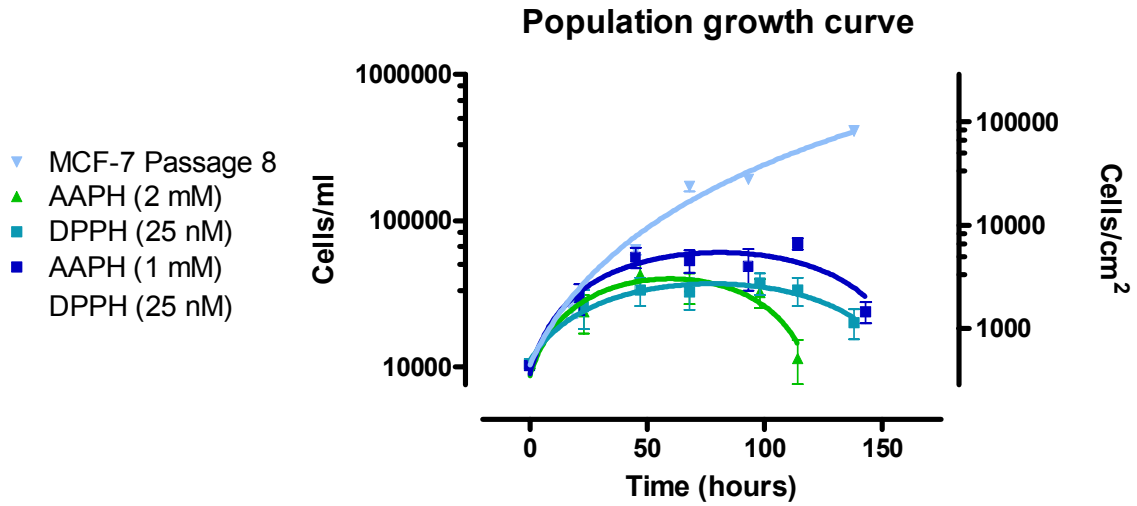

Figure 3.29*. Response to free radical generator. MCF-7 cells** (▼, passage 8) treated with low level radical; ***AAPH (▲ , 1 mM); ***DPPH*** (■, 25 nM); ***AAPH*** (1 mM)/ ***DPPH*** (25 nM, ■). Data shown as mean ± SE.

3.4.4 DNA Isolation and Quantification

Isolation of cell line DNA from MCF-7 cells treated with various levels of free radicals was successful. Figure 3.30 depicts the quality of DNA obtained. Table 10 gives the absorbance values for DNA samples at 260 and 280 nm.

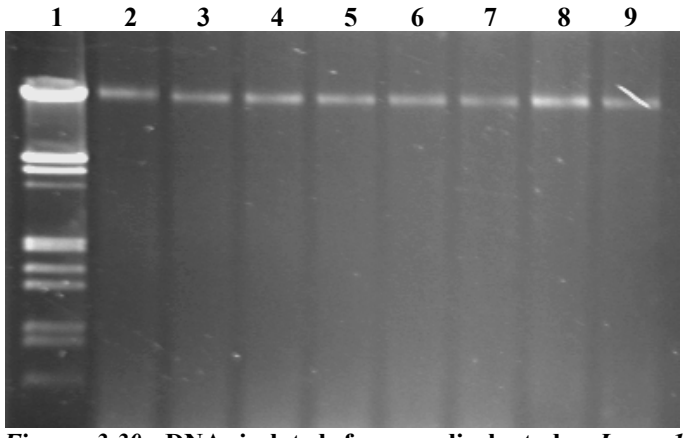

Figure 3.30*. DNA isolated from radical study.** ***Lane 1 λ*HindIII*/*EcoR1* marker, ***lane 2 and 3,*** MCF-7 cell DNA (53rd generation), ***lane 4 and 5,*** AAPH treated cell DNA; ***lane 6 and 7,*** DPPH treated cell DNA; ***lane 8 and 9,*** AAPH/DPPH treated cell DNA.

Table 3.12. **Genomic DNA quantification.**

DNA	A_{260}	A_{280}	$A_{260/A280}$	Quantity (µg/µl)
MCF-7*	0.130	0.107	1.21	0.650
AAPH 2 mM	0.140	0.108	1.30	0.700
AAPH 4mM	0.013	0.008	1.63	0.065
DPPH 25 nM	0.024	0.014	1.71	0.120
AAPH(1 mM)/ DPPH(25 nM)	0.009	0.004	2.25	0.045

AAPH and DPPH refer to MCF-7 cells treated with free radicals at the indicated concentrations
***MCF-7 cells in their 53rd generation**

PCR products were obtained for genes ND1, COI, Cytb and D-loop for all DNA sample in Table 3.12. These PCR products are from the low free radical generator concentrations with continuous treatment and the MCF-7 cells grown over an extended period of time. Figure 3.31 shows the PCR product from the Cytb gene from the low-level free radical generator study. Figures 3.32, 3.33 and 3.34 show the PCR product for the low-level radical generator study for genes ND1, COI and D-loop, respectively. Additional PCR products for the mitochondrial DNA extraction and one hour free radical generator incubation can be seen in Appendix C (PCR and sequencing). ABI chromatograms for these PCR products can also be found in Appendix C.

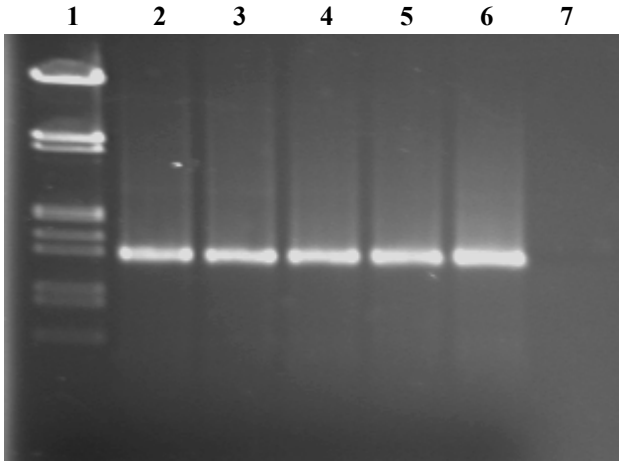

Figure 3.31. **PCR precipitate of the Cytb gene.** ***Lane 1,*** molecular marker λ*HindIII*/*EcoRI*; ***lane 2,*** MCF-7; ***lane 3,*** AAPH (2 mM) treated cell culture DNA; ***lane 4,*** DPPH (25 nM) treated cell culture DNA; ***lane 5,*** AAPH (1 mM) and DPPH (25nM) treated cell DNA, ***lane 6***, negative control.

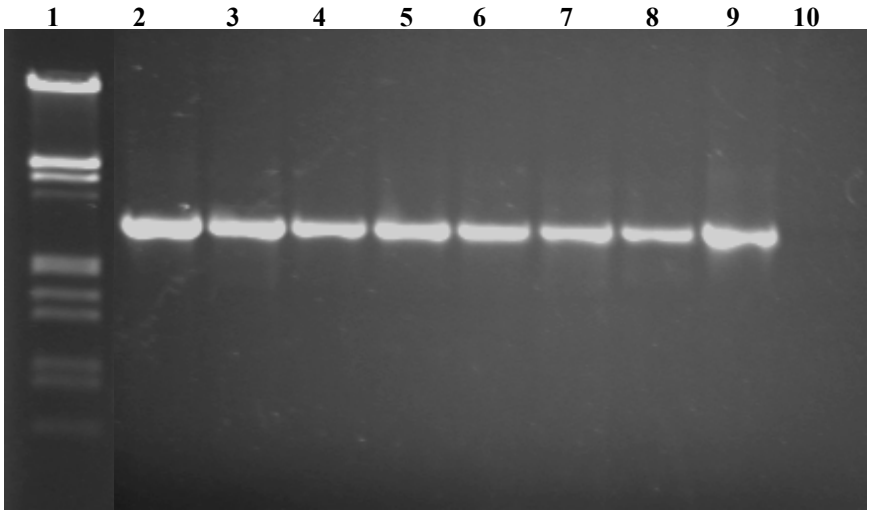

Figure 3.32. **PCR of the ND1 gene.** ***Lane 1*****,** molecular marker λ*HindIII/EcoRI*, ***lane 2 and 3,*** MCF-7; ***lane 4 and 5,*** AAPH (2 mM) treated cell culture DNA; ***lane 6 and 7,*** DPPH (25 nM) treated cell culture DNA; ***lane 8 and 9,*** AAPH (1 mM) and DPPH (25nM) treated cell culture DNA; ***lane 10,*** negative control

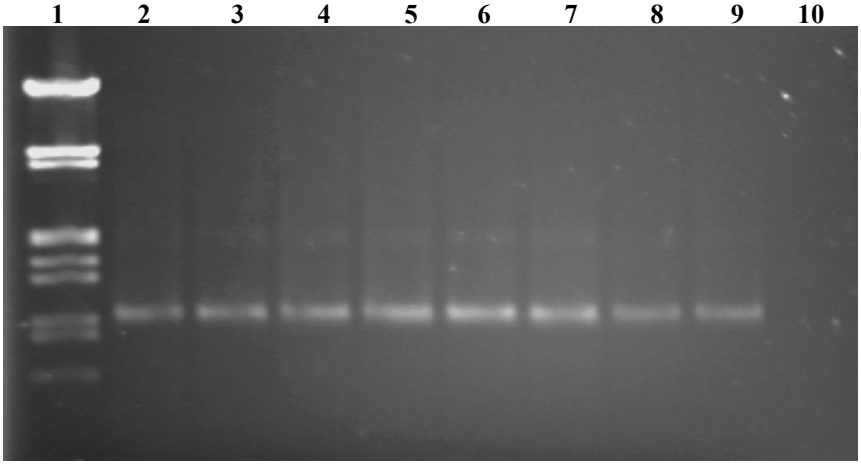

Figure 3.33. **PCR precipitate of the COI gene.** ***Lane 1*****,** molecular marker λ*HindIII/EcoRI*; ***lane 2 and 3,*** MCF-7; ***lane 4 and 5,*** AAPH (2 mM) treated cell culture DNA; ***lane 6 and 7,*** DPPH (25 nM) treated cell culture DNA; ***lane 8 and 9,*** AAPH (1 mM) and DPPH (25nM) treated cell culture DNA; ***lane 10,*** negative control

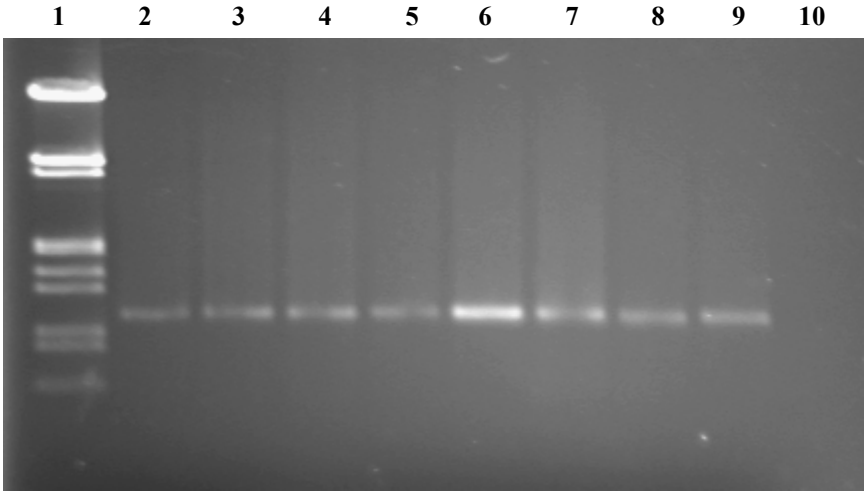

Figure 3.34. **PCR precipitate of the D-loop gene.** ***Lane 1*****,** molecular marker λ*HindIII/EcoRI*; ***lane 2 and 3,*** MCF-7; ***lane 4 and 5****,* AAPH (2 mM) treated cell culture DNA; ***lane 6 and 7,*** DPPH (25 nM) treated cell culture DNA; ***lane 8 and 9,*** AAPH (1 mM) and DPPH (25nM) treated cell culture DNA; ***lane 10,*** negative control

3.4.5 AAPH and DPPH Treatment of DNA

Figure 3.35 demonstrates the adverse effect AAPH has on DNA, making it a potential candidate for DNA mutation. Figure 3.36 demonstrates possible degradation at 500 nM treatment of MCF-7 DNA with DPPH. This experiment simply shows the negative interaction of these two radicals have with mitochondrial DNA. For AAPH, this has been well documented (Kristal *et al*., 1994). For DPPH, it is largely unknown whether any deleterious effects may be induced by its presence.

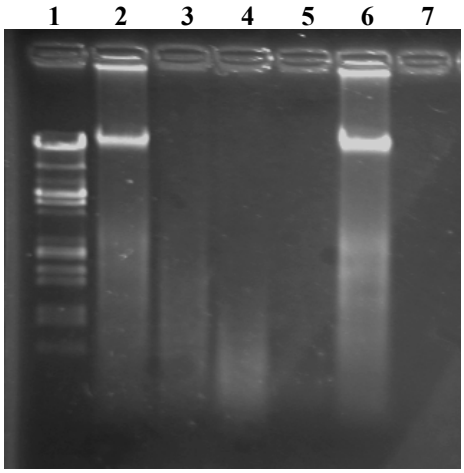

Figure 3.35. **AAPH treated DNA.** ***Lane 1,*** molecular marker λ*HindIII*/*EcoR*I; ***lane 2***, MCF-7 DNA; ***lane 3***, MCF-7 DNA with 20 mM AAPH; ***lane 4***, 50 mM AAPH; ***lane 5***, 100 mM AAPH; **lane 6**, MCF-7 DNA, incubated for 2 hours.

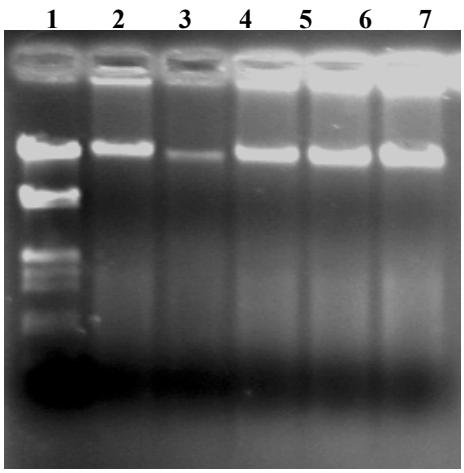

Figure 3.36. **DPPH treated DNA.** ***Lane 1*****,** molecular marker λ*HindIII*/*EcoR1*; ***lane 2***, MCF-7 DNA; ***lane 3***, MCF-7 DNA with 500 nM DPPH; ***lane 4***, 250 nM DPPH; ***lane 5***, 100 nM DPPH; ***lane 6***, MCF-7 DNA, incubated for 2 hours

3.4.6 AAPH and DPPH Treatment of Isolated Mitochondria

Isolated intact mitochondria were treated with both AAPH (20 mM) and DPPH (250 nM) for 1 hour at 37˚C. DNA was isolated from these mitochondrial fractions by phenol/chloroform extraction (Section 2.2.2.1). The mitochondrial genes ND1, COI, Cytb and D-loop were amplified by PCR and sequenced using ABI fluorescent sequencing. No DNA base modification or DNA heteroplasmy was observed for these genes. Additional PCR products and sequences from this study can be found in Appendix C (PCR and sequencing).

3.4.7 Transformation of the MCF-7 Cell Line with AAPH

Figure 3.37 B shows MCF-7 cells that have undergone transformation with 4 mM AAPH. A clustered morphology is observed which is very similar to the C12 clone

(Figure 3.37 A) isolated from the MCF-7 stock culture. The C12 clone did not undergo any radical treatment.

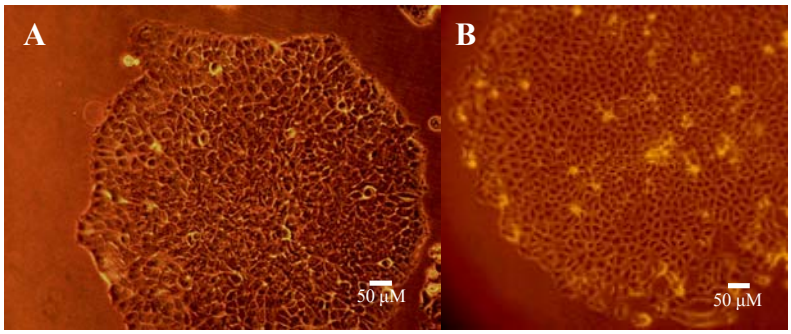

Figure 3.37. **Potential transformation of MCF-7 cells with AAPH. *A*,** C12 isolated single cell clone from MCF-7 stock, ***B***, MCF-7 stock treated with 4 mM AAPH over 72 hours.

CHAPTER 4

DISCUSSION

4.1 MCF-7 Growth Characteristics

The mammary epithelial cell line MCF-7 is widely used as a cell line model and is well characterized (Sutherland *et al*., 1983; Taylor *et al*., 1983; Taylor *et al*., 2001; Devarajan *et al*., 2002; Hand and Craven, 2003; Zou and Matsumura, 2003; Lacroix and Leclercq, 2004; Zivadinovic *et al*., 2004) It has been used to test the effect of reactive oxygen species in cell cultures (Chang *et al*., 2002; Hand and Craven, 2003). The MCF-7 cell line has particular features such as subpopulations (Zou and Matsumura, 2003). These sub-populations of MCF-7 may posses DNA variation and produce different levels of reactive oxygen species as some cultures were shown to proliferate faster than others.

4.1.1 Growth Characteristics of Single Cell Clones

In order to obtain genetically homogenous cell lines, single cell clones were isolated from the MCF-7 stock. Cell proliferation of single cell clones demonstrated different growth patterns between cultures. Further, markedly different growth morphology was also observed. In particular, the clustered morphology of the C12 clone was distinctive. This clone was the slowest to proliferate (PDT 41 hours), which may be due to competition for nutrient from the culture media because of the tight clustering growth habit, a difficulty in proliferation due to limited space within the cluster, or DNA mutation. In contrast, clone B5 was the most proliferative (PDT 25.5 hours) and displayed contact inhibition, and clone G8 (PDT 31.76 hours) with a moderate growth rate exhibited a slightly clustered morphology. Thus, the growth habit of a cell line may reflect the speed in which a cell population will proliferate.

Clone C12 displayed cluster morphology, which was concomitant with reduced mtDNA copy number indicated by a lower activity of citrate synthase in this culture (Chapter 3, Table 3.6). Citrate synthase activity is an indicator of mtDNA copy number. Further, clone G8 exhibited a tendency toward the cluster morphology (Figure 3.2C) and also has reduced mtDNA copy number. Lowering of mtDNA copy number and the cluster morphology were observed in a culture of human diploid fibroblasts that had undergone transformation by SV-40 Torroni *et al*. (1990). It is possible that the C12 culture may be a transformed cell culture. Clone C12 (Figure 3.37 A) displayed a lack of heteroplasmy within the Cytb gene (bp 15807), which was present in other clones. However, this does not appear to be related to the favour of cluster formation.

4.1.2 Isolation of Non-proliferative Single Cell Clones

Single cell clones that failed to proliferate after 45 days (C6, F2, F9) may have harboured mitochondrial DNA mutation or heteroplasmy that prevented proliferation and facilitated cell death. Enriquez *et al.* (2000) determined the rate of trans-complementation of mitochondrial DNA carrying a homoplasmic mutation A8344G in which the recipient trans-complementing clones were notably ‘sluggish’ and experienced substantial cell death (22-28%) (Enriquez *et al*., 2000). Such mutation may be significant in impairing the function of oxidative phosphorylation. A similar study described non-proliferative growth curves in human muscle and myoblast cells resulting from a G6930A mitochondrial mutation, which produced a stop codon, terminating 170 amino acids from the COX I gene product (Bruno *et al*., 1999). Hence, a difficulty encountered in using a cell line model (with single cell clone

isolation) to study mtDNA mutation is the potential for mutant cells to be non-proliferate and/or have a high rate of cell death. Therefore, natural variation between single cell clones may be difficult to obtain. The severity of mitochondrial defect depends largely on the nature of the mutation, and also the ratio of mutant and wild type DNA, i.e. the level of mitochondrial heteroplasmy (Bruno *et al*., 1999; Quintana-Murci *et al*., 2001). Nuclear mutation may also have been present in non-proliferative clones, thereby altering OXPHOS efficiency and lowering energy production required for proliferation.

It is possible that sub-populations exist within the MCF-7 cell line that are non-proliferative. It is unknown if this is due to a mitochondrial defect because it was not possible to isolate the DNA from these cells for analysis. Studies using human fibroblasts carrying NARP (neurologic muscle weakness, ataxia and retinitis pigmentosa) G8993C (85-90% mtDNA) indicate slowly growing cells contained little or no mtDNA (Vergani *et al*., 1999). This may have been a factor in the inability to isolate mtDNA from the limited proliferation cultures. An additional aspect to consider is the phenomenon of cancer cell senescence. Cancer cell senescence is a tumour suppressive mechanism. Senescence can be divided into two categories; replicative senescence (shortening of the chromosomes telomeres) and DNA damage preventing cell cycle progression (Langdon, 2004). As viable single cell clones were isolated, it is unlikely the former mechanism of senescence is active, though the latter mechanism may be involved as the non-proliferative cells remained alive for at least one month. This is in agreement with the observation of senescence cell growth arrest at G_1 but remaining metabolically active and thus, being sustained for a period of time (Langdon, 2004). Moreover, ROS have been implicated in cellular senescence

(Behrend *et al*., 2003; Hand and Craven, 2003) and mutant mtDNA may be prone to producing higher levels of ROS, inducing cellular senescence. The morphology of potential senescent cells could be compared to an MCF-7 stock culture that was induced into cellular senescence by SN38 at 6 nM with subsequent X-gal staining. Senescent positive cells typically exhibit an increased granular appearance and a blue precipitate from positive β–galactosidase activity (Langdon 2004).

4.2 Mitochondrial DNA Modification and OXPHOS

4.2.1 The MCF-7 Cancer Cell Line and Mitochondrial Mutation Rate

The MCF-7 cell line mitochondrial DNA deviates from the NCBI sequence NC-001078 (April 2005) and has the common 73 bp associated with the highly mutagenic prostate tumour lines (Chen, 2003). At the very least, a significant subset of human tumours experience frequent mutational events within the mtDNA. This is proposed to occur as the cell shifts from a benign epithelial cell to a malignant cell, of high oxygen consumption particularly in prostate tumours (Costello and Franklin, 2000). For this reason, a simple study was conducted with MCF-7 cells grown over an extended period to encompass 53 generations. The mitochondrial genes ND1, COI, Cytb and the hypervariable D-loop were amplified and sequenced (Chapter 3, Section 3.4.4). No mutations or mitochondrial heteroplasmy was encountered when compared to stock MCF-7 mtDNA. This may suggest a slower mutation rate of human mtDNA than estimated by some studies. However, in the present study the cells had gone through only 57 generations and only a small number of genes were analysed.

4.2.2 MCF-7 Cell Line and Clone Enzyme Activity

One purpose of this thesis was to assess the differences in respiratory chain enzyme activity between isolated single cell clones from the MCF-7 stock. Heteroplasmy was found in three mitochondrial genes, with different levels of heteroplasmy present in clones for the gene Cytb. The enzyme activities of all respiratory complexes were measured to determine if there was a correlation between mitochondrial heteroplasmy observed and relative enzyme activity (Chapter 3, Table 3.11). These are discussed in turn. Figure 4.1 demonstrates the interaction between complexes. The combined effects of OXPHOS when one or more complexes have low activity are important in the relationship between enzyme activity and PDT. Each enzyme complex of the respiratory chain is responsible for supplying substrates to the following complex, and/or creating the proton gradient across the inner membrane.

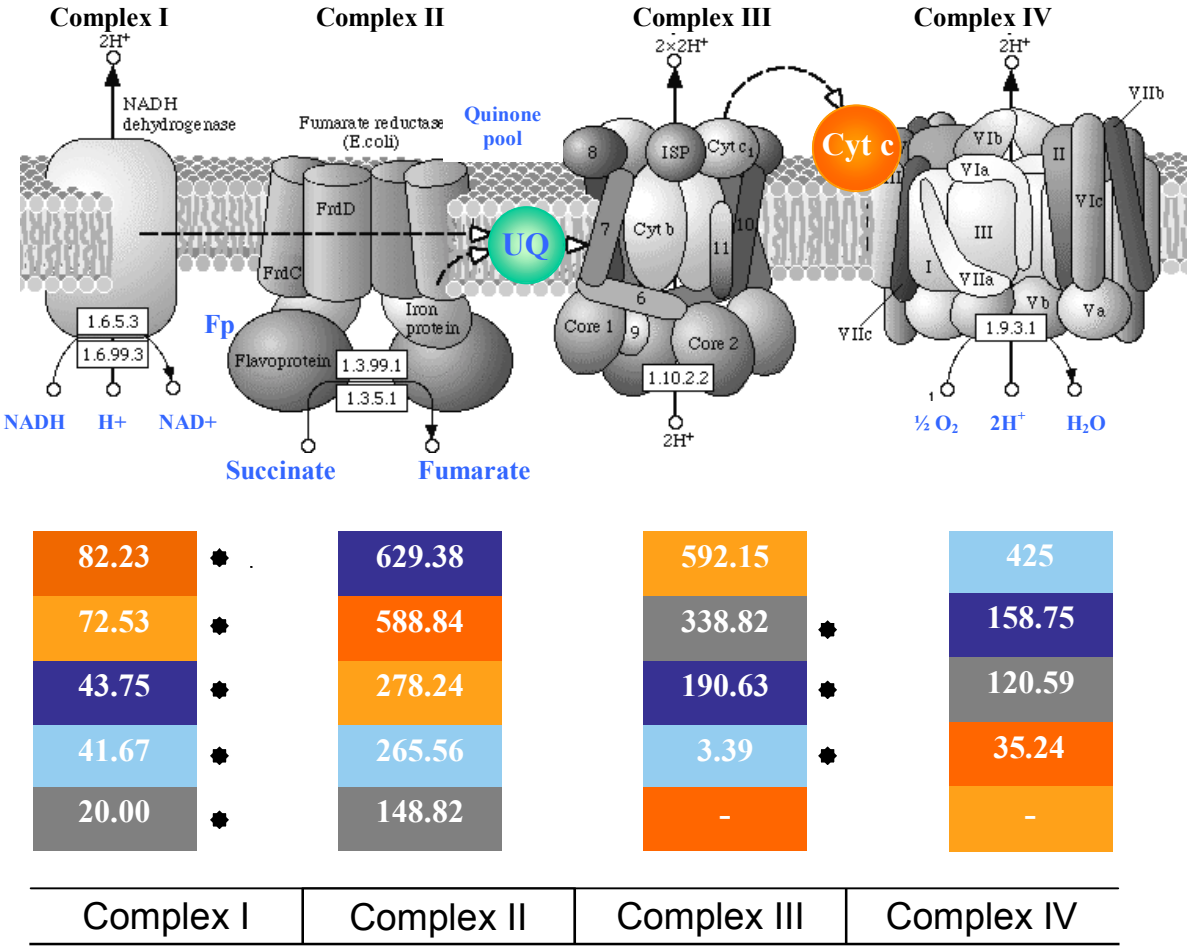

Figure 4.1. **OXPHOS enzyme activities in relation to function in µg/sec/mg protein**. MCF-7 (PDT 27 hours), B5 (PDT 25.5), C12 (PDT 41), E1 (PDT 28.79), and G8 (PDT 31.76) (±SE not shown see Section 3.3.4). This shows relative enzyme activity in relationship with enzyme function. The ✹ symbol indicates complexes with heteroplasmy in their coding genes.

Therefore, the presence of one defective enzyme within the respiratory chain may impair the overall energy production of OXPHOS. This may occur via the lowered production of substrate required by another complex or the decrease in the transport of protons across the inner membrane.

4.2.2.1 Complex I- NADH-Coenzyme Q Reductase

B5 has the lowest complex I activity (PDT 25.5 hours, enzyme activity, 20 µg/sec/mg protein), and C12 the highest (PDT, 41 hours, enzyme activity, 82.23 µg/sec/mg protein). There appears to be little influence of complex I in relation to PDT in terms

of lowered enzyme activity. Additionally, heteroplamsy was observed within the ND6 gene in all clones (A14300C at 20% for all clones) producing a stop codon from tyrosine. Enzyme activities observed for all clones may be low due to the introduction of the stop codon. This resulted in a truncation of the protein by 50 residues. It appears the ability of complex I to transport protons across the inner mitochondrial membrane may be impaired in the MCF-7 cell line and derivative clone cultures. Further, a lowered production of the complex III substrate ubiquinone by complex I may also be influential, though complex II also produces this substrate. However, clone B5 had low activity for both complex I and II but still had the fasted PDT. The differences in activities in complex I in the present research may be due to changes in the coding genes of the nuclear DNA. Deficiency in complex I activity has been shown to increase the production of superoxide radicals, whilst simultaneously inducing superoxide dismutase in human skin fibroblasts (Pitkanen and Robinson, 1996). Superoxide is a prime character in the initiation of lipid peroxidation (Murphy *et al*., 2003). In the present research, clone B5 PDT does not appear to be impaired, despite the potential for greater production of superoxide. A threshold may exist for the increased production of superoxide to become deleterious and impair cellular respiration.

In a study similar to the aspirations of this thesis, mammalian mitochondrial NADH dehydrogenase (complex I) was examined for mitochondrial heteroplasmy in isolated murine fibroblasts (Bai *et al*., 2004). Mutational analysis was carried out on the mitochondrial DNA. The mutant cells were selected due to their resistance to rotenone (1.2 μM), an inhibitor of complex I (Hofhaus *et al*., 1995; Bai *et al*., 2004). Complex I functional analysis was achieved by measuring the enzyme activity (capacity) of cells

displaying rotenone resistance. An experiment was performed in which a heteroplasmy threshold for the ND5 gene was determined. For this, a consistent nuclear background was applied by employing a p^o mitochondrial re-population technique. The identified mutation ND5 C12081A is a nonsense mutation resulting in truncation of the encoded protein (Bai *et al*., 2004). Total mRNA level was examined. For all except those near mutant homoplasmy the ND5 mRNA level was constant. This suggests an independence of the level of heteroplasmy from mRNA transcription until a very high threshold is reached.

This thesis found levels of mitochondrial heteroplasmy around 20% (ND6 T14300G and Ctyb G15807A) and up to 50% (ATPase6 C9119T). These levels may be below a critical threshold to influence mRNA transcription, and hence, protein synthesis. Complex I heteroplasmy in single cell clones was 20%.

4.2.2.2 Complex II- Succinate-Coenzyme Q Reductase

Upon comparing enzyme activity to population doubling time, there appears to be little influence of the activity of complex II to cell clone population doubling time. As clone C12 (PDT 41 hours, 588.84 μg/sec/mg protein) has a higher activity than the fastest clone, B5 (PDT 25.5 hours, 148.82 μg/sec/mg protein). Mutation or heteroplasmy in the nuclear genes may play a role in the reduced enzyme efficiency of the clone B5.

4.2.2.3 Complex III- Coenzyme Q-Cytochrome c Reductase

There was no detectable activity for the clone C12. This may mean a severe reduction in the amount of cytochrome c (II) supplied to complex IV in C12. Complex IV activity for C12 is very low also (35.24 μg/sec/mg protein), suggesting the influence of a defective complex III protein and/or complex IV protein. There may be other factors involved however, as the activity of the MCF-7 stock (3.39 μg/sec/mg protein) in supplying reduced cytochrome c to complex IV is not reflected in complex IV activity (425 μg/sec/mg protein). MCF-7 displayed G15807A heteroplasmy in the Cytb gene at 15%. From mutational analysis, C12 (could not detect enzyme activity) did not harbour detectible levels of heteroplasmy in any complex III genes. Conversely, G8 also did not display heteroplasmy but had the highest activity (592.15 μg/sec/mg protein) in complex III. This suggests that the differing activities observed for complex III are not due to mitochondrial heteroplasmy, but may be of nuclear origin. An additional aspect to consider is that complex III is the site of superoxide production (Ramachandran *et al*., 2002). Hence, high complex III activity may confer a disadvantage by producing higher levels of ROS, damaging surrounding proteins.

4.2.2.4 Complex IV- Cytochrome c Oxidase

For complex IV clone G8 did not have detectible activity. Clone C12 had the second lowest activity (PDT 41, 35.24 μg/sec/mg protein). Clone B5 had an intermediate activity (PDT 25.5, 120.59 μg/sec/mg protein), and the stock culture had the highest activity (PDT 27, 425 μg/sec/mg protein). MCF-7 stock had the lowest complex III

activity (3.39 μg/sec/mg protein), yet it had the highest complex IV activity. On the contrary, clone G8 had the highest complex III activity, yet no detectible complex IV activity. Thus, it appears that complex IV activity was not influenced by the amount of substrate produced by complex III. Furthermore, a number of human cell types have a low in-vivo complex IV capacity (Villani *et al.,* 1998). No mitochondrial mutation was detected in the complex IV genes for any of the clones. The lower activity of complex IV in clone G8 may be due to mutations in some nuclear encoded genes.

Complex IV is a key enzyme in OXPHOS in terms of regulation (Bruno *et al*., 1999; Roberts and Pique, 1999, Zhen *et al*., 1999; D'Aurelio *et al*., 2001). Mitochondrial encoded subunits I and II form the catalytic centre of the complex (Roberts and Pique, 1999; Zhen *et al*., 1999; D'Auelio *et al*., 2001). D'Aurelio *et al*. (2001) found a correlation between the levels of mutant complex IV encoding mitochondrial DNA, mutant mRNA and cell proliferation in cybrid human osteosarcoma 143B cells after excluding mitochondria with ethidium bromide. The mutation COX I G6930A results in truncation of the protein by 170 residues (Bruno *et al*., 1999; D'Aurelio *et al*., 2001). COX I DNA and mutant COX I mRNA, were positively correlated, however total levels of COX I and mRNA were unchanged (D'Aurelio *et al*., 2001). Complex IV activity was measured relative to mutation load and was found to decrease proportionally. Additionally, the activities of complexes I and III were unchanged in mutant complex IV harbouring cells. For complex I and III therefore, there is no mutant threshold or indeed compensatory increase, affecting complex activities. Growth studies were performed, which demonstrated cells harbouring greater than

50% mutant mtDNA were slow to proliferate, and greater than 70% were not able to divide (D'Aurelio *et al*., 2001). This describes a direct influence of mitochondrial heteroplasmy on cell population growth, corroborated by an analogous study (Bruno *et al*., 1999).

In the present research, levels of heteroplasmy present in clone cultures may simply be too low to affect cell division and proliferation. A larger sample size is needed to determine the heteroplasmy threshold and particular cases of heteroplasmy that are influential on growth characteristics. Ideally, a number of different cell lines displaying mitochondrial heteroplasmy would be useful in obtaining a broader understanding of the influence of heteroplasmy on the respiratory chain in cultured human cells.

4.2.2.5 ATP Synthase

ATP synthase was not assayed in this research. Heteroplasmy (G9119A 50%) was found in all clone cultures and the MCF-7 stock. There may be an overall effect seen in the activity of ATPase *in vivo*, in which the combined effort of the respiratory chain to create the proton gradient between clones may differ. As complexes I, III and IV create the proton gradient utilised by ATP synthase, the lowered activities of C12 for complexes III and IV responsible for the transfer of protons across the inner mitochondrial membrane may result in lowered ATP production (hence, cell proliferation) due to a lower $\Delta\Psi m$. This may partially account for the longer population doubling time for C12. Nuclear mutation may play a significant role also.

4.2.3 OXPHOS Substrate Supplementation

Research performed by Folgero *et al.* (1993) studied the relationship between human spermatozoa and OXPHOS substrate supplementation (Folgero *et al.*, 1993). Spermatozoa motility was assessed by the swim up method. They found that 12% of spermatozoa were motile in media containing 0.5 mM glucose, and an almost three-fold increase (34%) in motile spermatozoa was observed in a medium containing 0.1 mM succinate (complex II substrate) and 0.2 mM pyruvate (complex I substrate) in addition to glucose. After 20 hours 60% of spermatozoa were motile. Further, control subjects (n=2) had higher motility (68%) in the presence of pyruvate, with a detectible increase upon the addition of succinate (82%) (Folgero *et al.*, 1993). This study has a very small sample size, but is intriguing in regards to sperm motility and supplementation of respiratory chain substrate. There is potential for the addition of respiratory complex substrates to human cultured cells, which may further elucidate the mechanism involved in this study. Thus, if complexes are defective in their ability to produce substrate within the respiratory chain, supplementation of required biomolecules may show a difference in PDT, demonstrating that the lowered energy output was due to substrate deficiency. Conversely, if supplementation does not aid proliferation, mitochondrial or nuclear DNA mutation or increased ROS production may be influential factors. This could be another means to test the heteroplasmy threshold, as addition of exogenous substrate could compensate for a certain level of heteroplasmy that may lower protein function thereby supplying the substrate the defective protein is unable to produce at physiological levels. For the present research, supplementation of ubiquinone and cytochrome c for clones G8 and C12 respectively, may elicit a change in complex III and IV activities for these clones.

Defects of oxidative phosphorylation can have a negative impact as poor enzyme function results in increasing bursts of ROS (Lucas and Szweda, 1998; Chen *et al*., 2003). This can have the knock-on effect of increasing mtDNA mutation resulting in greater ROS production. This process may well be in action in hyper-mutagenic prostate cancer cell lines, resulting in a downward spiral of mutation and superoxide production, eliciting more mutation.

4.3 Reactive Oxygen Species in Cultured Cells

One of the most common ROS is hydrogen peroxide. It can exist at damaging levels in a physiological environment. In addition, it can undergo many reactions producing more potent ROS, such as hydroxyl radicals that can elicit DNA damage.

4.3.1 Hydrogen Peroxide and MCF-7 Cells

Hydrogen peroxide has further implications for mitochondria with the induction of apoptosis (Miller *et al*., 2001; Fujii *et al*., 2002; Behrend *et al*., 2003), the reduction of cellular membrane potential ($\Delta\Psi m$), DNA fragmentation (Fujii *et al*., 2002) and induction of neoplastic transformation (Arnold *et al*., 2001; Takabe *et al*., 2001). Addition of H_2O_2 to human bronchial epithelium cells (transformed by SV-40) at levels >200 μM induced a dose-dependant DNA modification. Concentrations of 1 mM H_2O_2 resulted in 20% of cell DNA being modified as compared with 5% in the control (Fujii *et al*., 2002). Since the repair mechanism in mitochondria is significantly lower than the nuclear base excision and repair system in MCF-7 cells

(Croteau *et al*., 1997; Mambo *et al*., 2002), any DNA damage induced by AAPH or DPPH should be evident without the concern of self-repair in MCF-7 cells (Behrend *et al*., 2003).

4.3.2 Antioxidants in Cell Culture

In the present research AAPH and DPPH were used to treat the MCF-7 cell culture. When used in conjunction, the culture experienced a degree of protection from cell death as opposed to treatment with AAPH or DPPH alone (Figure 3.29). This may be due to a protective effect of DPPH acting as a spin-trap for the carbon centred radicals generated from AAPH. Further, there may be a protective effect of membrane proteins acting as sacrificial antioxidants due to their abundance in relation to nucleic acid. If these sacrificial antioxidants are exhausted there is potential for nucleic acid modification by ROS (Genova *et al*., 2003). The hydroxyl radical, superoxide, hydrogen peroxide or lipid peroxides may mediate this directly or indirectly.

4.3.3 Acrolein Involvement in Transformation

Lipid peroxidation has been implicated in male infertility, atherosclerosis and cancer (Folgero *et al*., 1993; Twigg *et al.,* 1998; Aitken and Krausz, 2001; Miller *et al*., 2001; Takabe *et al*., 2001; Holstein *et al*., 2003). The effects of lipid peroxides include DNA damage, alteration of cellular biochemistry (Twigg *et al*., 1998; Uchida, 1999; Said *et al*., 2005) and the production of mutagenic adducts (Takabe *et al*., 2001). A highly mutagenic (and common) lipid peroxidation product is acrolein (Uchida, 1999; Takebe *et al*., 2001).

An early event in the exposure of mouse embryo C3H/10T1/2 fibroblast cells was the generation of a highly mutagenic lipid peroxidation product, acrolein (Takabe *et al*., 2001). The presence of acrolein was observed from the exposure of the culture to H_2O_2 generated indirectly by AAPH. ELISA was used to determine the presence of acrolein using a monoclonal antibody raised against acrolein-lysine adducts. Acrolein formation was suppressed by the addition of α-tocopherol (supplying a proton for abstraction). Takabe *et al*. (2001) pre-treated C3H/10T1/2 cells with benzo[a]pyrene (0.5 μM) before the addition of AAPH (200 μM). The treated fibroblasts underwent transformation. It was found that acrolein significantly induced transformation of pre-treated cells but not the control sample involving 200 μM AAPH alone. This thesis research demonstrated the potential induction of transformation with 4mM AAPH treatment for 72 hours in MCF-7 cells, without pre-treatment of benzo[a]pyrene (Section 3.4.1, Figure 25C). Close to 80% of the cells underwent cell death. The surviving fraction was very sluggish, taking 10 days to reach 50% confluence (Figure 3.37B). There is a notable change in growth habit between the AAPH treated cells (Figure 3.37B) and the MCF-7 stock (Figure 3.2E). Figure 3.37A demonstrates the morphology of the C12 clone isolated from stock MCF-7. This clone was not treated with AAPH or any radical agent, but appears to be a natural sub-population of MCF-7 that may be more carcinogenic (Zou and Matsumura, 2003).

A possible suggestion for the morphological change after AAPH treatment is the production of acrolein, which may be formed in MCF-7 cells upon treatment with 4 mM AAPH, 2 mM AAPH did not affect the viability of murine fibroblasts (Takabe *et al*., 2001) or the human MCF-7 cell line in the present study. This has bearing on many disease states, as ROS, largely lipid peroxidation products, are progenitors of

tissue damage and ensuing disease (Aitken and Krausz, 2001; Takabe *et al*., 2001; Khorowbeygi *et al*., 2004; Sanocka and Kurpisz, 2004).

Despite an 80% reduction in cell number following the AAPH treatment at 4 mM for 72 hours, no mitochondrial DNA damage was observed in the mitochondrial genes sequenced (one third of the mitochondrial genome). This is in contrast to research that suggests a correlation between lipid peroxidation, transformation, and the induction of DNA damage by mutagenic lipid products in murine fibroblasts (Takabe *et al*., 2001). This may be due to other bio-molecules (for instance sacrificial proteins) being oxidised before lipids. Gieseg *et al*. (2000) found that the peroxidation of proteins occurs before lipids in U937 cells (Gieseg *et al*., 2000). Thus, substantial ROS exposure experienced in some diseases may induce mtDNA damage via lipid adducts after sacrificial proteins are exhausted (Gil-Guzman *et al*., 2001).

4.3.5 DNA Modification

DNA fragmentation is a pro-mutagenic change that may be the result of oxidative stress, abortive Fas-mediated apoptosis or disruption of processes such as recombination and chromatin packaging, inducing strand breaks (Aitken and Krausz, 2001). For the purposes of this thesis the primary focus will be on oxidative stress in relation to DNA mutation and cell death.

4.3.6 Apoptosis in Free Radical Generator Studies

Apoptosis is commonly referred to as programmed cell death and is a decisive process in which a cell initiates a biochemical cascade resulting in cell death (Gieseg *et al*., 2000; Chang *et al*., 2002). Apoptosis can be induced in a number of ways including caspase activation and nitric oxide induction, but common to all is the release of mitochondrial cytochrome c accompanied by a loss of mitochondrial membrane potential ($\Delta\Psi m$) (Ide *et al*., 2001; Sanchez-Alcazar *et al*., 2001; Lachaud *et al*., 2004).

The free radical generator studies conducted in this thesis explored AAPH and DPPH as candidates for inducing mitochondrial DNA mutation. AAPH generates peroxyl radicals while DPPH (a stable free radical) is primarily used to test antioxidant effectiveness (Kristal *et al*., 1994; Jin and Chen, 1998; Hussain *et al*., 2003). Sporadic reports have indicated a deleterious oxidant function of DPPH against guinea pig cardiac tissue (Jin and Chen, 1998). The findings in the present study were that AAPH at 20 mM (1 hour treatment), 2 mM and 4 mM (72 hour treatment) induced cell death. Also DPPH at 250 nM (1 hour treatment), and 25 nM (72 hour treatment) induced cell death. This AAPH induced cell death was potentially due to apoptosis consistent with previous AAPH treatment studies in cell culture (Kristal *et al*., 1994; Hussain *et al*., 2003). In regards to cell proliferation, all levels of AAPH treatment reduced cell number leaving a surviving fraction that resulted in a longer lag phase compared to the control. Similarly, DPPH treatment at 250 nM resulted in cell death similar in morphological change to that of AAPH induced cell death, and resulted in a surviving fraction with expectedly longer lag phase. Population doubling times for both AAPH and DPPH treated cultures increased by 1 and 0.5 hours, respectively. This confirms a

negative impact of both AAPH and DPPH on MCF-7 cell cultures. Thus, lowered cellular energy output could be the result of excessive ROS production. This could be by endogenous defective respiratory function, or exogenous sources such as defective surrounding cells (Gil-Guzman *et al*., 2001). In the present research, cells that underwent free radical generator treatment did not experience mtDNA modification.

4.4 Future Aspirations

An intriguing experiment would be a study on the *in organelle* foot-printing of MCF-7 cell mitochondrial DNA, by monitoring the effects of AAPH (or other mutagenic agent) on transcription. AAPH may induce mitochondrial DNA mutation in hypotonic media (an experiment not conducted in this research), as the pores created on the mitochondrial membrane (as mitochondria swell) may be large enough to allow AAPH passage. Any induction of mitochondrial mutation or heteroplasmy could provide invaluable information by monitoring RNA synthesis. This may differentially affect the rates of mRNA and/or rRNA synthesis providing insight into the effect of mitochondrial DNA modification on transcription (Vander Heidan *et al*., 2000; Emmerson *et al*., 2001). The idea stems from the experiment performed by Micol *et al*. (1997), using HeLa cell isolated mitochondria. In their study ethidium bromide and ATP were employed to investigate their effect on transcription rate. It was found that the intercalating agent ethidium bromide and ATP decreased the rate of rRNA synthesis, but not mRNA synthesis.

An additional study will involve the use of a radioactively labelled RNA-synthesizing system using intact mitochondria. This could be another means of studying the

processing pattern of intact mitochondria harbouring mutant or heteroplasmic DNA. By using radioactive label, an *in-vivo* like processing system can be simulated, estimated to be at least 10-15% the *in-vivo* rate (Gaines and Attardi, 1984). This may elucidate the effect of silent mutations on transcription rate and/or processing. Messenger RNA transcription of mutant mtDNA is of interest, with a particular focus on heteroplasmy and thresholds thereof. As expected, this system is dependant on ATP concentration (Gaines and Attardi, 1984; Micol *et al*., 1997). Much research is needed to further elucidate the effect of mitochondrial mutations and mitochondrial heteroplasmy on human disease states and ROS production.

4.5 Conclusions

The aspirations of this thesis were to characterize the mammary epithelial cell line MCF-7 and assess the relevance natural mitochondrial mutation and OXPHOS function in relation to cell proliferation. This was achieved by the isolation of single cell, and establishment of genetically homogeneous, clones from the MCF-7 stock and characterization of their morphological and proliferate features. Mitochondrial mutations were determined by sequencing. Three cases of heteroplasmy were identified. One case of heteroplasmy Cytb gene G15807A) was different between single cell clones. This mutation did not correlate with population doubling time or enzyme activity of the encoded complex III. The effect of free radicals on DNA modification and cell proliferation was studied using free radical generators AAPH and DPPH. AAPH at 4 mM caused transformation in MCF-7 cells but did not induce mitochondrial DNA mutation. DPPH also did not induce mitochondrial DNA mutation or transformation in MCF-7 cells consistent with current research. However,

AAPH and DPPH did induce cell death that may implicate ROS in the production of lipid peroxides and mutagenic adducts facilitating apoptosis. MCF-7 was not found to be a hyper-mutagenic cancer cell line, and did not experience mtDNA mutation at the rates estimated by some research. Corroboration of these conclusions requires a larger sample size of variable single cell clones from MCF-7 and a number of cell lines to be investigated in the same manner. Analysis of nuclear coding genes is required to determine if variation in enzyme activity stems from nDNA mutation or heteroplasmy, or is a result of inadvertent laboratory variation. Furthermore, a number of means to estimate respiratory complex function in addition to the biochemical method used in this research could be used to eliminate error. In addition, a wider range of concentrations of AAPH could be used to treat MCF-7 cells to determine if a process of transformation is indeed in place and what concentration of AAPH is required to induce it. A study of PDT of treated cells may shed more light of the importance of MCF-7 growth habit in determining cell proliferation between potential transformed and non-transformed cells.

APPENDIX A

ABBREVIATIONS

AAPH 2,2′-azobis(2-amido propane)dihydrochloride

APS Ammonium persulphate

ATCC American type culture collection

ATP Adenosine triphosphate

ddH_2O Distilled, deionised water

DNA Deoxyribonucleic acid

dNTP Deoxyribonucleoside triphosphate

ddNTP Dideoxyribonucleoside triphosphate

DMEM Dulbecco's modified eagles medium

DMSO Dimethyl sulfoxide

DPPH 1,1-Diphenyl-2-picryl-hydrazyl

DTNB 5,5'-dithiobis-(2- nitrobenzoate)

EDTA Ethylenediaminetriacetic acid

GC Guanosine/Cytosine pairs

GM Growth medium

HEPES 4-(2-hydroxyethyl)-1-piperazineethanesulfonic acid

M Molar

mA Milliamps

mtDNA Mitochondrial DNA

NADH Nicotinamide adenine dinucleotide

nDNA Nuclear DNA

PBS Phosphate buffered saline

PCR Polymerase chain reaction

PDT Population doubling time

ROS Reactive oxygen species

SNP Single nucleotide polymorphism

TE8 Tris/EDTA, pH8

TAE Tris-acetate/EDTA

Taq *Thermus aquaticus*

TBE Tris-borate/EDTA

TMED N, N, N', N'-Tetramethyl-etheylenediamine

UV Ultraviolet

V Volts

W Watts

WST-1 (4-[3-(4-Iodophenyl)-2-(4-nitorphenyl)-2H-5-tetrazolio]-1,3-benzene-disulfonate)

w/v Weight per volume

Units:

g	grams
mg	milligrams
µg	micrograms

Prefixes:

c	centi (10^{-2})
m	milli (10^{-3})
µ	micro (10^{-6})
n	nano (10^{-9})
p	pico (10^{-12})

APPENDIX B

CHEMICAL SUPPLIERS

Product	Supplier
Acrylamide:bisacrylamide 19:1 (40%)	**BioRad**
Agarose	**Sigma**
Ammonium acetate	**BDH**
Ammonium persulfate	**Boehringer Mannheim**
Ascorbate	**Sigma**
2,2′-azobis(2-amido propane) dihydrochloride (AAPH)	**Sigma**
Bovine serum albumin V	**Boehringer Mannheim**
Bromophenol blue	**Sigma**
Chlofoform	**BDH**
Deoxynucleoside triphosphates (dNTPs)	**Eppendorf**
Dimethyl sulfoxide (DMSO)	**Gibco (Invitrogen)**
1,1-Diphenyl-2-picryl-hydrazyl (DPPH)	**Sigma**
5,5'-dithiobis-(2- nitrobenzoate) (DTNB)	**Sigma**
1, 4-Dithiothreitol (DTT)	**Boeringer Mannheim**
Dulbecco's modified eagle's media (DMEM)	**Gibco (Invitrogen)**
Ethanol	**BDH**
Ethidium bromide	**Sigma**
Ethylene diaminetetra acetic acid (EDTA)	**BDH**
Foetal bovine sera	**Gibco**
Hepes	**Boehringer Mannheim**
Isoamyl alcohol	**BDH**
Isopropanol	**BDH**
Mineral oil	**Sigma**
Nicotinamide adenine dinucleotide (NADH)	**Sigma**
Orange G	**Sigma**
Oxaloacetate	**Sigma**
Penicillin/ Streptomycin	**Gibco (Invitrogen)**
Phenol	**Scharlau (Scientific Supplies Ltd)**
Potassium cyanide	**Sigma**
Proteinase K	**Roche**
Sephadex G-25	**Amersham**
Sephadex G-50	**Amersham**
Sodium acetate	**BDH**
Sodium borohydride	**Sigma**
Sodium chloride	**BDH**
Sodium dodecyl sulfate (SDS)	**Gibco (Invitrogen)**
Sodium hydroxide	**BDH**
N,N,N',N'-Tetramethyl-ethylelediamine (TMED)	**Sigma**
Taq	**Roche**
Tris base	**Boehringer Mannheim**
Ubiquinone	**Sigma**
Urea	**BDH**
Xylene cyanol	**Sigma**

APPENDIX C

PCR AND SEQUENCING

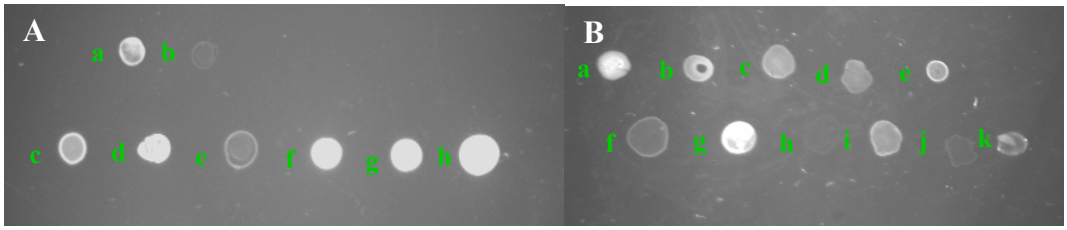

Figure 1A*. DNA spotting to visualise relative quantities of isolated DNA compared to a known quantity of λ DNA. A, *a*,** λ 0.1 µg; ***b*,** λ 0.01 µg; ***c*,** MCF-7; ***d, G8; ***e***, C12; ***f***, B5; ***g***, E1; ***h***, AAPH treated cell culture DNA. **B**, ***a*,** λ 0.1 µg; ***b*,** λ 0.06 µg; ***c*,** λ 0.04 µg; ***d*,** λ 0.02 µg; ***e*,** λ 0.01 µg; ***f*,** C12; ***g*,** B5; ***h*,** MCF-7; ***i*,** E1; ***j*,** DPPH treated cell culture DNA ***k*,** G8.

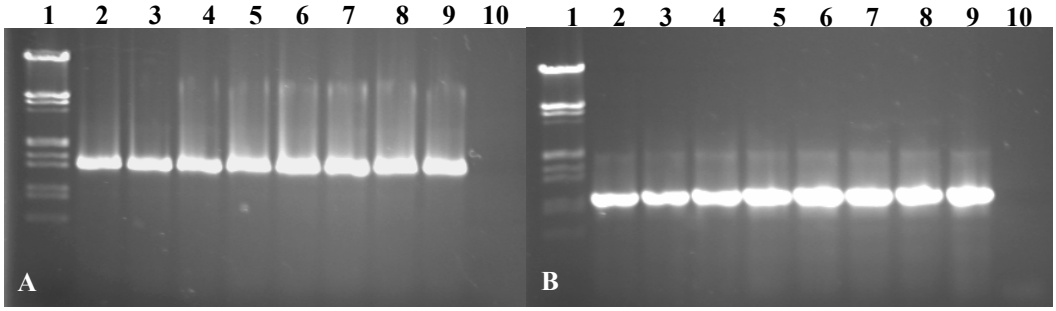

Figure 1.* A, PCR product from the D-loop gene for radical treated cell culture DNA. *Lane 1, molecular marker λ*HindIII/EcoRI*; ***lane 2 and 3,*** MCF-7 continuous growth DNA; ***lane 4 and 5,*** 2 mM AAPH treated cell culture DNA; ***lane 6 and 7,*** 25 nM DPPH treated cell culture DNA; ***lane 8 and 9,*** AAPH and DPPH treated cell culture DNA; ***lane 10,*** negative control. ***B,* PCR product from the COII gene for radical treated cell culture DNA. *Lane 1,*** molecular marker λ*HindIII/EcoRI*; ***lane 2 and 3,*** MCF-7 continuous growth DNA; ***lane 4 and 5,*** 2 mM AAPH treated cell culture DNA; ***lane 6 and 7,*** 25 nM DPPH treated cell culture DNA; ***lane 8 and 9,*** AAPH and DPPH treated cell culture DNA; ***lane 10,*** negative control.

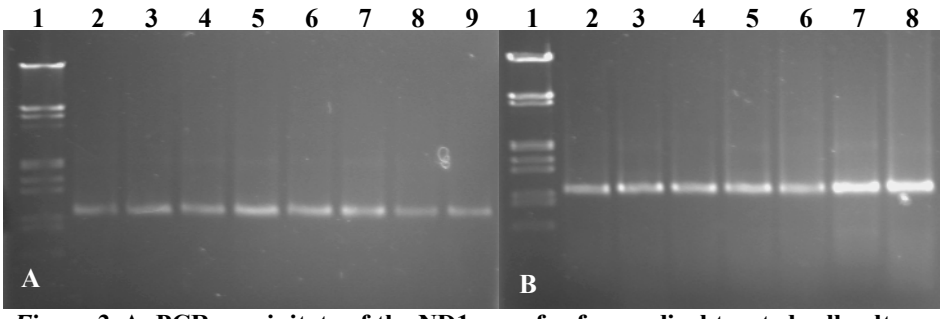

Figure 2.* A, PCR precipitate of the ND1 gene for free radical treated cell cultures. *Lane 1, molecular marker λ*HindIII/EcoRI*; ***lane 2 and 3,*** MCF-7 continuous growth DNA; ***lane 4 and 5,*** 2 mM AAPH treated cell culture DNA; ***lane 6 and 7,*** 25 nM DPPH treated cell culture DNA; ***lane 8 and 9,*** AAPH and DPPH treated cell culture DNA. B, PCR precipitate

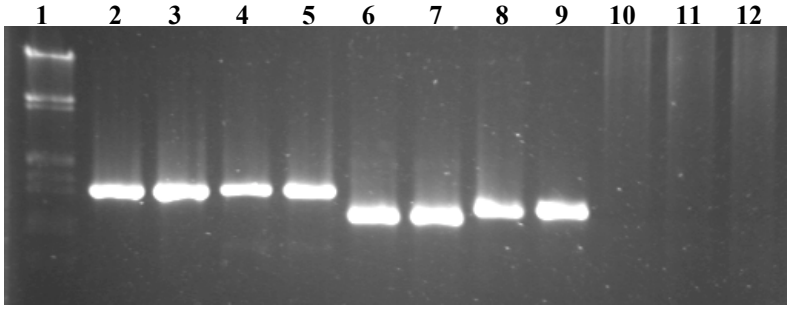

Figure 3. **PCR of mitochondrial genes with MCF-7 DNA from cell culture treated with AAPH 20 mM for 1 hour.** ***Lane 1,*** molecular marker *λHindIII/EcoRI*; ***ane 3 and 3,*** Cytb gene product; ***lane 4 and 5,*** D-loop gene product; ***lane 6 and 7,*** COI gene product; ***lane 8 and 9,*** ND1 gene product; ***lanes 10 to 12***, negative controls

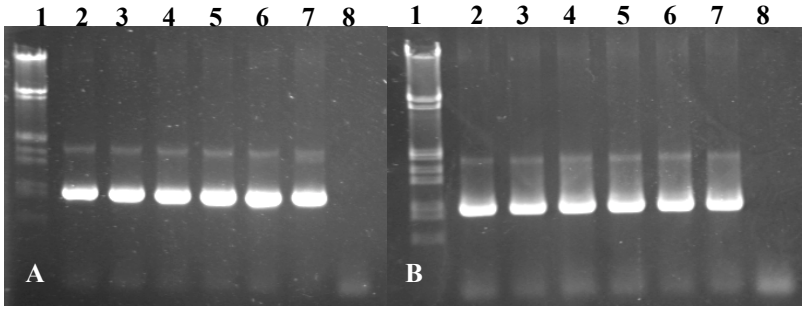

Figure 4. **A. B. PCR product of the ATPase gene for MCF-7.** ***Lane 1,*** molecular marker λ*HindIII/EcoRI*; ***lane 2 to 7,*** ATPase product; ***lane 8,*** negative control.

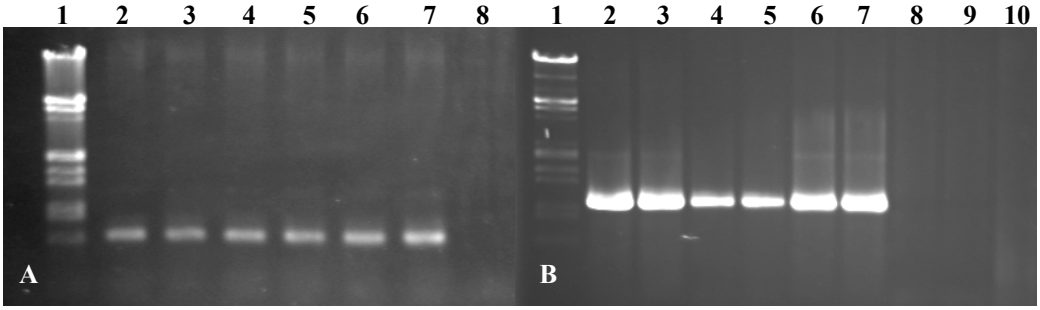

Figure 5. **A, PCR product for the ND6 gene.** ***Lane 1,*** molecular marker λHindIII/EcoRI; ***lane 2 to 6,*** ND6 gene product; ***lane 7,*** negative control.

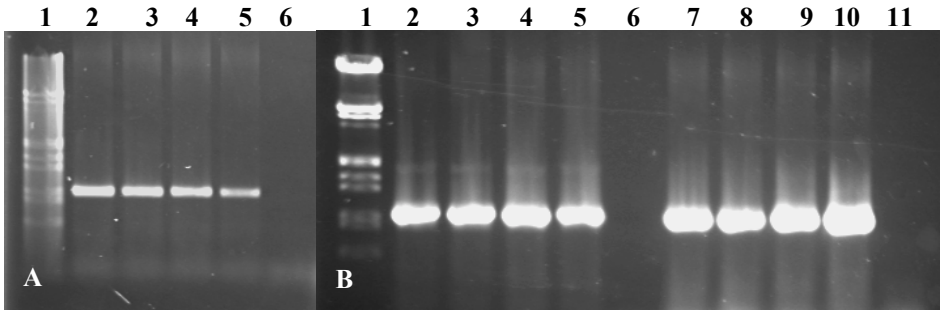

Figure 6. **A, PCR product for the COI gene for MCF-7.** ***Lane 1,*** molecular marker λ*HindIII/EcoRI*; ***lane 2 to 5,*** MCF-7; ***lane 6,*** negative control. **B,** PCR product for mitochondrial genes for MCF-7. ***Lane 1,*** molecular marker λHindIII/EcoRI; ***lane 2 to 5,*** PCR product of the COI gene; ***lane 6,*** negative control; ***lane 7 to 10,*** PCR product of the COIII gene; ***lane 11,*** negative control.

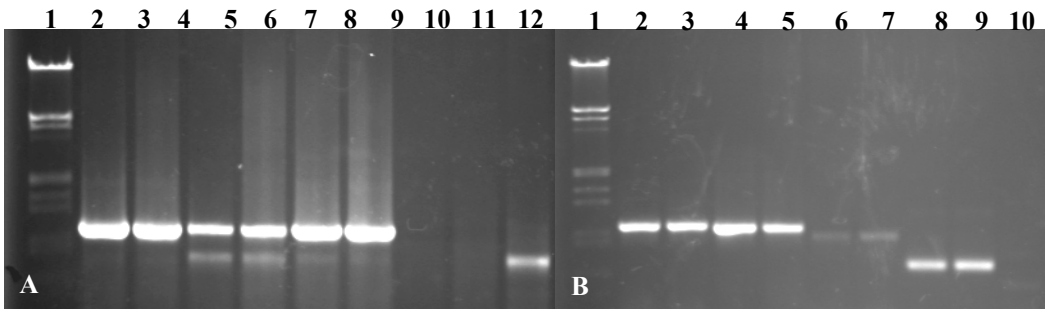

Figure 7. **A, PCR product from the 12S gene.** ***Lane 1,*** molecular marker λ*HindIII/EcoRI*, ***lane 2 and 3,*** G8 clone; ***lane 4 and 5,*** E1 clone; ***lane 6 and 7,*** B5 clone, ***lane 8 and 9,*** C12 clone, ***lane 10,*** negative control. ***B,*** **PCR products of mitochondrial genes for C12 clone**. ***Lane 1,*** molecular marker λ*HindIII/EcoRI*; ***lane 2 and 3,*** COIII gene; ***lane 4 and 5,*** COI gene; ***lane 6 and 7,*** ATPase gene; ***lane 8 and 9,*** ND6 gene; ***lane 9,*** negative control for ND6. Other controls had no banding (not shown).

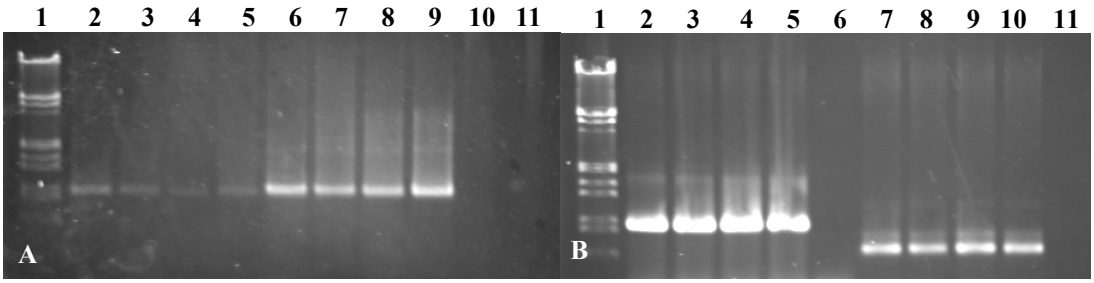

Figure 8. **PCR product for MCF-7. A,** ***Lane 1,*** molecular marker λ*HindIII/EcoRI*; ***lane 2 to 5,*** product for the COI gene; ***lane 6 to 9,*** product for the COIII gene; ***lane 10 and 11,*** negative controls. ***B,*** **PCR product for mitochondrial genes for MCF-7.** ***Lane 1,*** molecular marker *λHindIII/EcoRI*; ***lane 2 to 5,*** product for the ATPase gene; ***lane 6,*** negative control for ATPase; ***lane 7 to 10,*** product for the ND6 gene; ***lane 11,*** negative control for ND6.

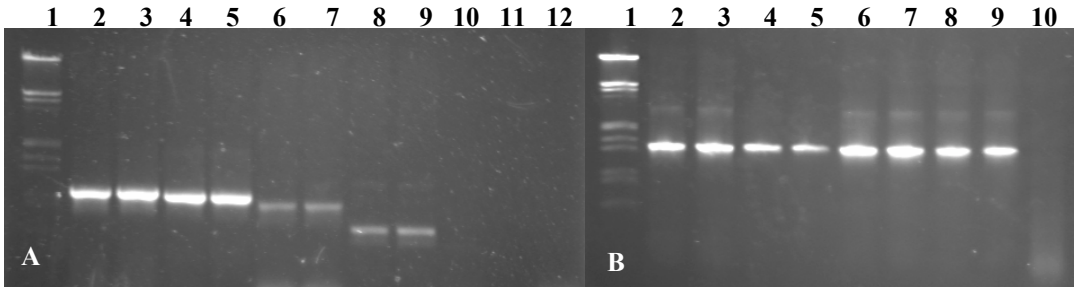

Figure 9. **A, PCR products of mitochondrial genes for G8 clone**. ***Lane 1,*** molecular marker λ*HindIII/EcoRI*; ***lane 2 and 3,*** COIII gene; ***lane 4 and 5,*** COI gene; ***lane 6 and 7,*** ATPase gene; ***lane 8 and 9,*** ND6 gene; ***lane 10 to 14*** negative controls. ***B,*** **PCR product for the ND4 gene.** ***Lane 1,*** molecular marker λ*HindIII/EcoRI*; ***lane 2 and 3,*** G8 clone; ***lane 4 and 5,*** C12 clone; ***lane 6 and 7***, E1 clone; ***lane 8 and 9,*** B5 clone; ***lane 10,*** negative control.

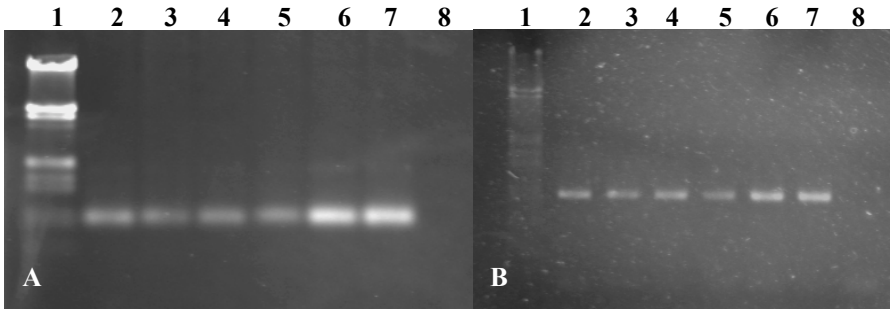

Figure 10. **A. PCR precipitate of the ATPase gene. Lane 1,** molecular marker λHindIII/EcoRI; lane 2 to 7, ATPase precipitate. **B. PCR product for the ATPase gene. *Lane 1,*** molecular marker λHindIII/EcoRI; ***lane 2 to 6,*** ND6 gene product; ***lane 7,*** negative control.

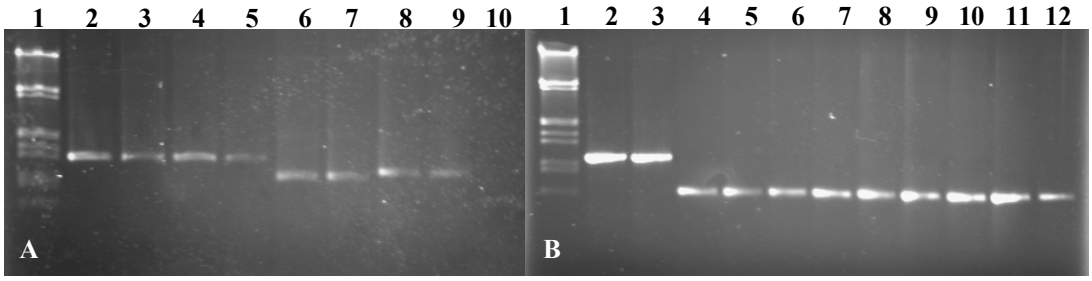

Figure 11. A, **PCR precipitate of mitochondrial gene products form MCF-7 DNA from cell culture treated with 20 mM AAPH for 1 hour. *Lane 1,*** molecular marker *λHindIII/EcoRI*; **l*ane 2 and 3,*** Cytb gene product; ***lane 4 and 5,*** D-loop gene product; ***lane 6 and 7,*** COI gene product; ***lane 8 and 9,*** ND1 gene product; ***lanes 10 to 12,*** negative controls. ***B,*** **PCR precipitate from mitochondrial gene products. *Lane 1,*** molecular marker λ*HindIII/EcoRI*; ***lane 2 and 3,*** E1 clone product for 12S; ***lane 4 and 5,*** E1 clone product for ND2; ***lane 6 and 7,*** MCF-7 product for ND2; ***lane 8 and 9,*** G8 clone product for ND2; ***lane 10 and 11,*** B5 clone product for ND2; ***lane 12,*** C12 clone product for ND2. (Negative controls not pictured).

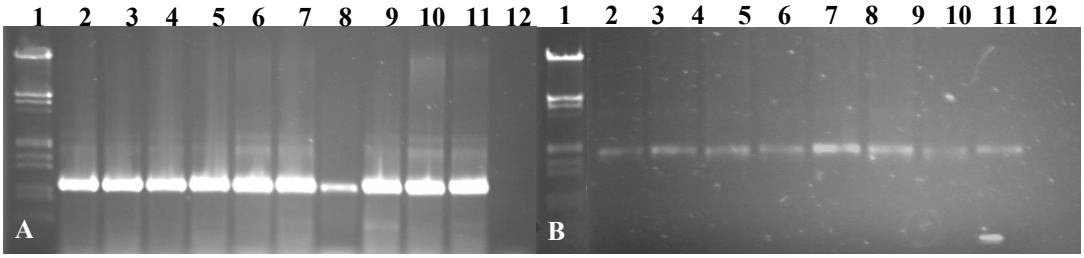

Figure 12. **A, PCR product for the COII gene. *Lane 1,*** molecular marker λ*HindIII/EcoRI*; ***lane 2 and 3,*** MCF-7; ***lane 4 and 5,*** clone E1; ***lane 6 and 7,*** clone G8; ***lane 8 and 9,*** clone C12; ***lane 10 and 11,*** clone B5; ***lane 12,*** negative control. **B, PCR precipitate of the COII gene for continuous radical treated cells. *Lane 1,*** molecular marker λ*HindIII/EcoRI*; ***lane 2 and 3,*** MCF-7; ***lane 4 and 5,*** clone E1; ***lane 6 and 7,*** clone G8; ***lane 8 and 9,*** clone C12; ***lane 10 and 11,*** clone B5; ***lane 12,*** negative control.

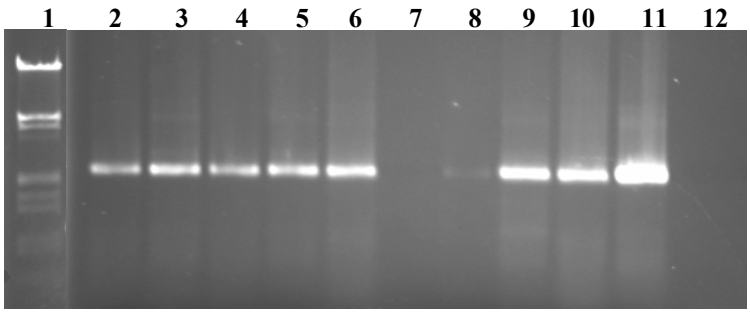

Figure 13. **PCR precipitate for the COIII gene.** ***Lane 1,*** molecular marker λ*HindIII/EcoRI*; ***lane 2 and 3,*** MCF-7; ***lane 4 and 5,*** clone E1; ***lane 6 and 7,*** clone G8; ***lane 8 and 9,*** clone C12; ***lane 10 and 11,*** clone B5; ***lane 12,*** negative control.

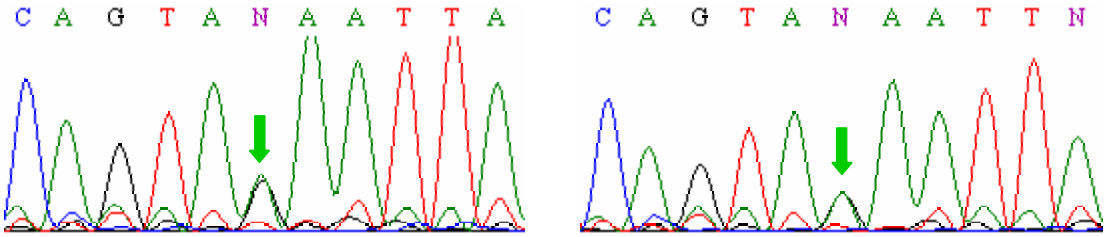

Figure 14. **ABI Chromatographs of the ATPase gene** (reverse sequence shown) displaying C→T base heteroplasmy. ***A,*** C12. ***B,*** G8.

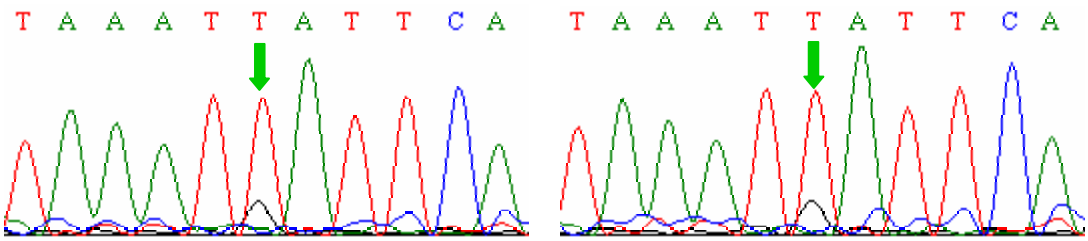

Figure 15. **ABI Chromatographs of the ND6 gene.** (forward sequence shown) displaying T→G heteroplasmy. ***A,*** C12. ***B,*** B5.

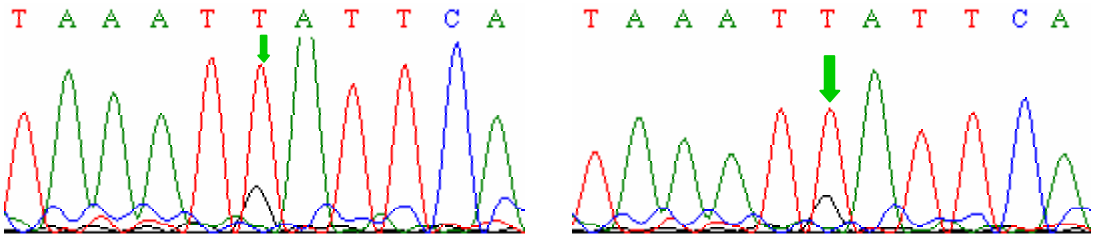

Figure 16. **ABI Chromatographs of the ND6 gene.** (forward sequence shown) displaying T→G heteroplasmy. ***A,*** E1. ***B,*** G8.

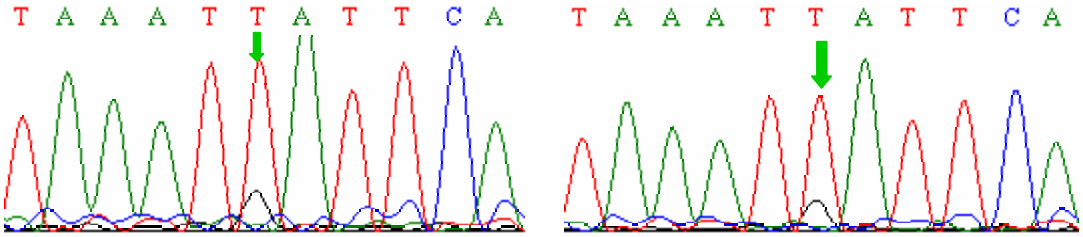

Figure 17. **ABI Chromatographs of the ND6 gene.** (forward sequence shown) displaying T→G heteroplasmy. ***A,*** MCF-7 ***B,*** E1.

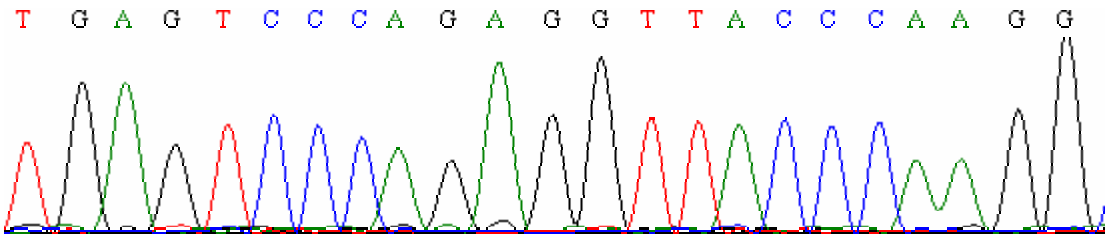

Figure 18. **ABI Chromatograph of a portion of the ND2 gene from MCF-7** (reverse sequence shown).

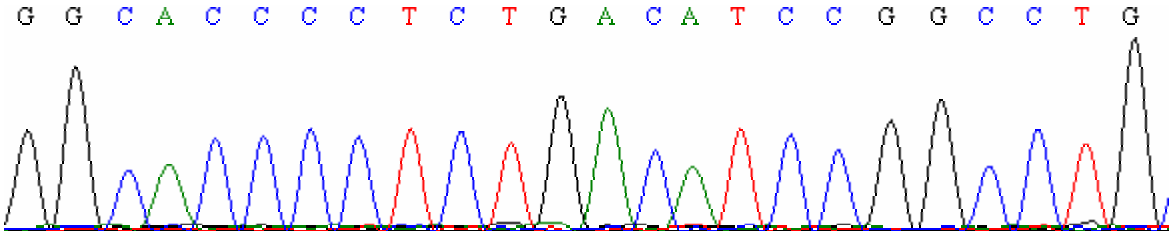

Figure 19. **ABI Chromatograph from a portion of the ND2 gene of MCF-7** (forward sequence shown).

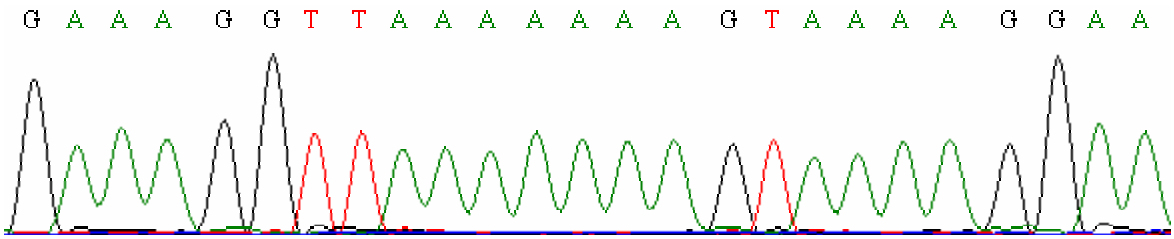

Figure 20. **ABI Chromatograph of a portion of the 16S gene of MCF-7** (forward sequence shown).

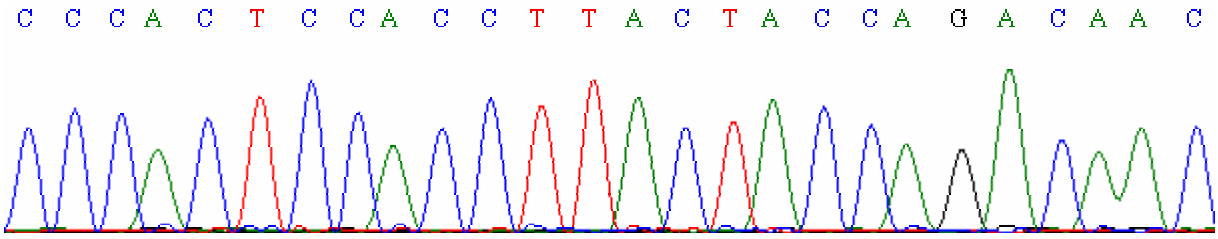

Figure 21. **ABI Chromatograph of a portion of the 16S gene of MCF-7** (forward sequence shown).

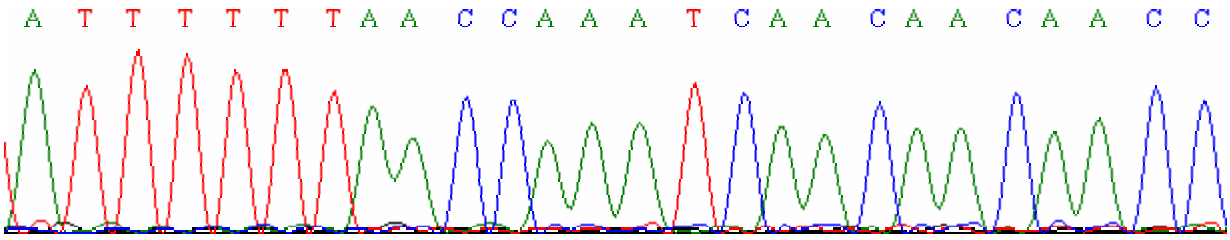

Figure 22. **ABI Chromatograph of a portion of the ND4 gene of MCF-7** (forward sequence shown).

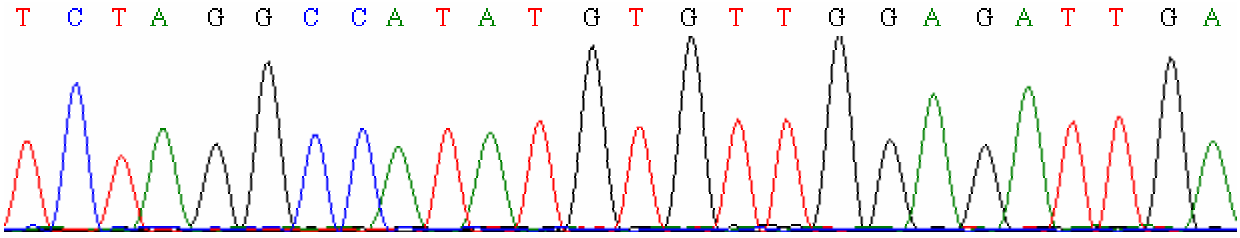

Figure 23. **ABI Chromatograph of a portion of the ND4 gene of MCF-7** (reverse sequence shown).

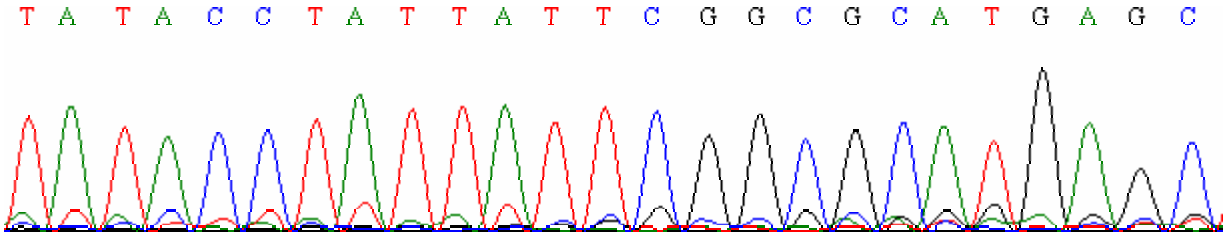

Figure 24. **ABI Chromatograph of a portion of the COI gene of MCF-7** (forward sequence shown).

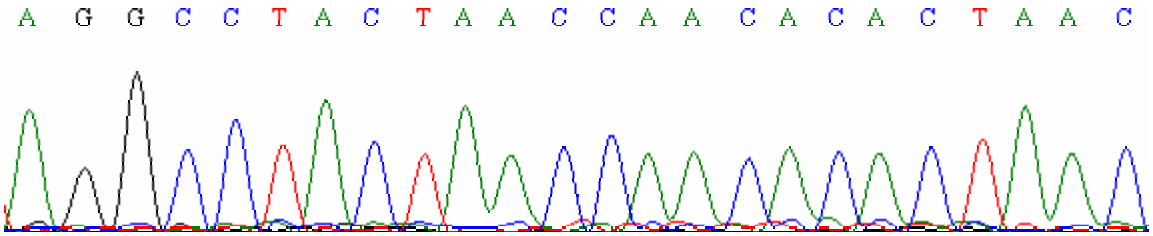

Figure 25. **ABI Chromatograph of a portion of the COIII gene of MCF-7** (forward sequence shown).

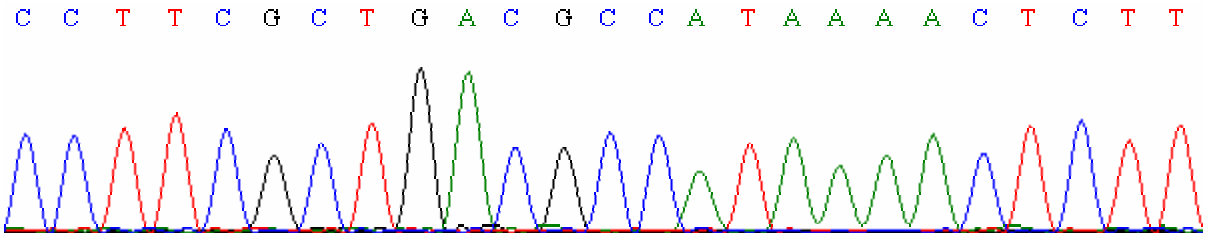

Figure 26. **ABI Chromatograph of a portion of the ND1 gene of MCF-7** (forward sequence shown).

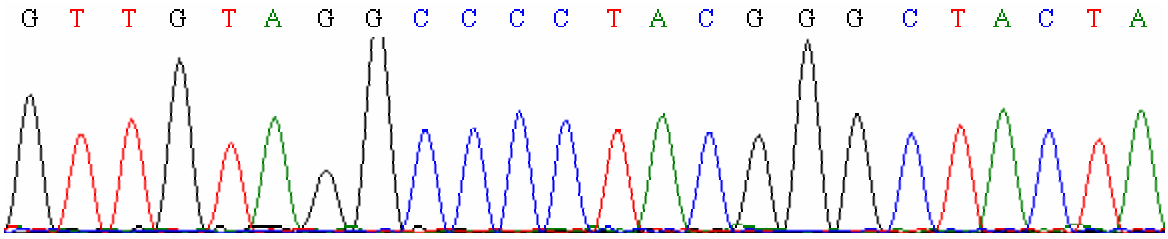

Figure 27. **ABI Chromatograph of a portion of the D-loop gene of MCF-7** (forward sequence shown).

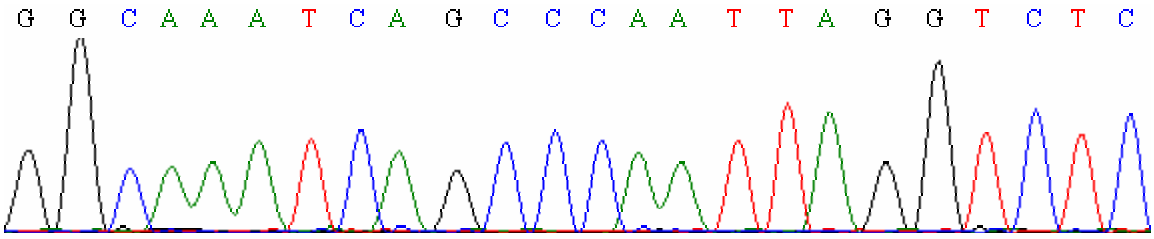

Figure 28. **ABI Chromatograph of a portion of the ND5 gene of MCF-7** (forward sequence shown).

REFERENCES

Aggeler, R., Coons, J., Taylor, S., Ghosh, S., Garcia, J., Capaldi, R., Marusich, M. (2002). "A functionally active human F1F0 ATPase can be purified by immunocapture from heart tissue and fibroblast cell lines." *J. Biol. Chem*. **277**(37): 33906-33912.

Aitken, R., Krausz, C. 2001. Oxidative stress, DNA damage and the Y chromosome. *Reprod.* **122**: 497-506.

Aitken, R., Fisher, H., Fulton, N., Gomez, E., Knox, W., Lewis, B., Irvine, S. (1997). "Reactive oxygen species generation by human spermatozoa is induced by exogenous NADPH and inhibited by the flavoprotein inhibitors diphenylene iodonium and quinacrine." *Mol. Reprod. Dev.* **47**: 468-482.

Allen, R., Keogh, B., Tresini, M., Gerhard, G., Volker, C., Pignolo, R., Horton, J., Cristofalo, V. (1997). "Development and age-associated differences in electron transport potential and consequences for oxidant generation." *J. Biol. Chem.* **272**(40): 24805-24812.

Anderson, S, Bankier, A., Barrell, B., de Bruijin D., Colson, A., Drouin J, Eperon, I., Nierlich DP, Roe BA, Sanger F, Schreier PH, Smith, A., Staden, R., Young IG. (1981). "Sequence and organization of the human mitochondrial genome." *Nature*. **290**(5806): 457-65

Arnold, R., Shi, J., Murad, E., Whalen, A., Sun, C., Polavarapu, R., Parthasarathy, S., Petros, J., Lambeth, J. (2001). "Hydrogen peroxide mediates the cell growth and transformation caused by the mitogenic oxidase Nox1." *PNAS* **98**(10).

Bai, Y., Hu, P., Park, J., Deng, J., Song, X., Chomyn, A., Yagi, T., Attardi, G. (2004). "Genetic and functional analysis of mitochondrial DNA-encoded complex I genes." *Ann. N. Y. Acad. Sci.* **1011**: 272-283.

Ballard, J., Whitlock, M. (2004). "The incomplete natural history of mitochondria." *Mol. Ecol.* **13**: 729-744.

Barrientos, A. (2002). "In vivo and in organello assessment of OXPHOS activities." *Methods* **26**: 307-316.

Battersby, B., Loredo-Osti, J., Shoubridge, E. (2003). "Nuclear genetic control of mitochondrial DNA segregation." *Nat. Genet.* **33**(2): 183-186.

Behrend, L., Henderson, G., Zwacka, R. (2003). "Reactive oxygen species in oncogenic transformation." *Biochem. Soc. Trans*. **31**(6): 1441-1444.

Birch-Machin, M., Briggs, H./, Saborido, A., Bindoff, L., Turnbull, D. (1994). "An evaluation of the measurerment of the activities of complexes I-IV in the respiratory chain of human skeletal muscle mitochondria." *Biochem. Med. Metab.* **51**: 35-42.

Bourges, I., Ramus, C., Mousson de Camaret, B., Beugnot, R., Remacle, C., Cardol, P., Hofhaus, G., Issartel, J. (2004). "Structural organization of mitochondrial human complex I: role of

the ND4 and ND5 mitochondria-encoded subunits and interaction with prohibitin." *Biochem. J.* **383**: 491-499.

Bradford, M. (1976). "A rapid and sensitive method for the quantification of microgram quantities of protein utilizing the principle of protein-dye binding." *Anal. Biochem.* **7**(72): 248-254.

Brown, W., George, M., Wilson, A. (1979). "Rapid evolution of animal mitochondrial DNA`." *Proc. Natl. Acad. Sci.* **76**(4): 1967-1971.

Bruno, C., Martinuzzi, A., Tang, Y., Andreu, A., Pallotti, F., Bonilla, E., Shanske, S., Fu, J., Sue, C., Angelini, C., DiMauro, S., Manfredi, G. (1999). "A stop-codon mutation in the human mtDNA cytochrome c oxidase I gene disrupts the functional structure of complex IV." *Am. J. Hum. Genet.* **65**: 611-620.

Cavelier, L., Johannisson, A., Gyllensten, U. (2000). "Analysis of mtDNA copy number and composition of single mitochondrial particles using flow cytometry and PCR." *Exp. Cell. Res.* **259**: 79-85.

Chang, W., Lui, J., Chen, C., Huang, T., Lu, F. (2002). "Growth inhibition and induction of apoptosis in MCF-7 breast cancer cells by fermented soy product." *Nutrition and Cancer* **43**(2): 214-226.

Chen, J., Gokden, N., Greene, G. (2003). "Simultaneous generation of multiple mitochondrial DNA mutations in human prostate tumours suggests mitochondrial hyper-mutagenesis." *Carcinogenesis* **24**(9): 1481-1487.

Chomyn, A., Enriquez, J., Micol, V., Fernandez-Silva, P., Attardi, G. (2000). "The mitochondrial myopathy, encephalopathy, lactic acidosis, and stroke-like episode syndrome-associated human mitochondrial tRNALEU(UUR) mutation causes aminoacylation deficiency and concomitant reduced association of mRNA with ribosomes." *J. Biol. Chem.* **275**(25): 19198-19209.

Cortopassi, G., Shibata, D., Soong, N., Arnheim, N. (1992). "A pattern of accumulation of a somatic deletion of mitochondrial DNA in aging human tissues." *Proc. Natl. Acad.* **89**: 7370-7374.

Costello, L., Franklin, R. (2000). "The intermediary metabolism of the prostate: a key to understanding the pathogenesis and progression of malignancy" *Oncology*. **59**: 269-282.

Croteau, D., Bohr, V. (1997). "Repair of oxidative damage to nuclear and mitochondrial DNA in mammalian cells." *J. Biol. Chem.* **272**(41): 25409-25412.

Cummins, J., Jequier, A., Kan, R. (1994). "Molecular biology of human male infertility: links with aging, mitochondrial genetics, and oxidative stress?" *Mol. Reprod. Dev.* **37**: 345-362.

D'Aurelio, M., Pallotti, F., Barrientos, A., Gajewski, C., Kwong, J., Bruno, C., Beal, M., Manfredi, G. (2001). "In vivo regulation of oxidative phosphorylation in cells harbouring a stop-codon mutation in mitochondrial DNA-encoded cytochrome c oxidase subunit I." *J. Biol. Chem.* **276**(50): 46925-46932.

Devarajan, E., Chen, J., Multani, A. (2002). "Human breast cancer MCF-7 cell line contains inherently drug-resistant subclones with distinct genotypic and phenotypic features." *Inter. Jour. Oncology*. **20**: 913-920.

de Lamirande, E., Harakat, A. Gagnon, C. 1998. Human sperm capacitation induced by biological fluids and progesterone, but not by NADH or NADPH, is associated with the production of superoxide anion. *J. Androl.* **19**(2): 215-225.

Diaz, F., Bayona-Bafaluy, M., Rana, M., Mora, M., Hao, H., Moraes, C. (2002). "Human mitochondrial DNA with large deletions repopulates organelles faster that full-length genomes under relaxed copy number control." *Nucl. Acid. Res.* **30**(21): 4626-4633.

Diekert, K., de Kroon, A., Kispal, G., Lill, R. (2001). "Isolation and subfractionation of mitochondria from the yeast Saccharomyces cerevisiae." *Meth. Cell. Biol.* **65**: 37-49.

Diez-Sanchez, C., Ruiz-Pesini, E., Montoya, J., Perez-Martos, A., Enriquez, J. A., Lopez-Perez, M. J. (2003). "Mitochondria from ejaculated human spermatozoa do not synthesize proteins." *FEBS Letters* **553**: 205-208.

DiMauro, S., Andreu, A. (2000). "Mutations in mtDNA: are we scraping the bottom of the barrel?" *Brain Pathology* **10**: 431-441.

DiMauro, S., Schon, E. (2001). "Mitochondrial DNA mutation in human disease." *Am. J. Med. Genet.* **106**: 18-26.

Emmerson, C., Brown, G., Puolton, J. (2001). "Synthesis of mitochondrial DNA in permeabilised human cultured cells." *Nucl. Acid. Res.* **29**(2): 1-9.

Enriquez, J., Cabezas-Herrera, J., Bayona-Bafaluy, M., Attardi, G. (2000). "Very rare complementation between mitochondria carrying different mitochondrial DNA mutations points to intrinsic genetic autonomy of the organelles in cultured human cells." *J. Biol. Chem.* **275**(15): 11207-11215.

Felty, Q., Roy, D. (2005). "Estrogen, mitochondria, and growth of cancer and non-cancer cells." *Jour. Carcin.* **4**(1): 1-18.

Folgero, T., Bertheussen, K., Lindal, S., Torbergsen, T., Oian, P. (1993). "Mitochondrial disease and reduced sperm motility." *Human. Reprod.* **8**(11): 1863-1868.

Freshney, I. (2000). "*Culture of animal cells, forth edition*." Wiley-Liss, Inc Canada.

Fujii, Y., Tomita, K., Sano, H. Yamasaki, A., Hitsuda, Y., Adcock, I., Shimizu, E. (2002). "Dissociation of DNA damage and mitochondrial injury caused by hydrogen peroxide in SV-40 transformed lung epithelial cells." *Can. Cell. Inter.* **2**(16).

Gaines, G., Attardi, G. (1984). "Highly efficient RNA-synthesizing system that uses isolated human mitochondria: new initiation events and in vivo-like processing patterns." *Mol. Cell. Biol.* **4**(8): 1605-1617.

Garrett, R., Grisham, C. (1999). "*Biochemistry second edition*." Saunders College Publishing, USA.

GenomeNet, B. c., Institute for chemical research, Kyoto university. http://www.genomenet.jp (2004).

Genova, M. L., Pich, M. M., Biondi, A. (2003). "Mitochondrial production of oxygen radical species and the role of coenzyme Q as an antioxidant." *Exp. Biol. Med.* **228**: 506-513.

Gieseg, S., Duggan, S., Gebicki, J. (2000). "Peroxidation of proteins before lipids in U937 cells exposed to peroxyl radicals." *Biochem. J.* **350**: 215-218.

Gieseg, S., Pearson, J., Firth, C. (2003). "Protein hydroperoxides are a major product of low density lipoprotein oxidation during copper, peroxyl radical and macrophage-mediated oxidation." *Free Rad. Research*. **37**(9): 983-991.

Gil-Guzman, E., Ollero, M., Lopez, M., Sharma, R., Alvarez, J., Thomas, A., Agarwal, A. (2001). "Differential production of reactive oxygen species by subsets of human spermatozoa at different stages of maturation." *Hum. Reprod.* **16**(9): 1922-1930.

Grzybowski, T. (2000). "Extremely high levels of human mitochondrial DNA heteroplasmy in single hair roots." *Electrophoresis* **21**: 548-553.

Halliwell, B., Gutteridge, J. (1999). "Free radicals biology and medicine." Clarendon Press, Oxford, England.

Hand, R., Craven, R. (2003). "Hpr6.6 protein mediates cell death from oxidative damage in MCF-7 human breast cancer cells." *Jour. Cell. Biochem.* **90**: 534-547.

Hofhaus, G., Johns, D., Hurko, O., Attardi, G., Chomyn, A. (1996). "Respiration and growth defects in transmitochondrial cell lines carrying the 11778 mutation associated with Leber's hereditary optic neuropathy." *J. Biol. Chem*. **271**(22): 13155-13161.

Hofhaus, G. A., G. (1993). "Lack of assembly of mitochondrial DNA-encoded subunits of respiratory NADH dehydrogenase and loss of enzyme activity in a human cell mutant lacking the mitochondrial ND4 gene product." *EMBO J.* **12**: 3043-3048.

Hofhaus, G. A., G. (1995). "Efficient selection and characterization of mutants of a human cell line which are defective in mitochondrial DNA-encoded subunits of respiratory NADH dehydrogenase." *Mol. Cell. Biol.* **15**(2): 964-974.

Holstein, A., Schulze, W., Davidoff, M. (2003). "Understanding spermatogenesis is a prerequisite for treatment." *Reprod. Biol. Endo.* **107**(1).

Holt, I., Harding, A., Morgan-Hughes, J. (1989). "Deletions of muscle mitochondrial DNA in mitochondrial myopathies: sequence analysis and possible mechanisms." *Nucl. Acid. Res.* **17**(12): 4465-4469.

Hussain, S. P., Hofseth, l. J., Harris, C. C. (2003). "Radical causes of cancer." *Nature reviews* **3**: 276-285.

Ide, T., Tsutsui, H., Hayashidani, S. (2001). "Mitochondrial DNA damage and dysfunction associated with oxidative stress in failing hearts after myocardial infarction." *Circ. Res.* **88**: 529-535.

Jacobs, H. (2003). "Disorders of mitochondrial protein synthesis." *Hum. Mol. Genet.* **12**(2): 293-301.

Jin, Z. Q., Chen, X. (1998). "A simple reproducible model of free radical-injured isolated heart induced by 1,1-diphenyl-2-picryl-hydrazyl (DPPH)." *Jour. of Pharm. and Toxic. Meth.* **39**: 63-70.

Khosrowbeygi, A., Zarghami, N., Deldar, Y. (2004). "Correlation between sperm quality parameters and seminal plasma antioxidant status." *Iran. J. Reprod. Med.* **2**(2): 58-64.

King, M. P., Attardi, G. (1989). "Human cells lacking mtDNA: repopulatiopn with exogenous mitochondria by complementation." *Science* **246**: 500-503.

Kirino, Y., Yasukawa, T., Ohta, S., Akira, S., Ishihara, K., Watanabe, K., Suzuki, T. (2004). "Codon-specific translational defect caused by a wobble modification deficiency in mutant tRNA from a human mitochondrial disease." *PNAS* **101**(42): 15070-15075.

Kirino, Y., goto, Y., Campos, Y., Arenas, J., Suzuki, T. (2005). "Specific correlation between the wobble modification deficiency in mutant tRNAs and the clinical features of a human mitochondrial disease." *PNAS* **102**(20): 7127-7132.

Kirstal, B., Chen, J., Pal Yu, B. (1994). "Sensitivity of mitochondrial transcription to different radical species." *Free Rad. Biol. Med.* **16**(3): 323-329.

Klug, W., Cummings, M (1997). "*Concepts of genetics*." Prentice Hall New Jersey.

Lachaud, C., Tesarik, J., Canadas, M., Mendoza, C. (2004). "Apoptosis and necrosis in human ejaculated spermatozoa." *Hum. Reprod*. **19**(3): 607-610.

Lacroix, M., Leclercq, G. (2004). "Relevance of breast cancer cell lines as models for breast tumours: an update." *Breast cancer reaserch and treatment* **83**(3): 249-289.

Langdon, S. (2004). "*Cancer cell culture*." Humana Press, NJ, USA.

Larsson, N. G., Oldfors, A., Garman, J. D., Barsh, G. S., Clayton, D. A. (1997). "Down-regulation of mitochondrial transcription factor A during spermatogenesis in humans." *Hum. Mol. Genet*. **6**(2): 185-91.

Lucas, D., Szweda, L. (1998). "Cardiac reperfusion injury: aging, lipid peroxidation, and mitochondrial dysfunction." *Proc. Natl. Acad. Sci*. **95**: 510-514.

Mambo, E., Nyaga, S., Bohr, V., Evans, M. (2002). "Defective repair of 8-hydroxyguanine in mitochondria of MCF-7 and MDA-MB-468 human breast cancer cell lines." *Cancer Research* **62**: 1349-1355.

Max, B. (1992). This and that: hair pigments, the hypoxic basis of life and the Virgilian journey of the spermatozoon. *Trends Pharmacol. Sci.*, **13**, 272-276.

May-Panloup, P. M., Cheretein, M. F., Savagner, F., Vasseur, C., Jean, M., Malthiery, Y., Reynier, P. (2003). "Increased sperm mitochondrial DNA content in male infertility." *Hum. Reprod.* **18**(3): 550-556.

Micol, V., Fernandez-Silva, P., Attardi, G. (1997). "Functional analysis of in vivo and in organello footprinting of HeLa cel mitochondrial DNA in relationship to ATP and ethidium bromide effects on transcription." *J. Biol. Chem*. **272**(30): 18896-18904.

Miller, M., Angeles, F., Reuter, B., Bobrowski, P., Sandoval, M. (2001). "Dietary antioxidants protect gut epithelial cells from oxidant-induced apoptosis." *BMC* **1**(11).

MITOMAP. A human mitochondrial genome database, www.mitomap.org. (2005).

Moustafa, M., Sharma, R., Thornton, J., Mascha, E., Abdel-Hafez, M., Thomas, A., Agarwal, A. (2004). "Relationship between ROS production, apoptosis and DNA denaturation in spermatozoa from patients examined for infertility." *Hum. Reprod.* **19**(1): 129-138.

Murphy, M., Echtay, K., Blaikie, F., Asin-Cayuela, J., Cocheme, H., Green, K., Buckingham, J., Taylor, E., Hurrell, F., Hughes, G., Miwa, S., Cooper, C., Svistunenko, D., Smith, R., Brand, M. (2003). "Superoxide activates uncoupling proteins by generating carbon-centred radicals and initiating lipid peroxidation." *Jour. Biol. Chem.* **278**(49): 48534-48545.

Pitkanen, S., Robinson, B. (1996). "Mitochondrial complex I deficiency leads to increased production of superoxide radicals and induction of superoxide dismutase." *J. Clin. Invest.* **98**(2): 345-351.

Quintana-Murci, L., Rotig, A., Munnich, A., Rustin, P., Bourgeron, T. (2001). "Mitochondrial DNA inheritance in patients with deleted mtDNA." *J. Med. Genet.* **38**(28).

Ramachandran, A., Moellering, D., Ceaser, E. (2002). "Inhibition of mitochondrial protein synthesis results in increased endothelial cell susceptibility to nitric oxide-induced apoptosis." *PNAS* **99**(10): 6643-6648.

Rantanen, A., Jansson, M., Oldfors, A., Larsson, N. (2001). "Downregulation of Tfam and mtDNA copy number during mammalian spermatogenesis." *Mamm. Genome.* **12**(10): 787-792.

Richer, S., Ford, W. (2001). "A critical investigation of NADPH oxidase activity in human spermatozoa." *Mol. Hum. Reprod.* **7**(3): 237-244.

Roberts, V., Pique, M. (1999). "Definition of the interaction domain for cytochrome c on cytochrome c oxidase." *J. Biol. Chem*. **274**(53): 38051-38060.

Ross, J. (2004). " www.jdaross.mcmail.com."

Rossingnol, R., Letellier, T., Malgat, M. (2000). "Tissue variation in the control of oxidative phosphorylation: implication for mitochondrial diseases." *Biochem. J.* **347**: 45-53.

Ruiz-Pesini, E., Diez, C., Lapena, A. C., (1998). "Correlation of sperm motility with mitochondrial enzyme activities." *Clin. Chem*. **44**(8): 1616-1620.

Ruiz-Pesini, E., Lapena, A., Diez-sanchez, C., Perez-martos, A., Montoya, J., Alvarez, E., Diaz, M., Urries, A., Montoro, L., Lopez-perez, M., Enriquez, J. (2000b). "Human mtDNA haplogroups associated with high or reduced spermatozoa motility." *Am. J. Hum. Genet.* **67**: 682-696.

Ruiz-Pesini, E., Lapena, A., Diez, C., Alvarez, E., Enriquez, J., Lopez-Perez, M. (2000a). "Seminal quality correlates with mitochondrial functionality." *Clin. Chim. Acta.* **300**: 97-105.

Rustin, P., Parfait, B., Chretien, D., Bourgeron, T., Djouadi, F., Bastin, J., Rotig, A., Munnich, A. (1996). "Fluxes in nicotinamide adenine dinucleotides through mitochondrial membranes in human cultured cells." *Jour. Biol. Chem.* **271**(25): 14785-14790.

Said, T., Agarwal, A., Sharma, R., Thomas, A., Sikka, S. (2005). "Impact of sperm morphology on DNA damage caused by oxidative stress induced by beta-nicotinamide adenine dinucleotide phosphate." *Fertility and Sterility* **83**(1): 95-103.

Sanchez-Alcazar, J., Khodjakov, A., Schneider, E. (2001). "Anticancer drugs induce increased mitochondrial cytochrome c expression that precedes cell death." *Cancer Research* **61**: 1038-1044.

Sanocka, D., Kurpisz, M. (2004). "Reactive oxygen species and sperm cells." *Reprod. Biol. Endo.* **2**(12).

Shoubridge, E. A. (2001). "Nuclear genetic defects of oxidative phosphorylation." *Human Mol. Gen.* **10**(20): 2277-2284.

Siguroardottir, S., Helgason, A., Gulcher, J. R., Stefansson, K., Donnelly, P. (2000). "The mutation rate in the human mtDNA control region." *Am. J. Hum. Genet.* **66**: 1599-1609.

Simandan, T., Sun, J., Dix, T. (1998). "Oxidation of DNA bases, deoxyribonucleosides and homoploymers by peroxyl radicals." *Biochem. J.* **335**: 233-240.

Smith, C. (2004). "ATPases: diverse roles and common themes." *NZ Bioscience*: 32-36.

Snustad, D., Simmons, M. (1997). "*Principles of Genetics*", second edition, John Wiley and Sons New York.

Sottocasa, G. L., Kuylenstierna, B., Ernster, L. (1967). "An electron-transport system associated with the outer membrane of liver mitochondria." *Jour. Cell. Biol.* **32**: 415-438.

Srere, P. (1960). "Citrate Synthase." *Meth. Enzym.* **11**: 3-11.

St John, J. C., Jokhi, R. P., Barratt, C. L. R. (2001). "Men with oligoasthenoteratozoospermia harbour higher numbers of multiple mitochondrial DNA deletions in their spermatozoa, but individual deletions are not indicative of overall aetiology." *Mol. Hum. Reprod.* **7**(1): 103-111.

Sutherland, R., Hall, R., Taylor, I. (1983). "Cell proliferation kinetics of MCF-7 human mammary carcinoma cells in culture and effects of tamoxifen on exponentially growing and plateau-phase cells." *Cancer Research* **43**: 3998-4006.

Suzuki, T., Suzuki, T., Wada, T., Saigo, K., Watanabe, K. (2002). "Taurine as a constituent of mitochondrial tRNAs: new insights into the functions of taurine and human mitochondrial diseases." *The EMBO J.* **21**(23): 6581-6589.

Takabe, W., Niki, E., Uchida, K. (2001). "Oxidative stress promotes the development of transformation: involvement of a potent mutagenic lipid peroxidation product, acrolein." *Carcinogenesis* **22**(6): 935-941.

Taylor, I., Hodson, P., Green, M., Sutherland, R. (1983). "Effects of tamoxifen on cell cycle progression of synchronous MCF-7 human mammary carcinoma cells." *Cancer Research* **43**: 4007-4010.

Taylor, W., Taylor, G., Durham, S., Turnbull, D. (2001). "The determination of complete human mitochondrial DNA sequences in single cells: implications for the study of somatic mitochondrial DNA point mutations." *Nucl. Acid. Res.* **29**(15).

Torroni, A., Stepien, G., Hodge, J., Wallace, D. (1990). "Neoplastic transformation is associated with coordinate induction of nuclear and cytoplasmic oxidative phosphorylation genes." *J. Biol. Chem.* **265**(33): 20589-20593.

Tryoen-Toth, P., Richerts, S., Sohm, B. (2003). "Proteomic consequences of a human mitochondrial tRNA mutation beyond the frame of mitochondrial translation." *J. Biol. Chem.* **278**(27): 24314-24323.

Twigg, J., Fulton, N., Gomez, E., Irvine, D., Aitken, R. (1998). "Analysis of the impact of intracellular reactive oxygen species generation on the structural and functional integrity of human spermatozoa: lipid peroxidation, DNA fragmentation and effectiveness of antioxidants." *Hum. Reprod.* **13**(6): 1429-1436.

Uchida, K. (1999). "Current status of acrolein as a lipid peroxidation product." *TCM* **9**(5): 109-113.

Vander Heidan, M., Chandel, N., Li, X., Schumacker, P., Colombini, M., Thompson, C. (2000). "Outer mitochondrial membrane permeability can regulate coupled respiration and cell survival." *PNAS* **97**(9): 4666-4671.

Vergani, L., Rossi, R., Brierley, H., Hanna, M., Holt, I. (1999). "Introduction of heteroplasmic mitochondrial DNA (mtDNA) from a patient with NARP into two human po cell lines is associated either with selection and maintenance of NARP mutant mtDNA or failure to maintain mtDNA." *Hum. Mol. Genet.* **8**(9): 1751-1755.

Villani, G., Greco, M., Papa, S., Attardi, G. (1998). "Low reserve of cytochrome c oxidase capacity in vivo in the respiratory chain of a variety of human cell types." *J. Biol. Chem.* **273**(48): 31829-31836.

Wallace, D. (1986). "Mitotic segregation of mitochondrial DNAs in human cell hybrids and expression of chloramphenicol resistance." *Somat. Cell. Mol. Genet.* **12**(1): 41-49.

Wallace, D., Brown, M., Lott, M. (1999). "Mitochondrial DNA variation in human evolution and disease." *Gene* **238**: 211-230.

Wallace, D. C. (1999). "Mitochondrial diseases in man and mouse." *Science* **283**: 1482-1488.

Wang, X., Sharma, R., Sikka, S., Thomas, A., Falcone, T., Agarwal, A. (2003). "Oxidative stress is associated with increased apoptosis leading to spermatozoa DNA damage in patients with male factor infertility." *Fertility and Sterility* **80**(3): 531-535.

British Broadcasting Corporation, www.bbc.co.uk.

Yasukawa, T., Suzuki, T., Ishii, N., Ohta, S., Watanabe. (2001). "Wobble modification defect in tRNA disturbs codon-anticodon interaction in a mitochondrial disease." *EMBO J.* **20**(17): 4794-4802.

Zhen, Y., Hoganson, C., Babcock, G., Ferguson-miller, S. (1999). "Definition of the interaction domain for cytochrome c on cytochrome c oxidase." *J. Biol. Chem.* **274**(53): 38032-38041.

Zini, A., de Lamirande, E. Gagnon, C. 1995. Low levels of nitric oxide promote human sperm capacitation. *J. Androl.* **16**(5): 424-431.

Zivadinovic, D., Gametchu, B., Waston, C. (2004). "Membrane estrogen receptor-alpha levels in MCF-7 breast cancer cells predict c AMP and proliferation responses." *Breast Cancer Research* **7**(1): 101-112.

Zou, E., Matsumura, F. (2003). "Long-term exposure to beta-hexachlorocyclohexane (beta-HCH) promotes transformation and invasiveness of MCF-7 human breast cancer cells." *Biochem. Pharm.* **66**: 831-840.

ACKNOWLEDGEMENTS

Firstly, to my Lord and King Jesus Christ- anything that's good in me is because of you and your great love.

For Mum and Dad, Kelly and Dale who have believed in my abilities and encouraged me throughout, thank you, I love you. To all of my friends, workmates and flatmates that have been so caring of me and willing to help me in many different ways, especially Sarah and Lynette, thank you for your support. To my family at St Johns who have prayed for me, encouraged me and helped me to grow and continue to grow, especially Ailers, Chris, Sarah, Paula, Sophie, Aidan, Tim, Fiona, Melissa, Peter, Wally, and Ruth, who have encouraged me greatly.

Thanks to my supervisors Frank Sin, Steven Gieseg and Dru Mason for their advice and in supplying the cultures and equipment. Thank you to Jan McKenzie for her hard work and persistence with the inverted microscope and to Linda Morris for her care and dedication in managing the genetics lab and the teaching lab. Thanks heaps to the Gemmell lab for the farewell drinks! Thank you to all the lab members and in particular Maxine Bryant in giving her time to read this thesis and provide helpful comments.